

CCI+ PHASE 2 – NEW ECVS **PERMAFROST**

D4.1 PRODUCT VALIDATION AND INTERCOMPARISON REPORT (PVIR)

VERSION 5.1

30 OCTOBER 2025

PREPARED BY















Document Status Sheet

Issue	Date	Details	Authors
1.0	30.09.2019	CRDPv0 evaluation	B. Heim, M. Wieczorek (AWI), A. Bartsch, C. Kroisleitner (B.GEOS), Cécile Pellet, Reynald Delaloye, Chloé Barboux (UNIFR)
2.0	30.09.2020	Update of evaluation results of CRDPv1	A. Bartsch (B.GEOS), B. Heim, M. Wieczorek (AWI), Cécile Pellet, Reynald Delaloye (UNIFR)
2.1	14.01.2020	Inclusion of temporal stability	M. Wieczorek, B. Heim (AWI)
3.0	30.09.2021	Update of evaluation results of CRDPv2	B. Heim, S. Lisovski (AWI), Cécile Pellet, Reynald Delaloye (UNIFR), A. Bartsch (B.GEOS)
4.0	15.02.2024	Update of evaluation results of CRDPv3	B. Heim, M. Wieczorek (AWI), Cécile Pellet, Reynald Delaloye (UNIFR), A. Bartsch (B.GEOS)
5.0	15.09.2025	Update of evaluation results of CRDPv4	B. Heim, M. Wieczorek, L. Enguehard, E. Riegel (AWI), Cécile Pellet, Reynald Delaloye (UNIFR), A. Bartsch (B.GEOS)
5.1	30.10.2025	Inclusion of GT temporal stability for Antarctica and comparisons CRDPv4 and CRDPv3 evaluations	M. Wieczorek, B. Heim (AWI)

Author team

Birgit Heim, AWI

Mareike Wieczorek, AWI

Léa Enguehard, AWI

Elisabeth Riegel, AWI

Cécile Pellet, UNIFR

Reynald Delaloye, UNIFR

Annett Bartsch, B.GEOS

Tazio Strozzi, GAMMA

ESA Technical Officer: Frank Martin Seifert

EUROPEAN SPACE AGENCY CONTRACT REPORT

The work described in this report was done under ESA contract. Responsibility for the contents resides in the authors or organizations that prepared it.

TABLE OF CONTENTS

		· · · · · · · · · · · · · · · · · · ·	4
1	Intr	oduction	6
	1.1	Purpose of the Document	6
	1.2	Structure of the Document	7
	1.3	Applicable Documents	7
	1.4	Reference Documents	7
	1.5	Bibliography	8
	1.6	Acronyms	
	1.7	Glossary	9
2	Met	hods for Quality Assessment	11
	2.1.	Overview on the Quality Assessment Methods	
	2.2	Assessment of Permafrost Temperature	
	2.3	Assessment of Active Layer Thickness	
	2.4	Assessment of Permafrost Extent	27
3	Asse	essment Results: Permafrost Temperature	30
	3.1	Permafrost Temperature User Requirements	
	3.2	Permafrost_cci GTD Match-up Analyses with In Situ Data	
	3.3	Permafrost_cci GTD Comparison with PERMOS Permafrost Temperature	
	3.4	Permafrost_cci GTD Comparison with FT2T GT	
4	Asse	essment Results: Active Layer Thickness	52
	4.1	Active Layer Thickness User Requirements	52
	4.2	Permafrost_cci ALT Match-up Analyses with In Situ Data	
5	Asse	essment Results: Permafrost Extent	62
	5.1	Permafrost_cci PFR Match-up Analyses with In Situ Data	
	5.2	PERMOS Permafrost Extent Comparisons	
6	Sun	nmary	72
7	Refe	erences	74
	7.1	Bibliography	
	7.2	Acronyms	

EXECUTIVE SUMMARY

This document presents the Product Validation and Intercomparison Report (PVIR) v5 of the European Space Agency (ESA) Climate Change Initiative (CCI) Permafrost project (Permafrost_cci). CCI is ESA's global monitoring program whose main objective is to provide Earth Observation (EO)-based Essential Climate Variable (ECV) time series to the climate modelling and science user communities. Permafrost_cci phase I of CCI+ (2018–2021) has been selected for phase II (2022–2025) with the production of ECVs for permafrost, set by the Global Climate Observing System (GCOS)/World Meteorological Organisation (WMO). The PVIR describes the quality assessments of the Permafrost_cci *CRDPVv4* products: i) permafrost temperature expressed as Ground Temperature per Depth (GTD) [°C] ii) Active Layer Thickness (ALT) [m] and iii) permafrost extent expressed as Permafrost FRaction (PFR) [%] derived from GTD at 2 m depth.

The Committee on EO Satellites (CEOS) Working Group on Calibration and Validation (WGCV) defines validation as 'the process of assessing, by independent means, the quality of the data products derived from the system outputs' (*lpvs.gsfc.nasa.gov*). According to the CEOS Quality Assurance framework for Earth Observation (QA4EO) and ESA CCI guidelines, the validation data need to be independent from the product generation. In the QA4EO sense, suitable reference data are characterised by protocols and community-wide management practices and published openly. In Permafrost_cci accordingly, assessments of the Permafrost_cci products are carried out independently using in situ data mainly from the WMO/GCOS Global Terrestrial Network for Permafrost (GTN-P) managed by the International Permafrost Association (IPA) and suitable other international and national monitoring networks. Within the GTN-P/IPA framework, the Thermal State of Permafrost Monitoring (TSP) program is managing the temperature monitoring, whereas the Circumpolar Active Layer Monitoring program (CALM) is providing standardised global ALT monitoring. Permafrost_cci specifically involves the mountain permafrost monitoring program GTN-P/PERMOS in Switzerland to cope with the challenge of validation of the Permafrost_cci products in mountainous regions, providing PERMOS permafrost monitoring data at highest quality levels.

Standard statistical summaries and binary match-up analyses comparing in situ measurements with the Permafrost_cci products are used. Permafrost_cci is also innovatively undertaking assessments in comparing Permafrost_cci GTD with EO-microwave derived Freeze-Thaw to Temperature (FT2T) and for mountain permafrost areas using EO-derived inventories on rock glacier occurrence and dynamics, which was developed by Data User Element (DUE) GlobPermafrost since 2016 and continued in Permafrost_cci phase I and worldwide in 18 mountain regions in Permafrost_cci phase II.

Permafrost_cci GTD match-up evaluation (14,585 match-ups at 479 sites) shows a cold bias (median = -0.95 °C, mean = -0.76 °C ± 1.73) and high temporal stability for the Northern hemisphere for the bulk ground temperature data collection spanning all temperature regimes (permafrost and non permafrost) and across depths from the surface down to 10 m depth. The cold ground temperature regime representative for permafrost conditions (GTD < 1 °C) shows an even higher performance with a smaller bias (median = 0.23 °C, mean = 0.3 °C ± 1.70) across all depths and as well an high temporal stability. Therefore, we consider the Permafrost_cci GTD time series very well usable for the climate research communities. Users of Permafrost_cci GTD products should consider that GTD > 1 °C outside of the permafrost zones is characterised by a larger bias (median = -1.33 °C, mean = -1.16 °C ± 1.46).

D.4.1 Product Validation and Inter-	CCI+ PHASE II – NEW ECVS	Issue 5.1
Comparison Report (PVIR)	Permafrost	30 October 2025

This tendency in the warmer temperature subgroup towards too cold GTD is therefore characteristic for sporadic and discontinuous permafrost regions leading in turn to an overestimation of the areal extent of permafrost at the southern boundaries of Permafrost in Permafrost_cci PFR. The permafrost temperature range with GTD < 1 °C and PFR < 14 % is reliable as non permafrost.

Permafrost_cci ALT performance (with match-up pairs from China and Mongolia excluded) with 2,940 match-up pairs at 536 sites is characterised by a median bias of 0.03 m and a mean bias of 0.07 m, however with a large standard deviation of ± 0.56 m, but a robust temporal stability of 73 % for the Northern hemisphere. A large bias of > 1 m occurs only in a few match-up pairs in the more southern permafrost zones of Alaska, Canada and Russia, and > -1.5 m mainly in Svalbard and Scandinavia, and also in Antarctica, characteristic for rocky and pebble terrain with deep in situ active layer depths despite high latitudes and altitudes.

For the inland ice-free permafrost regions in Antarctica data are not sufficient for a thorough statistical analysis. The tendency of the Permafrost_cci products compared to the available in situ data for inland ice-free permafrost regions in Antarctica is negative, i.e. Permafrost_cci performs with too cold GTD and too shallow ALT depths.

PERMOS investigations in the Swiss Alps show that the performance of Permafrost_cci GTD and Permafrost_cci PFR further improved for high mountain regions. Permafrost_cci GTD shows a negative bias of -0.08 °C. At larger depth, Permafrost_cci GTD shows a positive bias of +1.06 °C at 10 m depth. Permafrost_cci PFR matches the majority of inventoried ESA GlobPermafrost slope movement products and Permafrost_cci rock glacier products that were located outside of the Permafrost_cci PFR up to Permafrost_cci CRDPv2.

D.4.1 Product Validation and Inter-	CCI+ PHASE II – NEW ECVS	Issue 5.1
Comparison Report (PVIR)	Permafrost	30 October 2025

1 INTRODUCTION

1.1 Purpose of the Document

This document is the Product Validation and Intercomparison Report (PVIR) v5 (update of [RD-1]) of the ESA CCI+ project Permafrost_cci [AD-1,2,3]. The PVIR describes the quality assessments of the Permafrost_cci *Climate Research Data Packages (CRDP)*, following CCI and CEOS Quality Assurance framework for Earth Observation (QA4EO) guidelines [AD-3,4,5, RD-2].

Besides the required WMO/GCOS Permafrost ECVs [AD-6] i) permafrost temperature and ii) active layer thickness, Permafrost_cci provides iii) permafrost extent (permafrost fraction within a pixel), as an additional variable derived from permafrost temperature: the areal fraction within the grid cell that fulfils the definition for the existence of permafrost (mean annual ground temperature (MAGT) < 0 °C for two consecutive years).

The generation of the Permafrost_cci *CRDP* i) MAGT from the surface down to 10 m in five different depths, ii) active layer thickness, and iii) permafrost fraction relies on the ground thermal model Permafrost_cci CryoGrid forced by EO time series of Land Surface Temperature (LST) and Snow Water Equivalent (SWE) with boundary conditions of EO-derived Land Cover [RD-3]. Therefore, Permafrost_cci *CRDPv4* [RD-4] released in 2025 as an update of *CRDPv3* includes three permafrost product time series covering the Northern hemisphere north of 30° N and for the first time in the production of Permafrost_cci *CRDPs* also the inland-ice free permafrost regions of Antarctica.

Permafrost cci CRDPv4 contains:

- simulated EO-forced mean annual Ground Temperature per Depth (GTD) in five discrete depths (0, 1.0, 2.0, 5.0, 10.0 m) from 1997 to 2023 [°C]
- simulated EO-forced annual Active Layer Thickness (ALT) from 1997 to 2023 [m]
- annual Permafrost FRaction (PFR) derived from GTD from 1997 to 2023 [0-1]

The CCI project team shall ensure independence for the validation, implying that the assessment of the Permafrost_cci product, as well as its uncertainties, is established with independent datasets and suitable statistical approaches [RD-2]. In addition, the validation needs to be carried out by team members not involved in the final algorithm selection [AD-3,4,5].

In Permafrost_cci phase II we continue the match-up based statistical validation for Permafrost_cci GTD, ALT and PFR time series for the Northern hemisphere, similarly now also for Antarctica, and for mountain permafrost areas including rock glacier abundance [RD-5] as in phase I [RD-6,7.8].

1.2 Structure of the Document

The PVIR is organised in six chapters. Chapter 1 provides the introduction and the overview on Permafrost_cci including applicable documents and the community glossary for Permafrost. Chapter 2 and its subsections describe the reference datasets and methods for the assessment of the Permafrost_cci products and their temporal stability. Chapters 3,4,5 present the results of the quality assessment for the Permafrost_cci products for Permafrost_cci Ground Temperature per Depth (GTD), Active Layer Thickness (ALT), and Permafrost FRaction (PFR) timeseries, respectively. Chapter 6 provides a summary and recommendations.

1.3 Applicable Documents

- [AD-1] IPA Action Group 'Specification of a Permafrost Reference Product in Succession of the IPA Map' (2016): Final report. https://ipa.arcticportal.org/images/stories/AG_reports/IPA_AG_SucessorMap_Final_2016.pdf
- [AD-2] Requirements for monitoring of permafrost in polar regions A community white paper in response to the WMO Polar Space Task Group (PSTG), Version 4, 2014-10-09. Austrian Polar Research Institute, Vienna, Austria, 20 pp.
- [AD-3] ESA 2017: Climate Change Initiative Extension (CCI+) Phase 1 New Essential Climate Variables Statement of Work. ESA-CCI-PRGM-EOPS-SW-17-0032
- [AD-4] GEO/CEOS Quality Assurance framework for Earth Observation (QA4EO) protocols 3-4
- [AD-5] ESA Climate Change Initiative. CCI Project Guidelines. EOP-DTEX-EOPS-SW-10-0002
- [AD-6] World Meteorological Organization (2022, updated 2025). The 2022 GCOS ECV Requirements (GCOS-245).

1.4 Reference Documents

- [RD-1] Heim, B., Wieczorek, M., Pellet, C., Delaloye, R., Bartsch, A., Strozzi, T. (2024): ESA CCI+ Product Validation and Intercomparison Report, v4.0
- [RD-2] Heim, B., Wieczorek, M., Pellet, C., Delaloye, R., Westermann, S., Bartsch, A., Strozzi, T. (2024): ESA CCI+ Product Validation Plan, v5.0
- [RD-3] Bartsch, A., Westermann, S., Strozzi, T., Wiesmann, A., Kroisleitner, C., Wieczorek, M., Heim, B. (2024): ESA CCI+ Permafrost Product Specifications Document, v5.0
- [RD-4] Bartsch, A., Westermann, S., Strozzi, T., Wiesmann, A. (2025): ESA CCI+ Permafrost Product User Guide, v5.0
- [RD-5] Rouyet, L., Schmid, L., Pellet, C., Delaloye, R., Onaca, A., Sirbu, F., Poncos, V., Kääb, A., Strozzi, T., Jones, N., Bartsch, A. (2024): CCN4 Mountain Permafrost: Rock Glacier Inventories (ROGI) and Rock Glacier Velocity (RGV) products Product Specification Document v2.1
- [RD-6] Heim, B., Wieczorek, M., Pellet, C., Barboux, C., Delaloye, R., Bartsch, A., B. Kroisleitner, C., Strozzi, T. (2019): ESA CCI+ Product Validation and Intercomparison Report, v1.0

- [RD-7] Heim, B., Wieczorek, M., Pellet, C., Delaloye, R., Bartsch, A., Jakober, D., Pointner, G., Strozzi, T. (2020): ESA CCI+ Product Validation and Intercomparison Report, v2.0
- [RD-8] Heim, B., Wieczorek, M., Pellet, C., Delaloye, R., Bartsch, A., Jakober, D., Pointner, G., Strozzi, T. (2021): ESA CCI+ Product Validation and Intercomparison Report, v3.0
- [RD-9] van Everdingen, Robert, ed. 1998 revised May 2005. Multi-language glossary of permafrost and related ground-ice terms. Boulder, CO: National Snow and Ice Data Center/World Data Center for Glaciology. (http://nsidc.org/fgdc/glossary/; accessed 23.09.2009)
- [RD-10] Bartsch, A., Westermann, S., Heim, B., Wieczorek, M., Pellet, C., Barboux, C., Delaloye, R., Kroisleitner, C., Strozzi, T. (2020): ESA CCI+ Permafrost Data Access Requirements Document, v2.0
- [RD-11] Nitze, I., Grosse, G., Heim, B., Wieczorek, M., Matthes, H., Rouyet, L., Echelard, T., Schmid, L., Pellet, C., Delaloye, R., Sirbu, F., Onaca, A., Poncho, V., Brardinoni, F., Rouyet, L., Kääb, A., Strozzi, T., Jones, N., Bartsch, A. (2024): ESA CCI+ Climate Assessment Report, v4.0
- [RD-12] Bartsch, A., Matthes, H., Westermann, S., Heim, B., Pellet, C., Onacu, A., Strozzi, T. (2024): ESA CCI+ Permafrost User Requirements Document, v4.0
- [RD-13] Nitze, I., Grosse, G., Heim, B., Wieczorek, M., Matthes, H., Bartsch, A., Strozzi, T. (2019): ESA CCI+ Climate Assessment Report, v1.0
- [RD-7] Bartsch, A., Matthes, H., Westermann, S., Heim, B., Pellet, C., Onacu, A., Kroisleitner, C., Strozzi, T. (2019): ESA CCI+ Permafrost User Requirements Document, v1.0
- [RD-8] Heim, B., Wieczorek, M., Pellet, C., Barboux, C., Delaloye, R., Bartsch, A., B. Kroisleitner, C., Strozzi, T. (2019): ESA CCI+ Product Validation and Intercomparison Report, v1.0
- [RD-9] Heim, B., Wieczorek, M., Pellet, C., Delaloye, R., Bartsch, A., Jakober, D., Pointner, G., Strozzi, T. (2020): ESA CCI+ Product Validation and Intercomparison Report, v2.0
- [RD-10] Rouyet, L., Schmid, L., Pellet, C., Delaloye, R., Onaca, A., Sirbu, F., Poncos, V., Kääb, A., Strozzi, T., Jones, N., Bartsch, A. (2023): CCN4 Mountain Permafrost: Rock Glacier Inventories (ROGI) and Rock Glacier Velocity (RGV) products Product Specification Document v1.0
- [RD-11] IPA Action Group 'Specification of a Permafrost Reference Product in Succession of the IPA Map' (2016): Final report. https://ipa.arcticportal.org/images/stories/AG_reports/IPA_AG_SucessorMap_Final_2016.pdf

1.5 Bibliography

A complete bibliographic list that supports arguments or statements made within the current document is provided in Section 7.1.

1.6 Acronyms

A list of acronyms is provided in section 7.2.

D.4.1 Product Validation and Inter-	CCI+ PHASE II – NEW ECVS	Issue 5.1
Comparison Report (PVIR)	Permafrost	30 October 2025

1.7 Glossary

The glossary below based on [RD-9] provides a selection of terms relevant for Permafrost_cci [AD-3]. A comprehensive glossary is available as part of the Product Specifications Document [RD-3].

active-layer thickness

The thickness of the ground layer that is subject to annual thawing and freezing above permafrost. The thickness of the active layer depends on factors such as the ambient air temperature, vegetation, drainage, soil or rock type and total water content, snowcover, and degree and orientation of slope. As a rule, the active layer is thin in the High Arctic (it can be less than 15 cm) and becomes thicker farther south (1 m or more). The thickness of the active layer can vary from year to year, primarily due to variations in the mean annual air temperature, distribution of soil moisture, and snowcover. The thickness of the active layer includes the uppermost part of the permafrost wherever either the salinity or clay content of the permafrost allows it to thaw and refreeze annually, even though the material remains cryotic (T < 0 °C).

Use of the term "depth to permafrost" as a synonym for the thickness of the active layer is misleading, especially in areas where the active layer is separated from the permafrost by a residual thaw layer, that is, by a thawed or noncryotic (T > 0 °C) layer of ground.

REFERENCES: Muller, 1943; Williams, 1965; van Everdingen, 1985

continuous permafrost

Permafrost occurring everywhere beneath the exposed land surface throughout a geographic region with the exception of widely scattered sites, such as newly deposited unconsolidated sediments, where the climate has just begun to impose its influence on the thermal regime of the ground, causing the development of continuous permafrost. For practical purposes, the existence of small taliks within continuous permafrost has to be recognized. The term, therefore, generally refers to areas where more than 90 percent of the ground surface is underlain by permafrost.

REFERENCE: Brown, 1970.

discontinuous permafrost

Permafrost occurring in some areas beneath the exposed land surface throughout a geographic region where other areas are free of permafrost. Discontinuous permafrost occurs between the continuous permafrost zone and the southern latitudinal limit of permafrost in lowlands. Depending on the scale of mapping, several subzones can often be distinguished, based on the percentage (or fraction) of the land surface underlain by permafrost, as shown in the following table.

Permafrost	English usage	Russian Usage				
Extensive	65-90%	Massive Island				
Intermediate	35-65%	Island				
Sporadic	10-35%	Sporadic				
Isolated Patches	0-10%	_				

SYNONYMS: (not recommended) insular permafrost; island permafrost; scattered permafrost.

D.4.1 Product Validation and Inter-	CCI+ PHASE II – NEW ECVS	Issue 5.1
Comparison Report (PVIR)	Permafrost	30 October 2025

REFERENCES: Brown, 1970; Kudryavtsev, 1978; Heginbottom, 1984; Heginbottom and Radburn, 1992; Brown et al., 1997.

mean annual ground temperature (MAGT)

Mean annual temperature of the ground at a particular depth. The mean annual temperature of the ground usually increases with depth below the surface. In some northern areas, however, it is not uncommon to find that the mean annual ground temperature decreases in the upper 50 to 100 metres below the ground surface as a result of past changes in surface and climate conditions. Below that depth, it will increase as a result of the geothermal heat flux from the interior of the earth. The mean annual ground temperature at the depth of zero annual amplitude is often used to assess the thermal regime of the ground at various locations.

permafrost

Ground (soil or rock and included ice and organic material) that remains at or below 0 °C for at least two consecutive years. Permafrost is synonymous with perennially cryotic ground: it is defined on the basis of temperature. It is not necessarily frozen, because the freezing point of the included water may be depressed several degrees below 0°C; moisture in the form of water or ice may or may not be present. In other words, whereas all perennially frozen ground is permafrost, not all permafrost is perennially frozen. Permafrost should not be regarded as permanent, because natural or man-made changes in the climate or terrain may cause the temperature of the ground to rise above 0 °C. Permafrost includes perennial ground ice, but not glacier ice or icings, or bodies of surface water with temperatures perennially below 0 °C; it does include man-made perennially frozen ground around or below chilled pipe-lines, hockey arenas, etc.

Russian usage requires the continuous existence of temperatures below $0\,^{\circ}\text{C}$ for at least three years, and also the presence of at least some ice.

SYNONYMS: perennially frozen ground, perennially cryotic ground and (not recommended) biennially frozen ground, climafrost, cryic layer, permanently frozen ground.

REFERENCES: Muller, 1943; van Everdingen, 1976; Kudryavtsev, 1978.

2 METHODS FOR QUALITY ASSESSMENT

This chapter provides an overview of methods used to evaluate the performance of the Permafrost_cci products analysed and discussed in the following order: Permafrost_cci Ground Temperature per Depth (GTD), Active Layer Thickness (ALT) and Permafrost FRaction (PFR).

2.1. Overview on the Quality Assessment Methods

2.1.1 Unbiased Validation

The CCI project team shall ensure independence for the validation, implying that the assessment of the Permafrost cci products is established with independent datasets and suitable statistical approaches [AD-3,4,5]: this implies that the validation needs to be carried out by team members not involved in the final algorithm selection [AD-3,4]. The validation in Permafrost cci is fully independent as the validation team is independent of the algorithm development team and uses fully independent validation datasets from the global GCOS Global Terrestrial Network for Permafrost (GTN-P) program and additional national measurement networks such as PERMOS in Switzerland and national monitoring programs in Russia, Canada and United States, as well as datasets from individual PIs [RD-10]. WMO/GCOS GTN-P managed by the International Permafrost Association (IPA) provides in situ measurements for the Permafrost ECVs from the Thermal State of Monitoring (TSP) and the Circumpolar Active Layer Monitoring program (CALM), including community standards for measurements and data collection (Brown et al., 2000, Clow, 2014, Biskaborn et al. 2015) [RD-10]. Specifically initiated by the International Polar Year (IPY 2007/2008), GTN-P established a temperature reference baseline for permafrost. Using this extended monitoring, the permafrost community could demonstrate that during the IPY reference decade (2007 to 2016/2017) permafrost temperature at depths of the Zero Annual Amplitude (ZAA) increased globally by around 0.3 °C (Biskaborn et al., 2019, GTN-P, 2018, 2021).

In addition to the community ground temperature data collection at depths of ZAA (GTN-P, 2018, 2021), there is an obvious need for a standardised ground temperature benchmark dataset across all different depths, specifically also standardising data for shallow depths, as has been stressed by user communities of climate and biosciences, as it does not yet exist [AD-1,2,5, RD-11,12]. Profoundly, land surface and climate models lack standardised data on ground temperature in shallow depths for a scientific evaluation of simulated ground thermal conditions and permafrost states. Land surface and climate models are parameterized down to depths of 3 m or 5 m depths only, not reaching the deeper ZAA depths in continuous permafrost at 10 to 20 m depths.

To validate the Permafrost_cci products, the team in Permafrost_cci responsible for validation has been thus compiling, checking and standardising all available communities' ground temperature (GT) and ALT data [RD-1,6,7,8,10,11]. The majority of the in situ data collection is contributed from GTN-P/IPA and its individual Principal Investigators (PIs) and for the Eurasian Permafrost region from the Russian meteorological monitoring network ROSHYDROMET (RHM) program, in addition with contributions from GTN-P PIs, datasets from the Canadian Data Repository Nordicana-D for Canada, and NASA Arctic-Boreal Vulnerability Experiment ABoVE datasets and United States Geological Survey (USGS) for Alaska (United States) were additionally collected. GTN-P and RHM time series and the data collections from additional networks and PIs provide a large data collection of in situ measured reference datasets [RD-1,6,7,8,10].

D.4.1 Product Validation and Inter-	CCI+ PHASE II – NEW ECVS	Issue 5.1
Comparison Report (PVIR)	Permafrost	30 October 2025

All these data are not easy-to-use or readily available in situ reference data that are data-fit for validation and round robin exercises. For example, the ground temperature data collection includes variable timeframes from hourly over annually to sporadic measurements, in different depths and not consistent over time. In addition, the in situ datasets, despite being produced according to community standards and published, contain a large number of caveats, including erroneous or imprecise coordinate locations and non-corrected measurement errors, depending on region, measurement program and PI. Within Permafrost_cci, these pre-existing community-based in situ data collections have been error-checked, homogenised, filtered and standardised. The newly compiled, harmonised Permafrost_cci in situ mean annual ground temperature (MAGT) data collections provides the first consistent reference dataset covering a wide range of common measurement depths for the circum-Arctic: it covers all permafrost zones from continuous to discontinuous, sporadic and isolated of the Northern hemisphere with all available measurement depths down to 10 m [RD-10].

The validation and evaluation efforts also consider high-mountain permafrost regions, using in situ observations of surface and ground temperatures provided by GTN-P PERMOS in Switzerland. In addition, the EO-derived inventories on rock glacier occurrence, which was developed by the ESA Data User Element (DUE) GlobPermafrost team since 2016 and which is continued in Permafrost_cci phase I and II, are innovatively used for assessments of the Permafrost_cci products. The PERMOS monitoring data and the rock glacier inventories compiled in 18 regions around the globe in the framework of Permafrost_cci [RD-5] supports the validation in mountain areas, where the Permafrost_cci products contain the highest uncertainties [RD-1,6,7,8].

The IPA Permafrost mapping action group contributed in its active IPA Action Group phase as an important collaborator for validation in Permafrost_cci phase I [RD-12]. Dr. Isabelle Gärtner-Roer, University of Zurich, CH, former vice president of IPA and former leader of the IPA Permafrost mapping action group, and Science Officer of the World Glacier Monitoring Service (WGMS), was stating that a very profound validation is being performed in Permafrost_cci by using the in situ data from GTN-P and from PERMOS [RD-12]. IPA agrees on the fact that in situ data are clustered in regions with active permafrost monitoring programs/projects, and that therefore some regions are underrepresented. For the validation in Permafrost_cci, IPA further provides the recommendation that the validation of the Permafrost_cci ground temperature product is the most important as it builds the base for the other products, such as active layer thickness and permafrost extent [RD-12].

Permafrost_cci entirely acknowledges the efforts of the international permafrost community in this impressive realisation of circumpolar measurements, and all national initiatives from US, Canada, Switzerland, Russia and Norway and from individual PI's for making the measurement data publicly available. The Permafrost_cci match-up dataset and its characteristics as well as data sources and availability, as also the PERMOS mountain permafrost products are described in detail in [RD-10] and [RD-5], respectively. The previous product quality assessments are described in [RD-1,6,7,8].

D.4.1 Product Validation and Inter-	CCI+ PHASE II – NEW ECVS	Issue 5.1
Comparison Report (PVIR)	Permafrost	30 October 2025

2.1.2 Validation Process

The required Permafrost ECVs by WMO/GCOS for Permafrost are [AD-3,5,6] i) **permafrost temperature** and ii) **active layer thickness**. Permafrost_cci added iii) **permafrost extent** (permafrost fraction) as a gridded permafrost variable, which is the fraction within an area (pixel) at which the definition for the existence of permafrost (ground temperature < 0 °C for two consecutive years) is fulfilled. The main focus of Permafrost_cci lies on the ECV permafrost temperature as its derivation also forms the base for the derivation of active layer thickness and permafrost fraction [RD-12].

The Permafrost cci products are evaluated using pixel-based match-up analyses between Permafrost cci GTD, ALT and PFR and the compiled in situ reference data at individual locations, relying on statistical metrics for its common usage. On one hand, the Permafrost cci in situ reference data collections of ground temperature are characterised by spatial and temporal biases related to regions, time covered and measurement depths due to the high variety in national measurement programs, PIs and funding sources. We are also facing a spatial-scale mismatch between in situ measurements, i.e., individual borehole locations or the 100×100 m² (0.01 km²) CALM grid ALT measurements versus the ~1 km² Permafrost cci grid cells. Already with the native MODIS LST product-derived sinusoidal geometry, that is the base for the native CryoGrid simulation grid cells, each location of an in situ measurement is moved already away from its original location to the center of the CryoGrid cell. In addition, the WGS84 geographic reprojection that is finally applied to the Permafrost cci products requires interpolated CryoGrid grid cell infilling, further smoothing out landscape heterogeneity. In addition, the comparison of in situ measurements in shallow ground depths to CryoGrid prescribed ground depths further compromises the precision, as permafrost landscapes contain heterogeneous micro-topography, leading to an inconsistent depth extrapolation for shallow depths. Despite these challenges, the Permafrost cci match-up analyses do provide the most reliable estimation of the accuracy and usability of the Permafrost cci products.

For a cross-product assessment we applied the Freeze-Thaw to Temperature (FT2T) product, a spaceborne radar-derived ground temperature product, for comparison with Permafrost_cci GTD.

For the mountain permafrost use case, GTN-P PERMOS in Switzerland assesses the Permafrost_cci GTD and PFR products, using expert knowledge, in situ surface temperature, borehole ground temperature and the EO-derived inventories on rock glacier occurrence, which has been developed by the ESA Data User Element (DUE) GlobPermafrost team since 2016 and which is continued in Permafrost cci phase I and worldwide in 18 mountain regions in phase II [RD-5].

2.1.3 Statistical Assessments

The pixel-based pairwise Permafrost cci match-up data collection consists of

- Permafrost_cci GTD matched with in situ mean annual ground temperature (MAGT) in discrete and interpolated depths (0, 0.1, 0.2, 0.25, 0.4, 0.5, 0.6, 0.75, 0.8, 1.0, 1.2, 1.5, 1.6, 2.0, 2.4, 2.5, 3.0, 3.2, 4.0, 5.0, 10.0 m), in annual resolution from 1997 to 2023
- Permafrost cci ALT matched with in situ ALT, in annual resolution from 1997 to 2023
- Permafrost_cci PFR matched with a combination of in situ MAGT (integrated over 3 m depth) and in situ ALT, in annual resolution from 1997 to 2023

D.4.1 Product Validation and Inter-	CCI+ PHASE II – NEW ECVS	Issue 5.1
Comparison Report (PVIR)	Permafrost	30 October 2025

We use common statistical approaches: the characterization of errors and uncertainties is carried out using evaluation measures of bias, median absolute deviation and root mean square error.

In addition, we assess the temporal stability of the Permafrost_cci product time series using two approaches: a g-score approach and a bias stability approach.

The bias is the mean deviation of the product to the in situ data and calculated by

$$bias = \frac{\sum_{i=1}^{n} (Permafrost_{cci} - in \ situ)}{n}$$

Given that large deviations in positive and negative direction can result in a bias ~0, we additionally use the absolute bias (abs_bias), calculated by

$$abs_bias = \frac{\sum_{i=1}^{n} |(Permafrost_{cci} - in \, situ)|}{n}$$

The root mean square error (RMSE) is calculated by

RMSE =
$$\sqrt{\frac{\sum_{i=1}^{n} (Permafrost_{cci} - in \, situ)^{2}}{n}}$$

The median absolute deviation (MAD) is calculated by

$$MAD = median(|x_i-median|)$$

'Gleichläufigkeit' (g-score) approach

First, we check how many cases of Permafrost_cci GTD and ALT respectively, follow the same year-to-year trend like the in situ reference measurements. This means, if within both, the Permafrost_cci product time series and the in situ measurement time series, the slope value decreases/increases simultaneously in the same direction (positive or negative) per year, the value of 1 is assigned. If the two slopes develop in different directions, the value 0 is assigned, and if one slope changes direction while the other slope is constant, the value of 0.5 is assigned. The mean value of these year-to-year trend-values then gives the fraction of synchronised curve development. This approach, in dendrochronology called 'Gleichläufigkeit' or g-score, gives an impression on how well the Permafrost_cci variable follows the actual temperature and ALT trend, respectively. This method does not provide any information on the bias.

Bias Stability approach

Additionally, we check for the magnitude of the interannual variability of the bias. We assume that physically based, the bias should not largely change in magnitude from one year to the next. We thus calculate temporal stability by

$$ts = \frac{bias_j - bias_i}{year_j - year_i}$$

with i being the current year/bias and j being the previous year/bias. The difference is calculated on a year-to-year basis and rejected, for every missing year at a specific site/depth.

2.2 Assessment of Permafrost Temperature

2.2.1 Ground Temperature Reference Data

The major data provider for ground temperature time series is the WMO/GCOS Global Terrestrial Network for Permafrost, GTN-P (https://gtnp.arcticportal.org/), the global permafrost monitoring program of the International Permafrost Association, IPA. Compiled GTN-P and USGS ground temperature data collections are published openly with a shared licence across several repositories. Specifically, data compilations are published in the Arctic Data Center (US), e.g.: https://arcticdata.io/catalog/#view/doi:10.18739/A2KG55 (Wang et al. 2018). Several more important GTN-P collections and data from individual members of the Permafrost research community are published in the PANGAEA data repository for environmental research (DE) (Boike et. al. 2018a, https://doi.org/10.1594/PANGAEA.891140, Boike et. al. 2019, https://doi.pangaea.de/10.1594/ PANGAEA.905233, Boike et al. 2018b, GTN-P 2018, https://doi.pangaea.de/10.1594/ PANGAEA.884711, Bergstedt & Bartsch 2020a, https://doi.pangaea.de/ 10.1594/PANGAEA.912482). In addition, we received ground data from individual members of the Permafrost research community (PI A. Lewkowicz, GTN-P, University of Ottawa, CA; PIs V. Romanovski and A. Kholodov, GTN-P, University of Alaska Fairbanks, US; PI M. Ulrich, University of Leipzig, DE) connected to GTN-P but this data were not yet published within the GTN-P database. Therefore, we undertook MAGT data standardisation and processing together with the PI's and published following data publications in the PANGAEA data repository as an activity within Permafrost cci (Lewkowicz et al. 2025, https://doi.pangaea.de/10.1594/PANGAEA.971276; Kholodov al. 2025, https://doi.org/10.1594/PANGAEA.972733). The joint Permafrost cci MAGT GTN-P data collection is published Wieczorek et al. (dataset in review) https://doi.pangaea.de/10.1594/PANGAEA.972992. Further relevant data providers are the WMO **RHM** hydrometeorological Roshydromet national monitoring program Russia (http://meteo.ru/data/164-soil-temperature), Nordicana-D, the Canadian data repository for Polar research (https://nordicana.cen.ulaval.ca/index.aspx), for example with the data publications from Allard et al., 2020, CEN 2020a,b,c,d,e,f,g, Fortier et al. 2021) and the NASA Arctic-Boreal Vulnerability Experiment ABoVE https://above.nasa.gov/field_data_products.html. In addition, new datasets for Canada and Svalbard could be included in the current validation round. These originate from 2024, repository (Allard et al., https://doi.org/10.5885/45291SL-Nordicana D 34F28A9491014AFD) and further data from individual members of the Permafrost research published in the community, **PANGAEA** data repository (Boike 2022, https://doi.org/10.1594/PANGAEA.947032; Boike al. 2023, https://doi.org/10.1594/ et PANGAEA.962726, Grünberg et al. 2025, https://doi.org/10.1594/PANGAEA.969343, Miesner et al. 2023, https://doi.org/10.1594/PANGAEA.961867). These new datasets contribute around 600 match-up points in depths between 0 and 10 m between 1998 and 2023. The majority of these are in the range of cold temperature sites (MAGT < 1 °C).

Our match-up data collection optimized for the assessments of Permafrost_cci products, in the following called Permafrost_cci-Val MAGT, covers the Northern hemisphere (Fig. 2.2). There are also a few GTN-P borehole sites (n = 5, 112 match-up pairs) in inland ice-free permafrost regions in Antarctica that are used in a separate regional assessment, as Permafrost_cci *CRDPv4* GTD time series are also covering Antarctica. [RD-10] describes the data sources, measurement programs and the data compilation steps in detail.

For the build up of the Permafrost_cci-Val MAGT time series for the Northern hemisphere, we needed to standardise highly diverse GT per depth data, as they all vary in measurement depths and temporal measurement frequencies with also requirements to undertake coordinate corrections, outlier and error elimination. We processed shallow versus deep going GT depth profiles with two different processing steps: for shallow GT depth profiles that we define according to the data assessments and exchange with PIs down to 5 m depth, all discrete values were calculated as these depth profiles represent either sensor depth profiles installed directly in the subground or as narrow-diameter boreholes with sensors deployed. For GT depth profiles of 5 m depth and deeper, we discard all data < 2 m depth of boreholes with large diameters, as there is frequently artificial material in-filling or air. If the diameter is unknown, data < 2 m were only kept if confirmed reliable by the PI.

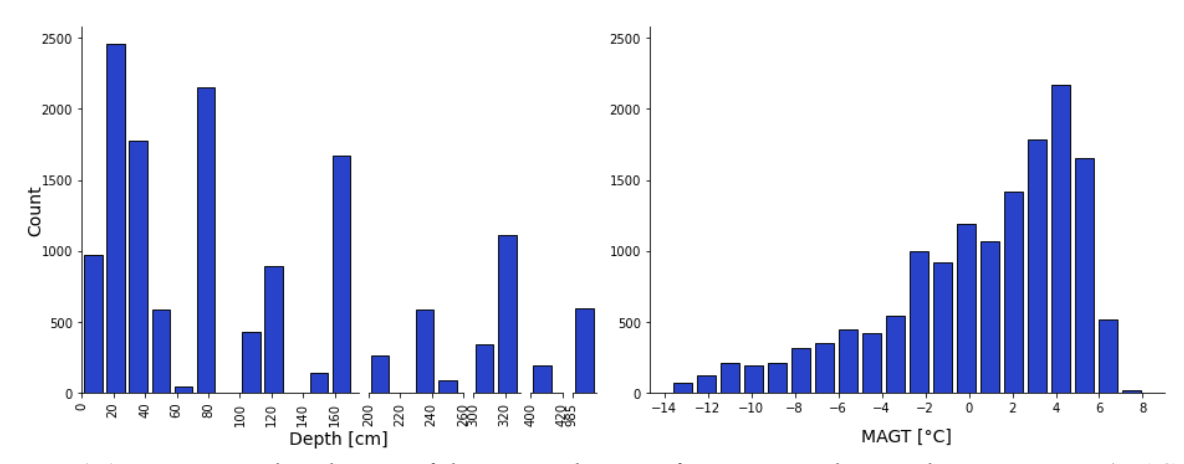


Figure 2.1. Frequency distribution of the in situ dataset of mean annual ground temperatures (MAGT) of the Northern hemisphere, Permafrost_cci-Val MAGT, used for the match-up analyses for the selected years covering CRDPv4 1997 to 2023 (left) at discrete depths and (right) across the temperature range.

Permafrost_cci-Val MAGT, the Permafrost_cci reference data consists of standardised mean annual Ground Temperature per Depth GTD from 1997 to 2023 (Figure 2.1), with product depths at 0, 0.1, 0.2, 0.25, 0.4, 0.5, 0.6, 0.75, 0.8, 1.0, 1.2, 1.5, 1.6, 2.0, 2.4, 2.5, 3.0, 3.2, 4.0, 5.0, 10.0 m. Figure 2.1 visualises the Permafrost_cci-Val MAGT data characteristics across the measurement depths and the temperature range.

Permafrost_cci-Val MAGT also holds metadata information, which allows assessing the quality of each temperature value (Table 2.1). These metadata comprise for yearly values the ratio of missing data per month/year (missing days per year/365) and the amount of completely missing months. Yearly means are not calculated if > 20 % of yearly values are not available or if more than one complete month is missing. An exception is made for data at the depth of Zero Annual Amplitude (ZAA) that represents a valid annual value as there is zero seasonal variation in GT at this depth.

The final Permafrost_cci match-up data collection v5 for the time frame of 1997 to 2023 covering the Permafrost_cci Northern hemisphere domain contains data from n=479 in situ measurement locations (Figure 2.2) (GTN-P/USGS n=313, RHM n=130, Nordicana-D n=30, NASA ABoVE n=6), with overall n=14,585 match-up pairs in time and depth. The temperature subset of the Permafrost_cci match-up data collection v5 <1 °C contains data from n=265 in situ measurement locations (GTN-P, USGS n=226, RHM n=19, Nordicana-D n=12, NASA ABoVE n=4) with overall n=4,898 match-up pairs in time and depth.

Table 2.1. Example of how the compiled dataset provides metadata information of yearly values across depths. Mxx = ratio of missing values per month/year at depth xx m. mMxx = number of missing months per year at depth xx m.

Site	Year	Type	M0	M0.2	M0.25	M0.4	M0.5	M0.75	M0.8	M1	mM0	mM0.2 r	mM0.2 n	nM0.4 ml	M0.5 mN	/10.7 m	M0.8	mM1	0	0.2	0.25	0.4	0.5	0.75	0.8	1
FB_dry_l	2006	Mean	1	1	1	1	1	1	1	1	12	12	12	12	12	12	12	12	NA							
FB_dry_l	2006	Max	1	1	1	1	1	1	1	1	12	12	12	12	12	12	12	12	NA							
FB_dry_l	2006	Min	1	1	1	1	1	1	1	1	12	12	12	12	12	12	12	12	NA							
FB_wet_	2006	Mean	0.414	0.414	0.414	0.416	0.414	NA	NA	NA	5	5	5	5	0 NA	N/	4	NA	1.33	1.64	1.56	1.35	1.12	NA	NA	NA
FB_wet_	2006	Max	0.414	0.414	0.414	0.416	0.414	NA	NA	NA	5	5	5	5	0 NA	N/	4	NA	18.9	12.7	12	10.4	8.07	NA	NA	NA
FB_wet_	2006	Min	0.414	0.414	0.414	0.416	0.414	NA	NA	NA	5	5	5	5	0 NA	N/	4	NA	-19.1	-12	-11.5	-10.2	-8.95	NA	NA	NA
FB_dry_l	2007	Mean	0.581	0.581	0.581	0.581	0.581	1	0.586	0.699	7	7	7	7	7	12	7	8	-3.58	-2.65	-2.53	-2.38	-2.44	NA	-2.4	-2.59
FB_dry_l	2007	Max	0.581	0.581	0.581	0.581	0.581	1	0.586	0.699	7	7	7	7	7	12	7	8	13.6	10.4	9.31	8.01	4.87	NA	1.73	0.63
FB_dry_l	2007	Min	0.581	0.581	0.581	0.581	0.581	1	0.586	0.699	7	7	7	7	7	12	7	8	-21.9	-17.5	-16.9	-16	-14.6	NA	-11.9	-8.83
FB_wet_	2007	Mean	0	0	0	0	0	NA	NA	NA	0	0	0	0	0 NA	N/	4	NA	-5.99	-5.41	-5.62	-5.48	-5.63	NA	NA	NA
FB_wet_	2007	Max	0	0	0	0	0	NA	NA	NA	0	0	0	0	0 NA	N/	4	NA	17.8	15.2	11.7	10.6	7.49	NA	NA	NA
FB_wet_	2007	Min	0	0	0	0	0	NA	NA	NA	0	0	0	0	0 NA	N/	4	NA	-30.2	-23.3	-22.7	-21.3	-20.3	NA	NA	NA
FB_dry_l	2008	Mean	0.18	0.18	0.18	0.18	0.18	1	0.183	0.183	3 2	2	2	2	2	12	2	2	-7.37	-6.62	-6.63	-6.63	-6.44	NA	-6.26	-5.82
FB_dry_l	2008	Max	0.18	0.18	0.18	0.18	0.18	1	0.183	0.183	3 2	2	2	2	2	12	2	2	18.7	13.2	11.8	9.48	8.1	NA	3.79	1.35
FB_dry_l	2008	Min	0.18	0.18	0.18	0.18	0.18	1	0.183	0.183	3 2	2	2	2	2	12	2	2	-28.7	-23.9	-23.2	-22.4	-20.7	NA	-18.2	-15.1
FB_wet_	2008	Mean	0.372	0.372	0.372	0.426	0.372	NA	NA	NA	4	4	5	4	0 NA	N/	4	NA	-6.62	-7.34	-7.43	-9.01	-7.73	NA	NA	NA
FB_wet_	2008	Max	0.372	0.372	0.372	0.426	0.372	NA	NA	NA	4	4	5	4	0 NA	N/	4	NA	18.2	12.4	11.8	9.71	9.12	NA	NA	NA
FB_wet_	2008	Min	0.372	0.372	0.372	0.426	0.372	NA	NA	NA	4	4	5	4	0 NA	N/	4	NA	-24.9	-22	-21.7	-20.7	-20.2	NA	NA	NA
FB_dry_l	2009	Mean	0.586	0.003	0	0.586	0	0.414	0.586	0.586	7	0	0	7	0	5	7	7	-13.2	-3.73	-3.9	-11.5	-3.92	0.11	-9.42	-7.8
FB_dry_l	2009	Max	0.586	0.003	0	0.586	0	0.414	0.586	0.586	7	0	0	7	0	5	7	7	-1.34	13.5	11.5	-3.74	7.1	3.58	-2	-1.09
FB_dry_l	2009	Min	0.586	0.003	0	0.586	0	0.414	0.586	0.586	7	0	0	7	0	5	7	7	-19.9	-18	-17.7	-17.3	-16.2	-5.97	-14.3	-11.9
FB wet	2009	Mean	0.414	0.416	0.416	1	0.414	NA	NA	NA	5	5	12	5	0 NA	N/	4	NA	1.95	1.65	1.65	NA	1.46	NA	NA	NA

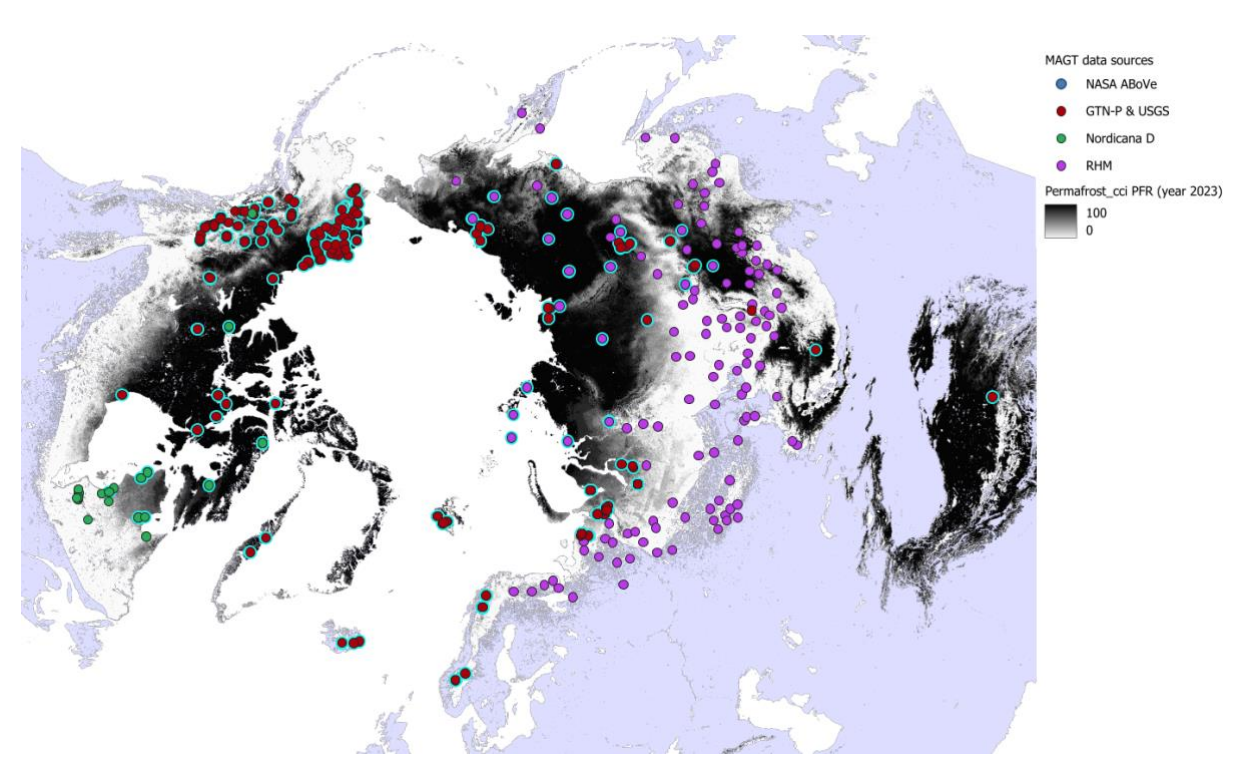


Figure 2.2. In situ sites and data sources of in situ MAGT (color-coded point symbols) over mapped $Permafrost_cci\ PFR\ 2023$ in the Northern hemisphere. Circle symbols with thick blue outlines represent sites with MAGT < 1 °C.

Versions of Ground Temperature Reference and Match-up Data Sets

GTD match-up dataset v1 (2003 to 2017) Exclusion of non-permafrost temperature value range (Validation in phase I, CRDPv0 2019)

For straightforward match-up analyses in the first validation round, we focused on the permafrost temperature range excluding all stations with in situ measurements of MAGT ≥ 1 °C at least once (independent of measurement depth) from the match-up analyses. We conducted the validation for the Northern hemisphere. This GTD match-up dataset in 0, 0.2, 0.25, 0.4, 0.5, 0.6, 0.75, 0.8, 1.0, 1.2, 1.6, 2.0, 2.4, 2.5, 3.0, 3.2, 4.0, 5.0, 10.0 m depth, with all 'non-permafrost temperature' station types excluded, contained n = 3,185 pairs in time and depth [RD-6].

GTD match-up dataset v2 (1997 to 2018) Inclusion of non-permafrost temperature value range, exclusion of sites in Yedoma regions in Siberia (Validation in phase I, CRDPv1 2020)

We conducted the validation of CRDPv1 GTD with in situ MAGT ≥ 1 °C included (depths down to 10 m). This GTD match-up dataset in 0, 0.2, 0.25, 0.4, 0.5, 0.6, 0.75, 0.8, 1.0, 1.2, 1.6, 2.0, 2.4, 2.5, 3.0, 3.2, 4.0, 5.0, 10.0 m depth contained n = 13,695 match-up pairs from n = 300 sites. [RD-7]. As especially the Russian RHM sites have no measurements at 1 or 2 m depth, we interpolated GT values fitting the Permafrost cci product depths. To achieve this, we only used sites with at least three sensors in the shallow depth range down to 1.20 m for interpolating these temperatures. At deeper depths, we allowed for more spacing between sensors due to less GT variability between depths. Interpolation was conducted by linear regression between two single GT measurement depths, resulting in separate equations for each sensor-pair and year. We conducted the validation for the Northern hemisphere. Please note that we excluded all sites that are not representative of the landscape-scale of in situ measurements from all three match-up data collections: these are selected mountain sites that are specifically assessed by PERMOS, small-scale landscape anomalies such as very local peatland patches or in situ measurements in pingos (ice hills, n = 3). Please also note that we excluded all sites within the Siberian Yedoma area (shape file from Bryant et al., 2017) due to incorrect parameterisation of Yedoma stratigraphy (n = 7) in CRDPv1 GTD [RD-7]. Swiss mountain permafrost sites were evaluated by PERMOS [RD-7].

GTD match-up dataset v3 (1997 to 2019) (Validation in phase I, CRDPv2 2021)

We conducted the validation of *CRDPv2 GTD* constructing an in situ MAGT data collection with interpolated depths down to 10 m. This GTD match-up dataset in 0, 0.2, 0.25, 0.4, 0.5, 0.6, 0.75, 0.8, 1.0, 1.2, 1.6, 2.0, 2.4, 2.5, 3.0, 3.2, 4.0, 5.0, 10.0 m depth included n = 14,107 match-up pairs in time and depth from n = 354 sites [RD-8]. We conducted the validation for the Northern hemisphere. The PERMOS mountain permafrost sites and landscape anomalies excluded in the previous validations were also excluded. However, all sites within the Siberian Yedoma area were included as *CRDPv2 GTD* contains no artefacts in the Yedoma regions [RD-8]. Swiss mountain permafrost sites were evaluated by PERMOS [RD-8].

GTD match-up dataset v4 (1997 to 2021) (Validation in phase II, CRDPv3 2023)

We conducted the validation of *CRDPv3 GTD* constructing an in situ MAGT data collection with interpolated depths down to 10 m. This GTD match-up dataset in 0, 0.1, 0.2, 0.25, 0.4, 0.5, 0.6, 0.75, 0.8, 1.0, 1.2, 1.5, 1.6, 2.0, 2.4, 2.5, 3.0, 3.2, 4.0, 5.0, 10.0 m depth included n = 13,614 match-up pairs from n = 477 sites and n = 27,389 match-up pairs for the interpolated dataset.

D.4.1 Product Validation and Inter-	CCI+ PHASE II – NEW ECVS	Issue 5.1
Comparison Report (PVIR)	Permafrost	30 October 2025

In this dataset, several sites lying directly in settlements with their coordinates were in addition excluded from the match-up dataset if the bias was higher than \pm 2.5 °C [RD-1]. We conducted the validation for the Northern hemisphere. The PERMOS mountain permafrost sites and landscape anomalies excluded in the previous validations were also excluded here in the general GT assessment. We kept some mountain sites outside the PERMOS region in the Swiss Alps, if they were not located in high mountain areas, e.g. if they were located below 1500 m [RD-1]. Swiss mountain permafrost sites were evaluated by PERMOS [RD-1].

Permafrost_cci-Val MAGT, GTD match-up dataset v5 (1997 to 2023) (Validation in phase II, CRDPv4 2025)

We conduct the validation of *CRDPv4 GTD* constructing an in situ MAGT data collection with interpolated depths down to 10 m. This GTD match-up dataset in 0, 0.1, 0.2, 0.25, 0.4, 0.5, 0.6, 0.75, 0.8, 1.0, 1.2, 1.5, 1.6, 2.0, 2.4, 2.5, 3.0, 3.2, 4.0, 5.0, 10.0 m depth includes n = 14,585 match-up pairs without interpolation in time and depth from n = 479 sites and n = 28,594 match-up pairs for the interpolated dataset. In Permafrost_cci-Val MAGT, we are even stricter with excluding sites in anomalies, mountain caps and too close to water and in addition, more sites lying directly in settlements are excluded from the match-up dataset, specifically if a bias higher than \pm 2.5 °C indicates local anomaly conditions. We conduct the validation for the Northern hemisphere and inland ice-free parts of Antarctica. For the Northern hemisphere assessment, the PERMOS mountain permafrost sites and landscape anomalies excluded in the previous validations are also excluded here. We keep some mountain sites outside the PERMOS region, if they are not located in high mountain areas, e.g., if they are located below 1500 m. Swiss mountain permafrost sites were evaluated by PERMOS.

2.2.2 Characteristics of GTD Match-up Data Set

The GTD match-up dataset v5 (2025) contains the cleaned and interpolated in situ MAGT at discrete depths matched with CRDPv4 Permafrost cci GTD at 0, 0.1, 0.2, 0.25, 0.4, 0.5, 0.6, 0.75, 0.8, 1.0, 1.2, 1.5, 1.6, 2.0, 2.4, 2.5, 3.0, 3.2, 4.0, 5.0, 10.0 m depth. The Permafrost cci GTD time series are provided at 0, 1, 2, 5, and 10 m depths. For the accuracy assessment, the Permafrost cci product development team produced in addition to the Permafrost cci GTD grid products at 0, 1, 2, 5, 10 m depths also per measurement site the additional depths as GTD time series. Figure 2.3 shows the frequency distribution of the match-up data collection v5 with n = 14,585 match-up points, Figure 2.4 with in situ MAGT ≥ 1 °C excluded, leaving $\frac{1}{3}$ of the match-up data collection with n = 4,898 match-up points in time, space and depth. The bulk match-up data collection peaks differently, between -1 °C and 2 °C for Permafrost cci GTD and between 2 °C and 4 °C for in situ MAGT (Figure 2.3). The data group within the warmer temperature range > 1 °C is mainly constructed with available data from the RHM longterm measurement network. The match-up data characteristics of the cold temperature range < 1 °C (Figure 2.4) show a bimodal distribution with a maximum around -8 °C and another one around -1 °C for Permafrost cci GTD and a maximum around -6 °C and another one from around -3 °C to -1 °C for in situ MAGT. The depth-specific frequency GTD distributions vary as the measurements cover different latitudes and regions depending on the measurement programs. RHM with main contributions to depths of 0.8, 1.2, 2.4 m covers fewer measurement sites at high latitudes than GTN-P and Nordicana-D that more frequently cover the depths of 0.75, 1 and 2 m (Figure 2.5).

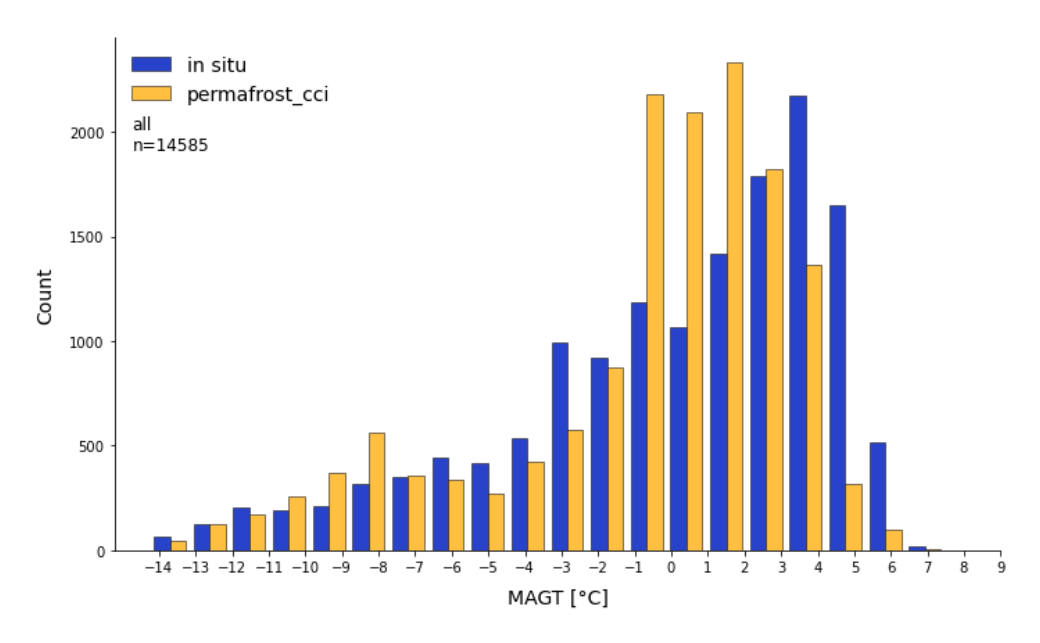


Figure 2.3. Frequency distribution across all non-interpolated sensor depths of the match-up data collection v5 at all discrete depths down to 10 m with steps of 1 °C, n = 14,583.

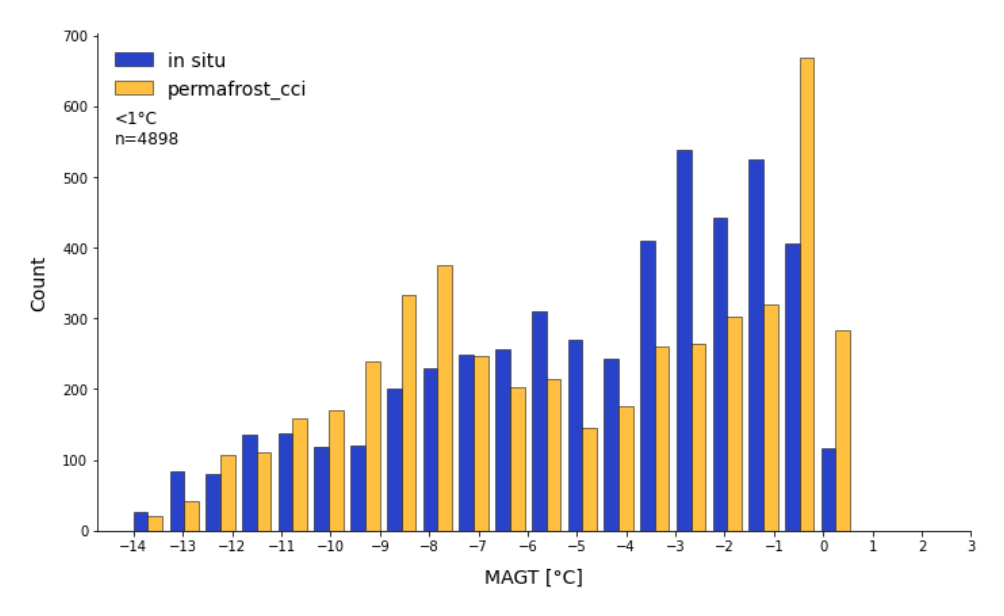


Figure 2.4. Frequency distribution across all non-interpolated sensor depths of the match-up data collection v5 at all discrete depths down to 10 m with steps of 1 °C, with sites $MAGT \ge 1$ °C being excluded, n = 4,898.

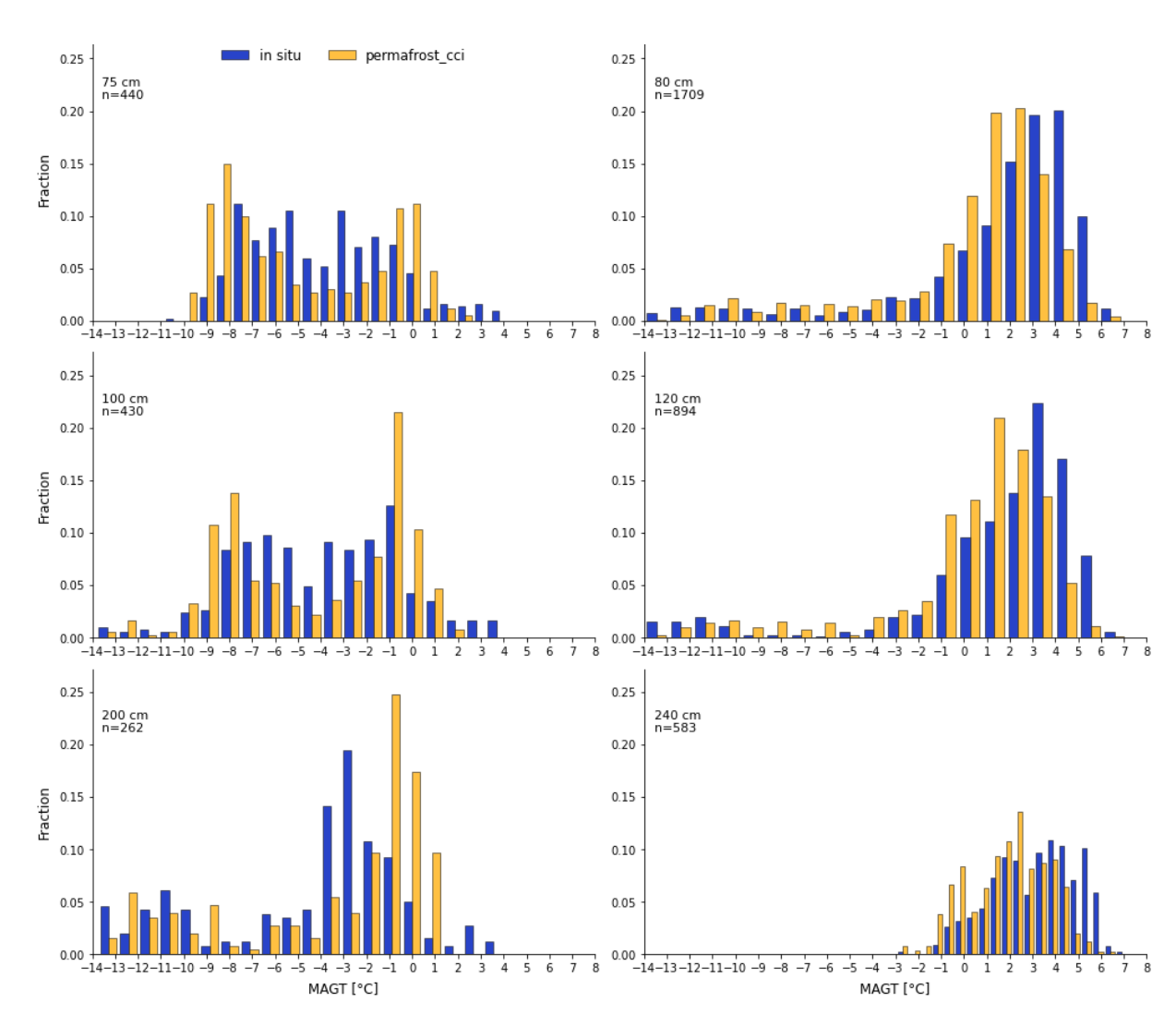


Figure 2.5. Frequency distribution across all non-interpolated sensor depths of the bulk match-up data collection v5 confined to match-up pairs in specific ground temperature sensor depths (75, 80, 100, 120, 200, 240 cm).

2.2.3 PERMOS Reference GST and GTD Data Generation

The PERMOS permafrost monitoring network currently comprises 27 boreholes distributed within 16 sites (Figure 2.8) across Switzerland, which continuously measure permafrost temperatures between 0 and 100 m depth. The sites are located in high mountain regions at elevations between 2400 m a.s.l. and 3400 m a.s.l. with boreholes drilled in bedrock, rock glaciers, talus slopes, steep rock walls or moraines [RD-1,6,7,8,10].

For each single borehole, PERMOS selected the thermistor closest to the depth of the Permafrost_cci GT product (0, 1, 2, 5 and 10 m) and compiled mean annual ground temperature (MAGT) in annual resolution over the period 1997 to 2023. Only data series with at least 80 % data completeness over the year were selected for computing MAGT.

The match-up of the 1 km² grid cells of the Permafrost_cci product with the in situ data functions by selecting the grid cells in which the boreholes are located. The in situ measured MAGT and Permafrost_cci GTD values are compared pairwise for each single borehole and depth. In mountainous terrains, the differences in the subsurface thermal regime due to varying climate conditions (i.e., latitudinal and regional gradients) are considered smaller than those caused by topography or surface and subsurface conditions of the different landforms. Therefore, we analyse Permafrost_cci product performance based on the landform typologies rather than based on climatic regions.

Ground surface temperature (GST) are temperature values measured between 0 and 10 cm depth by miniature loggers placed only with a small distance below the surface to avoid the influence of the direct shortwave radiation and to capture a slightly filtered temperature signal. Within the PERMOS network, GST is measured at 23 different sites across the Swiss Alps, each with four to more than 20 individual loggers adding up to 247 measurement points (see also Figure 2.8). Each logger measures continuously with a temporal resolution of 1 to 3 hours.

Based on this dataset, PERMOS filtered and gap-filled the time series using the approach of Staub et al. (2017). Mean annual ground surface temperature (MAGST) has been computed for each single logger over the period 1997 to 2023. Only series with at least 80 % data completeness over the year are selected for computing the annual mean. Thus, the number of MAGST available is variable from one year to the next. It ranges from 25 MAGST match-up data computed in 1997 to 160 MAGST match-up data in 2012. The MAGST data is highly variable depending on snow conditions, radiation and shading effects as well as surface and subsurface properties. The variability within one specific site (i.e., 4 to 30 loggers) is found to be in the same range as the variability in-between the different sites.

Given the high impact of topography and other (sub-)surface properties on the GST, a direct match-up between the 1 km² grid cell of the Permafrost_cci GTD product and single point locations is inapplicable. Therefore, we computed the average MAGST of all available GST logger within the PERMOS domain of the Swiss Alps and compared it to the average surface temperature at 0 m depth of all Permafrost_cci GT grid cells located between 2500 m a.s.l. and 3000 m a.s.l.

D.4.1 Product Validation and Inter-	CCI+ PHASE II – NEW ECVS	Issue 5.1
Comparison Report (PVIR)	Permafrost	30 October 2025

2.2.4 Satellite derived Freeze/Thaw Surface Status GT Evaluation Dataset Generation

The Freeze-Thaw to Temperature (FT2T) model is an empirical model, based on a linear regression analysis between the annual sum of frozen days, measured with in situ ground temperature measurements, but also possible to derive it from microwave EO sensors (Kroisleitner et al., 2018). It was initially developed for temperature retrieval at the coldest sensor depth spanning the years 2007 to 2013 available from Paulik et al. (2014). The method by Naeimi et al. (2012) which forms the basis for the 2007 to 2013 record of Paulik et al. (2014) has been applied to further records, extending the dataset to 2018. The method and set parameters were evaluated by in situ ground temperature records and C-band SAR data (Sentinel-1; Bergstedt et al. 2020b). A Metop ASCAT global gridded dataset available from EUMETSAT (SOMO12) has been used for this purpose. FT2T has been further developed for Permafrost_cci to represent the depths of the *CRDPv2* and calendar years. With respect to in situ data availability for the model calibration, only 1 m depth could be considered. Further improvements have been made regarding bias correction for lake fraction using Sentinel-1 SAR satellite data (Bergstedt et al., 2020b) applied to lake rich regions. FT2T records have been extracted for selected borehole locations of the match-up dataset for site comparisons and for regions in addition to the circumpolar comparison presented in [RD-1,6,7,8,13].

2.3 Assessment of Active Layer Thickness

2.3.1 Active Layer Thickness Reference Data

Same as for permafrost temperature, the major data provider for in situ ALT time series is the WMO/GCOS Global Terrestrial Network for Permafrost GTN-P, the global permafrost monitoring programme of the International Permafrost Association IPA. The comprehensive, continuously updated GTN-P data collection of ALT time series is available for download under the Circum-Polar Active Layer Monitoring (CALM) Network, https://www2.gwu.edu/~calm/ and http://gtnpdatabase.org. [RD-1,2,6,7,8,10] describe the CALM measurement program and our data compilation steps in detail. For a representative in situ estimation of ALT, it is relevant to measure active layer depths, ALD, at the end of the active-layer thawing season in late summer. This maximum thaw depth measured in late summer represents the ALT of a specific year. Within Permafrost_cci we error-checked and optimized CALM site coordinates and published this in situ ALT reference data collection together with GTN-P/CALM PI D. Streletskyi in the PANGAEA data repository under Streletskiy, et al. CALM, 2025, https://doi.org/10.1594/PANGAEA.972777.

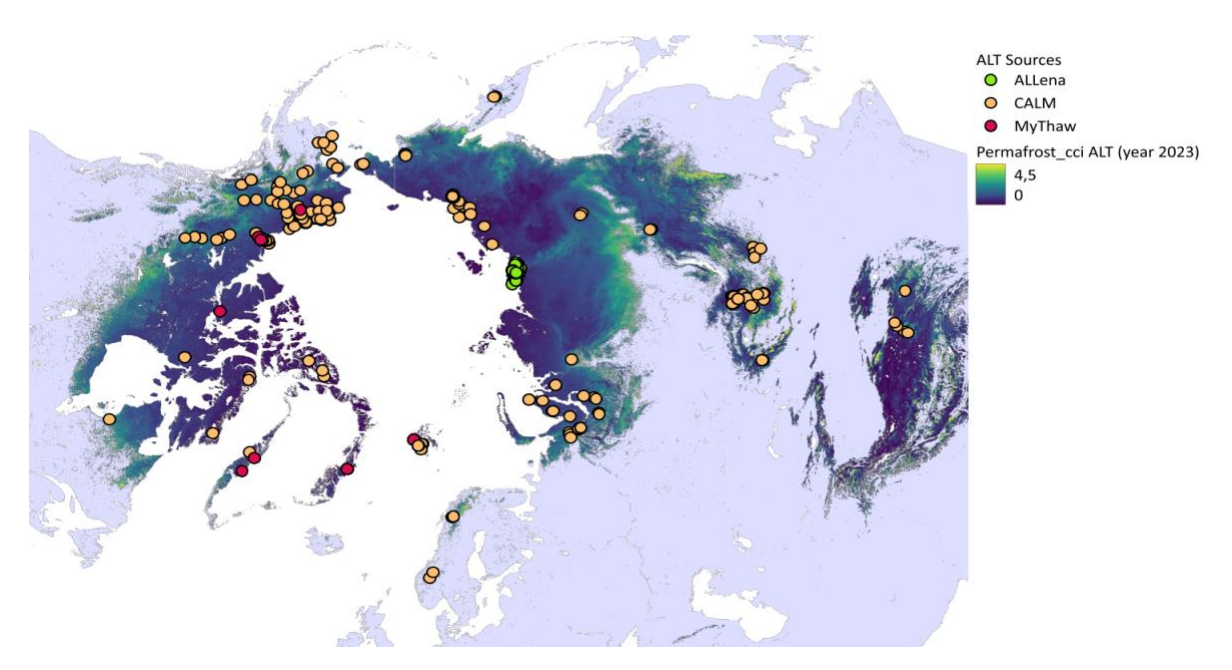


Figure 2.6. In situ sites and data sources of active layer thickness (ALT) (color-coded point symbols) over mapped Permafrost cci ALT 2023 in the Northern hemisphere.

We could extend the in situ ALT reference data collection further by including the 'ALLena' collection representing extensive Russian-German long-term ALT collections in the Lena River Delta in Arctic Siberia (Veremeeva et al., 2025, https://doi.org/10.1594/PANGAEA.974408) and data from the ongoing AWI MyThaw project set up in the framework of the Terrestrial Multidisciplinary distributed Observatories for the Study of the Arctic Connections (T-MOSAiC) IASC initiative (Boike et. al, 2021). MyThaw (Boike et. al, 2021) coordinated standardised ALT measurements in the circum-Arctic and optimised the technique at the CALM grids of the AWI measurement sites.

D.4.1 Product Validation and Inter-	CCI+ PHASE II – NEW ECVS	Issue 5.1
Comparison Report (PVIR)	Permafrost	30 October 2025

The MyThaw in situ ALT data collections are published in the PANGAEA data repository (Martin et al. 2023, https://doi.org/10.1594/PANGAEA.956039; Miesner et al., 2023, https://doi.org/10.1594/PANGAEA.961867). Figure 2.6 shows an overview on the CALM measurement network of the Northern hemisphere including the measurement sites in Mongolia, central Asia and in China on the Tibetan plateau and in the Alps in Europe and the newly assembled sites from the ALLena and MyThaw ALT projects.

Versions of ALT and Match-up Data Sets

ALT match-up dataset v1 (2003 to 2017) (Validation in phase I, CRDPv0 2019)

We conducted the validation of *CRDPv0 ALT* with in situ annual ALT time series from 2003 to 2017 with a circum-Arctic geographic coverage of the Northern hemisphere. The collection contained data from n = 324 sites (China + Mongolia: 67, Greenland + Svalbard + Scandes: 11, Canada: 6, Russia: 57, USA: 207), with 1,835 match-up pairs. However, we excluded for the match-up analyses all sites in China and Mongolia due to too different ground lithographies not covered in the Permafrost_cci CryoGrid parameterisation.

ALT match-up dataset v2 (1997 to 2018) (Validation in phase I, CRDPv1 2020)

We conducted the validation of *CRDPv1 ALT* with in situ annual ALT time series from 1997 to 2018 with a circum-Arctic geographic coverage of the Northern hemisphere. The collection was updated with ALT measurements from the GTN-P CALM program and contained in this version data from fewer sites, n = 156 sites. Please note that in this assessment we were stricter by excluding not only the sites in Mongolia, Central Asia, but also on the Tibetan Plateau (China). Please also note that we needed to exclude as well all sites within the Siberian Yedoma area (Bryant et al., 2017) due to incorrect parameterisation of Permafrost cci CryoGrid of the Yedoma stratigraphy.

ALT match-up dataset v3 (1997 to 2019) (Validation in phase I, CRDPv2 2021)

We conducted the validation of *CRDPv2 ALT* with in situ annual ALT time series from 1997 to 2019 with a circum-Arctic geographic coverage of the Northern hemisphere. The collection was updated with ALT measurements from the GTN-P CALM program, including the Yedoma regions and therefore, contained considerably more data, from n = 314 sites. Please note that we still excluded all sites in Mongolia, Central Asia, and Tibetan Plateau (China).

ALT match-up dataset v4 (1997 to 2021) (Validation in phase II, CRDPv3 2023)

We conducted the validation of *CRDPv2 ALT* with in situ annual ALT time series from 1997 to 2021 with a circum-Arctic geographic coverage of the Northern hemisphere. The collection was updated with ALT measurements from the GTN-P CALM program. Please note that we excluded all sites in Mongolia, Central Asia, and Tibetan Plateau (China). We experimentally included Russian ALD sites (Bartsch, oral communication, 2020), which are also included for PFR analyses. As these however do not provide the maximum thaw depth, the deviations to the model are higher. The overall influence on the validation is yet not high, as these sites comprise only one year of measurements (2018).

ALT match-up dataset v5 (1997 to 2023) (Validation in phase II, CRDPv4 2025)

We conduct the validation of *CRDPv2 ALT* with in situ annual ALT time series from 1997 to 2023 with a circum-Arctic geographic coverage of the Northern hemisphere. The collection is updated with ALT measurements from the GTN-P CALM program and additional programs such as MyThaw from Miesner et a. (2024) and the ALLena collection by Veremeeva et al (2025). We conduct the validation for the Northern hemisphere and for the inland ice-free parts of the permafrost regions in Antarctica. Please note that we still exclude all sites in Switzerland, Mongolia, Central Asia, and Tibetan Plateau (China). for Permafrost_cci ALT assessments in the Northern hemisphere. The in situ reference data collection contains data from n = 536 sites (Greenland + Svalbard + Scandes: 27, Canada: 33, Russia: 409 (345 of which coming from the ALLena dataset), USA: 67) for the Northern hemisphere with 2,940 match-up pairs. For the first time in Permafrost_cci we also conduct ALT assessments in Antarctica using n = 7 sites and n = 106 match-up pairs with in situ ALT reference data coming from the GTN-P CALM programme.

2.3.2 Characteristics of ALT Match-up Data Set

The ALT match-up v5 dataset (2025) contains standardised in situ ALT reference data matched with *CRDPv4* Permafrost_cci ALT. Figure 2.7 shows the frequency distribution of the match-up data. In situ ALT can, by definition, only occur within permafrost regions. Therefore, the characteristics of the ALT Permafrost_cci and ALT in situ data collections represent all data sampled in permafrost zones. The characteristics of Permafrost_cci ALT show an unimodal right-skewed distribution with a maximum around 0.4 m and 0.6 m ALT, and in situ ALT similarly with a maximum around 0.4 m ALT. Both Permafrost_cci ALT and in situ ALT show highest abundance in shallow ALT values.

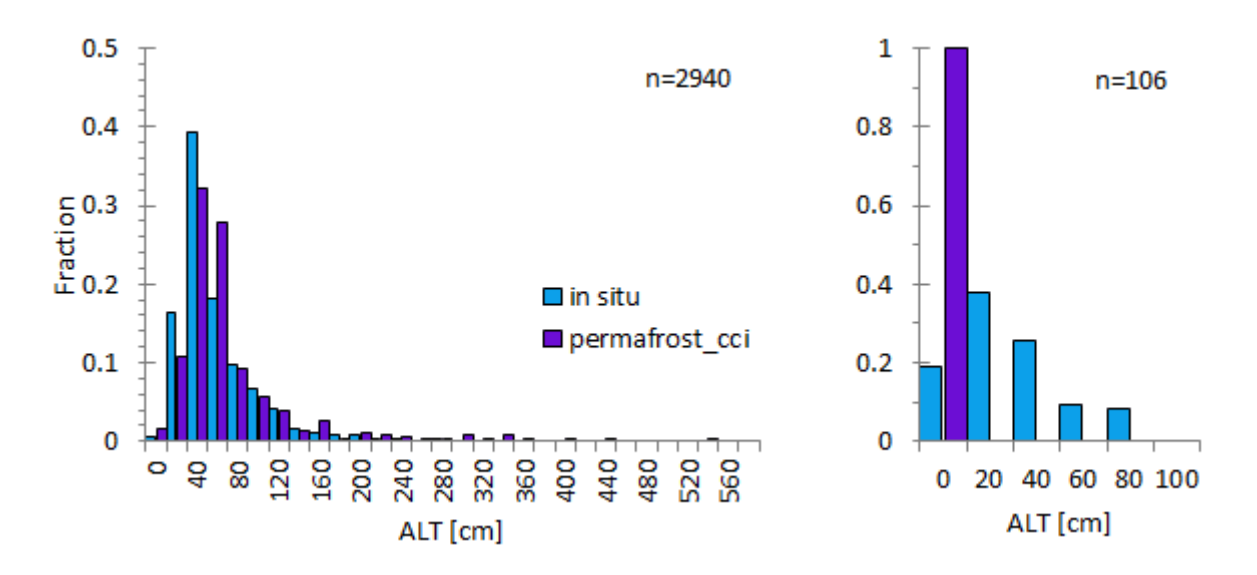


Figure 2.7. Frequency distribution of Permafrost_cci ALT and in situ ALT from 1997 to 2023 (left) in the Northern Hemisphere (sites in China, Mongolia and the Alp Mountains are excluded) with n = 2,940 match-up pairs and (right) sites in inland ice-free permafrost regions in Antarctica with n = 106 match-up pairs.

2.4 Assessment of Permafrost Extent

2.4.1 Permafrost Fraction Reference Data

In Permafrost_cci we approximate permafrost in-situ abundance with the in situ MAGT and ALT reference datasets [RD-1,2,6,7,8]. Since the first validation round v1 of Permafrost_cci $CRDPv0\ PFR$ we apply a binary match-up assessment [RD-6]. We allow a small variability around MAGT 0 °C not setting "permafrost" strictly as in situ MAGT < 0 °C in two consecutive years but define a cold temperature regime representative for permafrost regions with in situ MAGT \leq 0.5 °C. This approach described in detail in [RD-2,6] was successful and we applied it more in depth for the assessments of Permafrost_cci CRDPv1 to $CRDPv4\ PFR$ adding the ALT time series [RD-1,7,8].

Versions of PFR reference and match-up datasets

PFR match-up dataset v1 (2003 to 2017) (Validation in phase I, CRDPv0 2019)

- Northern hemisphere
- Permafrost cci PFR per site and year in 0, 20, 40, 60, 80, 100 % Permafrost
- Binary PFR dataset (permafrost/ no permafrost) compiled from in situ MAGT
- Yes if all MAGT measurements in depths (0-2 m) MAGT $\leq 0.5 \,^{\circ}\text{C}$.
- Criteria permafrost abundance yes / no

PFR match-up dataset v2 (1997 to 2018) (Validation in phase I, CRDPv1 2020)

- Northern hemisphere
- Permafrost cci PFR per site and year in 0, 14, 29, 43, 57, 71, 100 % Permafrost
- Binary PFR dataset (permafrost/ no permafrost) compiled from in situ MAGT and ALT
- ALD from Russian expeditions (Bartsch, oral communication, 2020)
- Yes if any MAGT measurements in depths (0 2.4 m) MAGT $\leq 0.5 \,^{\circ}\text{C}$
- and Yes to all ALD and ALT
- Criteria permafrost abundance yes / no

PFR match-up dataset v3 (1997 to 2019) (Validation in phase I, CRDPv2 2021)

- Northern hemisphere
- Permafrost cci PFR per site and year in 0, 14, 29, 43, 57, 71, 100 % Permafrost
- Binary PFR dataset (permafrost/ no permafrost) compiled from in situ MAGT and ALT
- ALD from Russian expeditions (Bartsch, oral communication, 2020)
- Yes if any MAGT measurements in depths $(0 2.4 \text{ m}) \text{ MAGT} \le 0.5 ^{\circ}\text{C}$
- and Yes to all ALD and ALT
- Criteria permafrost abundance yes / no

PFR match-up dataset v4 (1997 to 2021) (Validation in phase II, CRDPv3 2023)

- Northern hemisphere
- Permafrost cci PFR per site and year in 0, 14, 29, 43, 57, 71, 100 % Permafrost
- Binary PFR dataset compiled from in situ MAGT and ALT
- (case 1: Permafrost=no PFR <=14 %, case 2: Permafrost=no PFR 29 %)
- ALD from Russian expeditions (Bartsch, oral communication, 2020)

D.4.1 Product Validation and Inter-	CCI+ PHASE II – NEW ECVS	Issue 5.1
Comparison Report (PVIR)	Permafrost	30 October 2025

- Yes if any MAGT measurements in depths $(0 3 \text{ m}) \text{ MAGT} \le 0.5 \text{ }^{\circ}\text{C}$
- and Yes to all ALD and ALT
- Criteria permafrost abundance yes / no

PFR match-up dataset v5 (1997 to 2023) (Validation in phase II, CRDPv4 2025)

- Northern hemisphere and inland ice-free parts of Antarctica
- Permafrost cci PFR per site and year in 0, 14, 29, 43, 57, 71, 100 % Permafrost
- Binary PFR dataset (permafrost/ no permafrost) compiled from in situ MAGT and ALT
- (case 1: Permafrost=no PFR <=14 %, case 2: Permafrost=no PFR 29 %)
- ALD from Russian expeditions (Bartsch, oral communication, 2020)
- Yes if any MAGT measurements in depths (0 3 m) MAGT ≤ 0.5 °C and
- Yes to all ALD and ALT
- Criteria permafrost abundance yes / no

2.4.2 PERMOS Reference PFR Data Generation

The best visual expression of mountain permafrost at the land surface in high mountain areas is represented by rock glaciers, which, in contrast to the sub-ground permafrost itself, can be mapped and monitored directly using remotely sensed data. Rock glaciers are debris landforms generated by the former or current creep of frozen ground (permafrost), detectable in the landscape with the following morphologies: front, lateral margins and optionally ridge-and-furrow surface topography (RGIK, 2023). Their abundance can be used as validation for a high permafrost probability extent. The products on rock glacier abundance and extent could be produced within the ESA GlobPermafrost program for the Bas-Valais region in Switzerland (Figure 2.8) and extended within the CCI Permafrost phase I (see Rouyet et al., 2025) and II in 18 regions worldwide (Figure 2.9). These inventories are compared with the Permafrost_cci PFR time series.

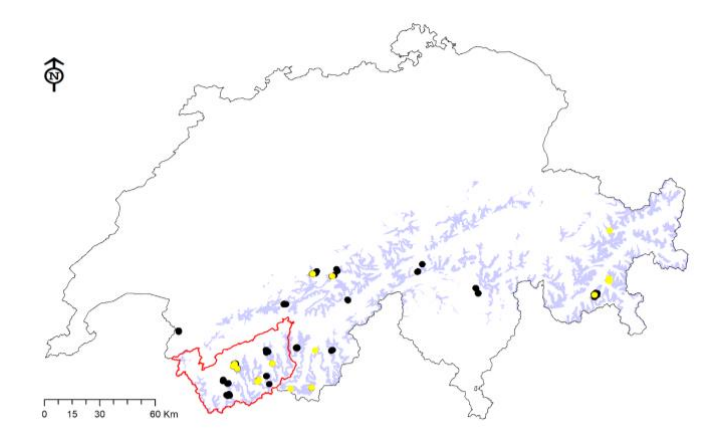


Figure 2.8. Location of the n = 247 GST loggers (black circles), n = 27 GT boreholes (yellow circles) and the extent of the ESA GlobPermafrost rock glacier inventory (red outline) used for the validation of the Permafrost_cci GTD and Permafrost_cci PFR products in the Swiss Alps. The bluish color-coded zones represent the areas located between 2500 m and 3000 m a.s.l.

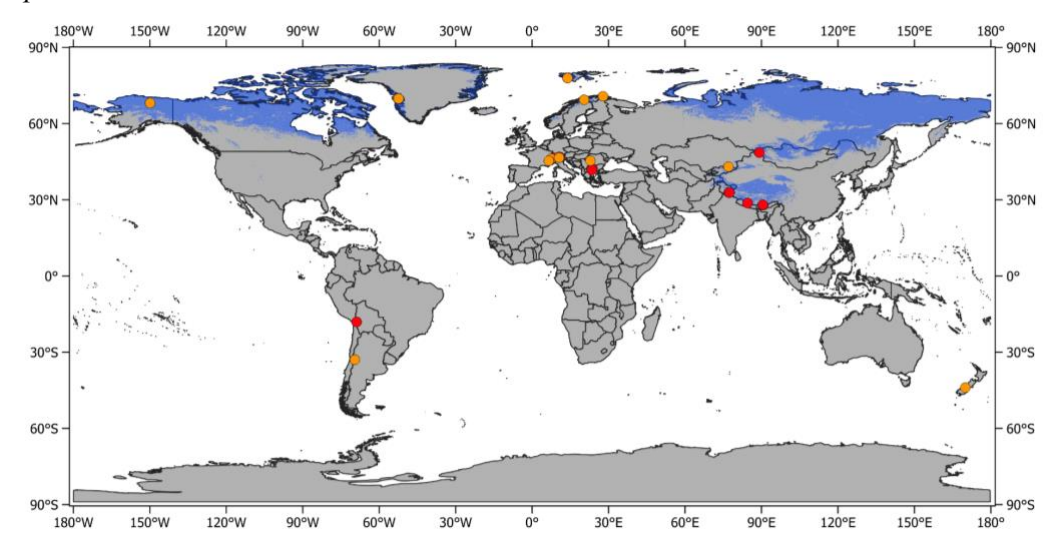


Figure 2.9. Location of the 12 rock glacier inventories compiled within Permafrost_cci phase I (orange dots, see RD-5, Rouyet et al. 2025) and the six inventories compiled within Permafrost_cci phase II (red dots). The blue color-coded areas represent the Permafrost_cci PFR (PFR > 0 %) in 2023.

3 ASSESSMENT RESULTS: PERMAFROST TEMPERATURE

3.1 Permafrost Temperature User Requirements

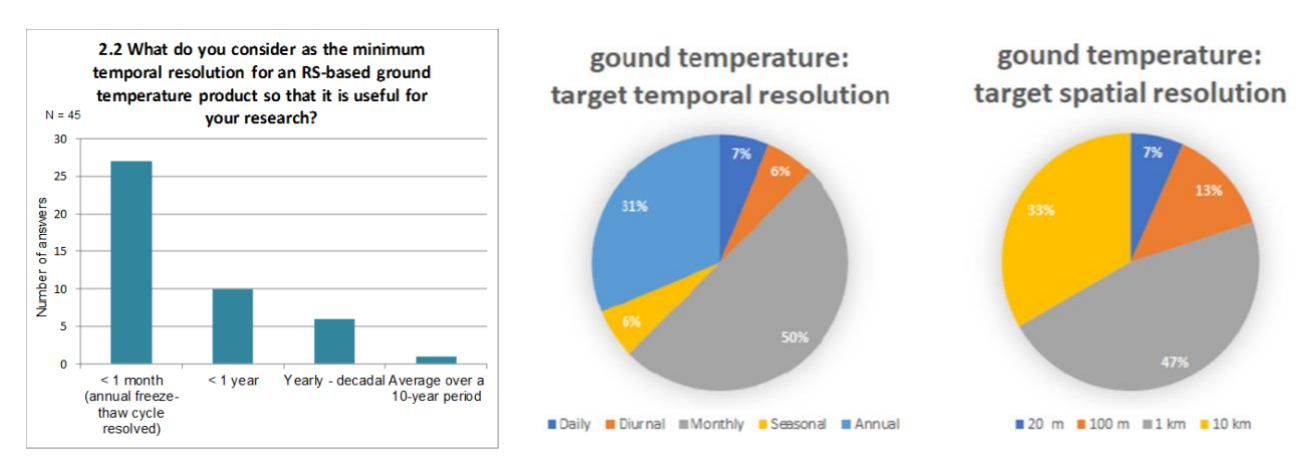


Figure 3.1a,b. User Survey results. Left: ESA DUE GlobPermafrost User Survey results, question 2.2 [RD-12]. Right: ESA CCI Permafrost User Survey results, Figure 3 [RD-12].

Users of potential products of permafrost temperature are interested in high temporal resolution: monthly or higher as documented in [RD-12]. However, 30 % of users also rated annual resolution as adequate as target temporal resolution in [RD-12]. Half of the user group are satisfied with a target spatial resolution of 1 km². The first release of the Permafrost_cci *CRDPv0 GTD* provided annual resolution with 1 km² spatial resolution over a range of depths (0, 1, 2, 5, 10 m) from 2003 to 2017, Permafrost_cci *CRDPv1* to *v4 GTD* provide an annual resolution with 1 km² spatial resolution over the same depths (0, 1, 2, 5, 10 m) and in addition covering longer time spans from 1997 to 2018, 1997 to 2019, 1997 to 2021, and 1997 to 2023, respectively.

3.2 Permafrost cci GTD Match-up Analyses with In Situ Data

The match-up is performed for Permafrost_cci GTD versus in situ MAGT across the measurement depths and interpolated depths using the entire data collection as well as the subset of measurements in the cold temperature only that more closely represents the permafrost (that we define by in situ MAGT < 1 °C). For each in situ point location and year, the pixel value in the Permafrost_cci products closest to the in situ measurement is extracted to compile the match-up dataset and calculate summary statistics. Residuals of the match-up pairs from the bulk regression line of the match-up data collection v5 come out with the equation of the residual = Permafrost_cci GTD - (0.84 × in situ MAGT -0.67). The summary statistics of the bulk dataset as well as the temperature related subsets are visualised and displayed in Figures 3.2, and 3.4 for the match-up analyses using the original in situ measurements and in Figure 3.3 for the match-up analyses using the depth-interpolated MAGT time series. Spatial mapping visualises potential geographic biases in residuals, see Figure 3.5a for the bulk match-up data collection and Figure 3.5b for the match-up data collection representative for permafrost temperature represented at 'cold sites' as we define it by MAGT < 1 °C.

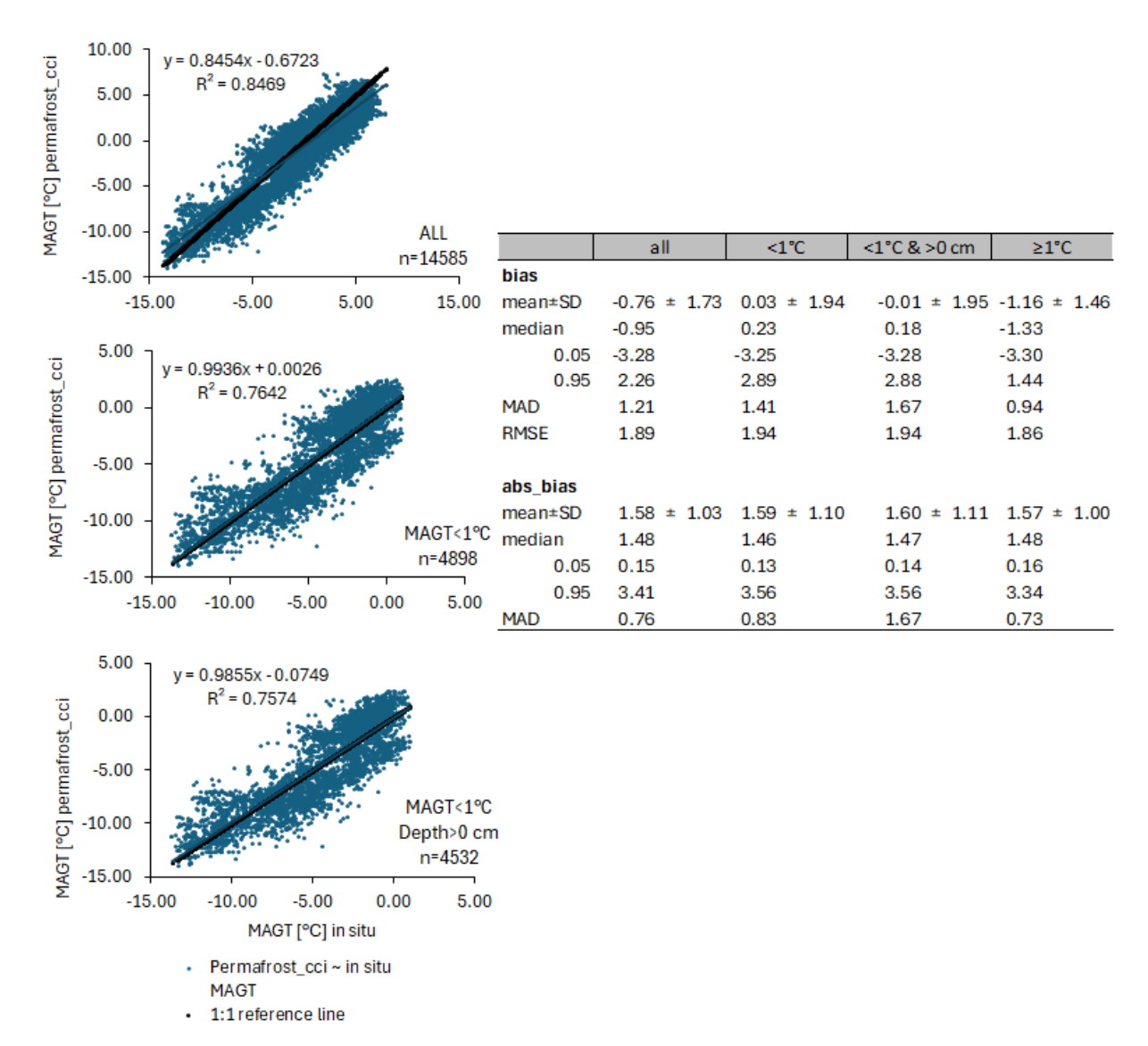


Figure 3.2. Regression of Permafrost_cci GTD versus in situ MAGT across all discrete depths and years (upper panel) for the bulk data set, (middle panel) for MAGT < $1\,^{\circ}$ C and (lower panel) for MAGT < $1\,^{\circ}$ C with depth = 0 m excluded. Summary statistics of Permafrost_cci GTD versus in situ MAGT in all discrete depths are given for the bulk dataset and the temperature related subsets. SD=standard deviation, MAD=median absolute deviation, RMSE=root mean square error.

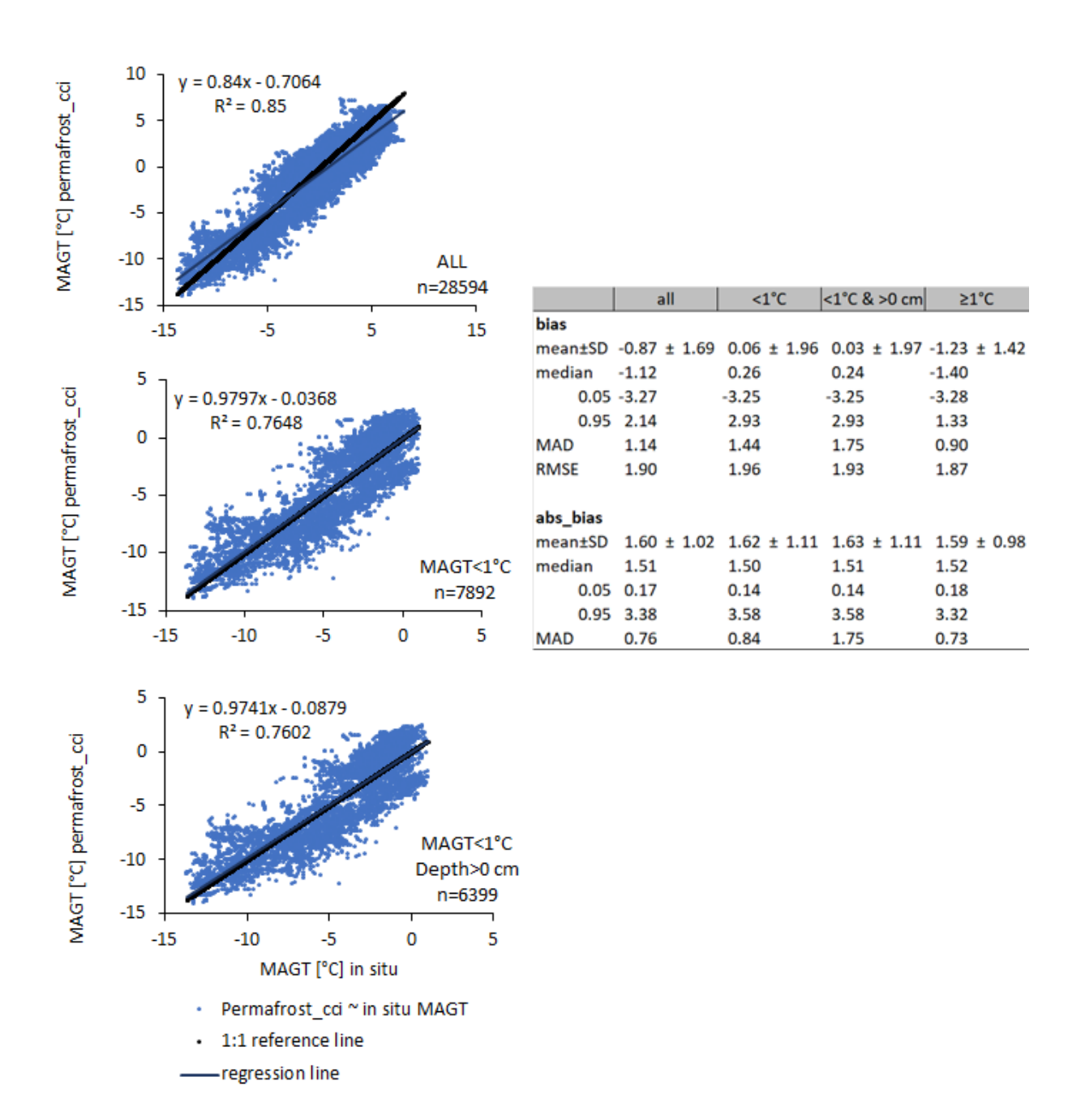


Figure 3.3. Regression of Permafrost_cci GTD versus in situ MAGT data interpolated through depth across all depths and years (upper panel) for the bulk data set, (middle panel) for MAGT < 1 °C and (lower panel) for MAGT < 1 °C with depth = 0 m excluded. Summary statistics of Permafrost_cci GTD versus in situ MAGT in all discrete depths are given for the bulk dataset and the temperature related subsets. SD=standard deviation, MAD=median absolute deviation, RMSE=root mean square error.

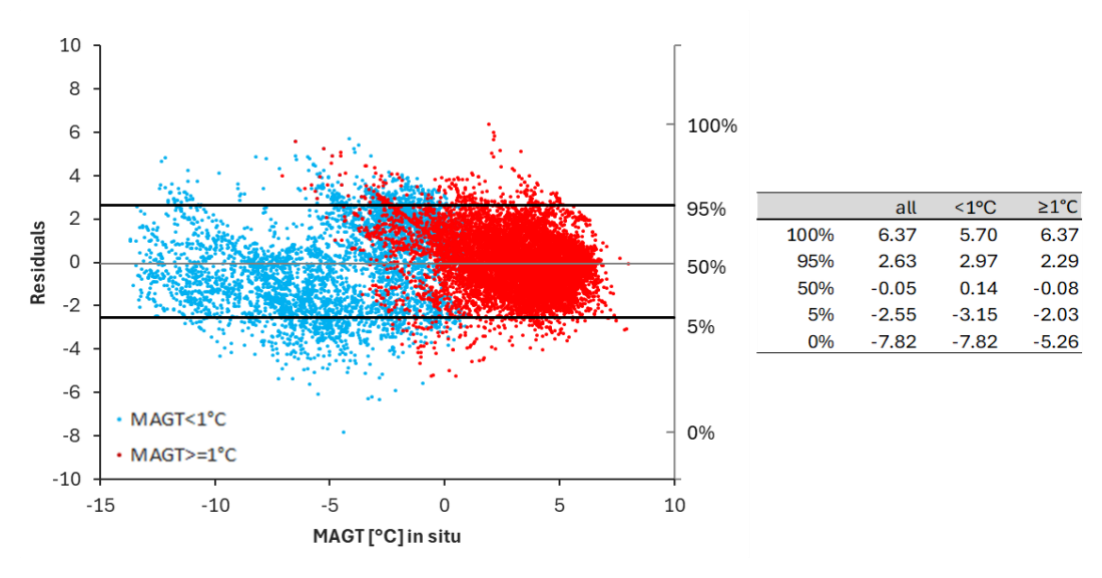


Figure 3.4. Residuals of Permafrost_cci GTD and in situ MAGT match-up (blue = MAGT < 1 °C, red = MAGT > 1 °C) with summary statistics for the bulk MAGT dataset and the temperature related subsets.

Table 3.1a. GTD bias across temperature subsets for original depths (in cm) across sampling depths.

Depth	ALL	#	<1°C	#	≥1°C	#
0	0.17	795	0.53	364	-0.13	431
10	-0.36	172	-0.21	120	-0.70	52
20	-1.11	1916	-0.27	344	-1.30	1572
25	-0.47	540	-0.54	441	-0.13	99
40	-1.13	1776	-0.19	314	-1.33	1462
50	-0.36	581	-0.39	496	-0.19	85
60	-0.91	38	-0.99	36	0.40	2
75	-0.73	440	-0.70	380	-0.93	60
80	-1.19	1709	-0.29	253	-1.34	1456
100	-0.21	430	-0.11	332	-0.54	98
120	-1.16	894	-0.25	107	-1.29	787
150	0.45	139	1.03	90	-0.62	49
160	-1.31	1670	-0.93	168	-1.35	1502
200	0.84	262	0.90	165	0.73	97
240	-1.29	583		0	-1.29	583
250	0.90	82	1.00	58	0.67	24
300	0.75	343	0.69	264	0.96	79
320	-1.40	1112	0.00	54	-1.47	1058
400	0.97	195	0.98	108	0.94	87
500	0.72	310	0.62	244	1.09	66
1000	0.78	598	0.75	560	1.24	38

Tables 3.1a,b show the Permafrost_cci GTD bias of originally measured and interpolated GT across sampling depths, visualised for the cold sites' temperature group as defined by us with the in situ MAGT threshold of < 1 °C with a positive bias of 0.53 °C, then a shift towards small negative bias < 1 °C characteristic for the shallower depths until ca 1 m, shifting to a positive bias from around 1.5 m depth down to deeper depths. The shifts in negative and positive bias dominance predominantly reflect the dominance of different data sources and measurement programs.

D.4.1 Product Validation and Inter-	CCI+ PHASE II – NEW ECVS	Issue 5.1
Comparison Report (PVIR)	Permafrost	30 October 2025

Table 3.1b. GTD bias across temperature subsets for the interpolated dataset across sampling depths.

Depth	ALL	#	<1°C	#	≥1°C	#
0	0.17	795	0.53	364	-0.13	431
10	0.09	256	0.28	175	-0.32	81
20	-1.05	1997	-0.10	390	-1.28	1607
25	-0.97	2161	-0.34	717	-1.28	1444
40	-0.97	2197	-0.29	660	-1.27	1537
50	-0.95	2094	-0.28	714	-1.29	1380
60	-1.06	1902	-0.40	559	-1.34	1343
75	-1.08	1966	-0.47	611	-1.35	1355
80	-1.08	2013	-0.33	503	-1.33	1510
100	-0.85	1241	-0.09	435	-1.26	806
120	-1.16	894	-0.25	107	-1.29	787
150	-0.96	970	0.24	180	-1.23	790
160	-1.16	1829	-0.27	250	-1.31	1579
200	-0.87	1464	0.90	221	-1.18	1243
240	-0.93	1462	0.88	206	-1.23	1256
250	-0.90	1292	0.89	215	-1.26	1077
300	-0.82	1411	0.66	318	-1.25	1093
320	-0.98	1382	0.52	221	-1.27	1161
400	0.78	314	0.76	211	0.84	103
500	0.78	356	0.65	275	1.23	81
1000	0.78	598	0.75	560	1.24	38

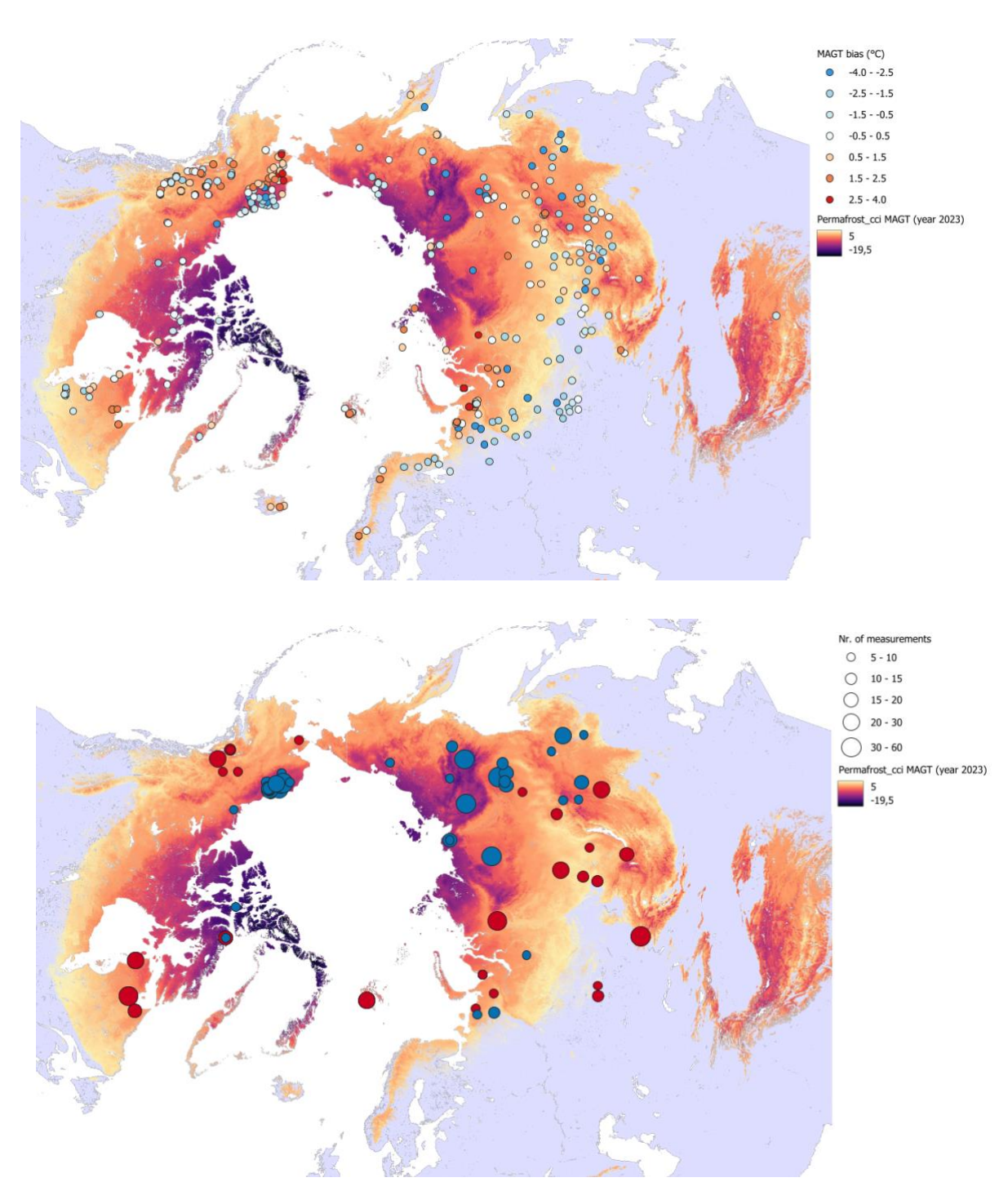


Figure 3.5a (upper panel) GTD bias and (lower panel) residuals > 95 % quantile (red) and < 5 % quantile (blue) over mapped Permafrost_cci GTD 2023 (2 m) in the Northern hemisphere. The size of the circle represents the number of samples with specific residuals at the particular location.

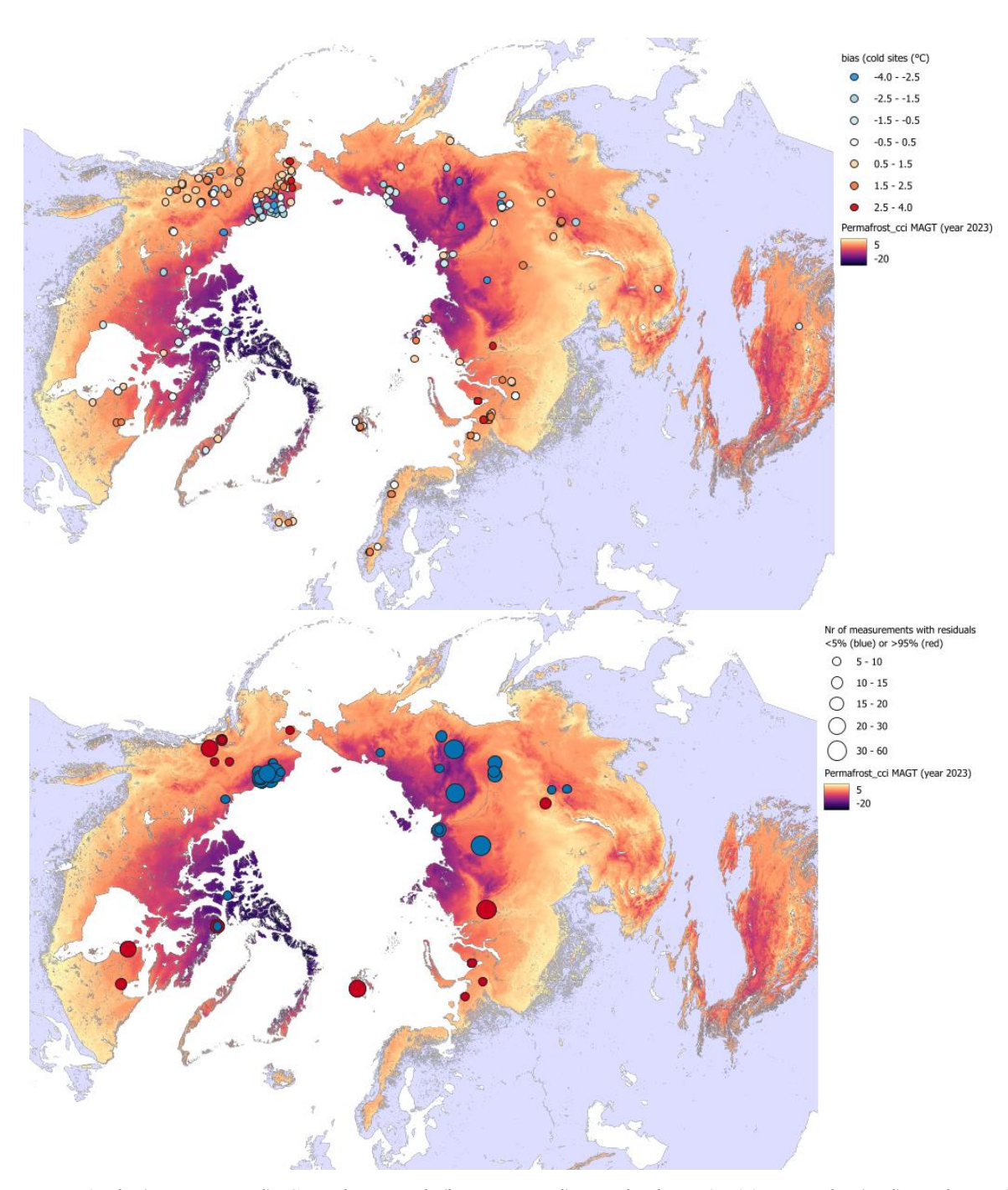


Figure 3.5b (upper panel) GTD bias and (lower panel) residuals > 95 % quantile (red) and < 5 % quantile (blue) for the in situ MAGT < 1 °C subset of sites over mapped Permafrost_cci GTD 2023 (2 m) in the Northern hemisphere. The color of circles represents the temperature subset and size of the circle represents the number of samples with specific residuals at the particular location.

D.4.1 Product Validation and Inter-	CCI+ PHASE II – NEW ECVS	Issue 5.1
Comparison Report (PVIR)	Permafrost	30 October 2025

Permafrost_cci GTD and in situ MAGT consensus in temporal trends

Table 3.2. Gleichläufigkeit (glk) and temporal stability (ts) per year for all sites, and the subsets MAGT < 1 °C and MAGT > 1 °C.

	ć	all		l de la companya de	MAGT<1	°C		MAGT≥1	°C
Year	glk	ts	#	glk	ts	#	glk	ts	#
1998	0.67	0.05	504	0.69	0.26	51	0.67	0.03	453
1999	0.66	0.03	512	0.47	-0.31	47	0.67	0.07	465
2000	0.63	-0.21	535	0.55	-0.17	58	0.64	-0.22	477
2001	0.70	0.06	556	0.60	0.37	70	0.72	0.01	486
2002	0.79	0.10	547	0.75	-0.19	79	0.80	0.15	468
2003	0.76	0.02	578	0.65	0.22	96	0.78	-0.02	482
2004	0.71	-0.13	585	0.48	0.06	89	0.75	-0.16	496
2005	0.66	-0.17	604	0.64	-0.56	104	0.67	-0.09	500
2006	0.70	-0.13	672	0.57	-0.61	163	0.74	0.03	509
2007	0.81	0.06	701	0.58	0.01	169	0.88	0.07	532
2008	0.60	-0.04	782	0.44	-0.12	225	0.66	-0.01	557
2009	0.67	0.16	835	0.69	0.22	270	0.67	0.13	565
2010	0.70	-0.10	888	0.64	0.11	303	0.74	-0.21	585
2011	0.66	0.09	907	0.61	0.06	324	0.69	0.11	583
2012	0.65	-0.16	773	0.72	-0.17	341	0.59	-0.16	432
2013	0.67	-0.13	436	0.70	-0.28	252	0.63	0.08	184
2014	0.72	0.00	458	0.82	-0.09	267	0.58	0.12	191
2015	0.64	-0.12	414	0.62	-0.12	243	0.67	-0.11	171
2016	0.73	0.41	215	0.72	0.56	147	0.76	0.10	68
2017	0.63	-0.23	190	0.53	-0.41	119	0.82	0.07	71
2018	0.56	0.08	177	0.49	-0.02	116	0.70	0.26	61
2019	0.66	-0.34	89	0.73	0.00	71	0.39	-1.66	18
2020	0.54	0.27	71	0.50	0.09	50	0.62	0.69	21
2021	0.53	-0.29	59	0.32	-0.45	34	0.80	-0.08	25
2022	0.72	0.54	60	0.65	0.67	46	0.93	0.14	14
2023	1.00	0.38	9	1.00	0.38	9			0
MEAN	0.68	-0.02		0.63	-0.05		0.71	-0.01	

Table 3.3. Summary statistics per site for Gleichläufigkeit (glk), temporal stability (ts) and absolute temporal stability (abs_ts)

all			MAG	Γ<1°C	MAGT	'≥1°C
	glk	ts	glk	ts	glk	ts
mean±SD	0.66 ± 0.23	-0.05 ± 0.40	0.63 ± 0.34	-0.09 ± 0.44	0.70 ± 0.34	0.00 ± 0.20
5%	0.24	-0.52	0.00	-0.75	0.00	-0.25
95%	1.00	0.40	1.00	0.47	1.00	0.25
median	0.69	-0.01	0.53	0.00	0.67	0.00

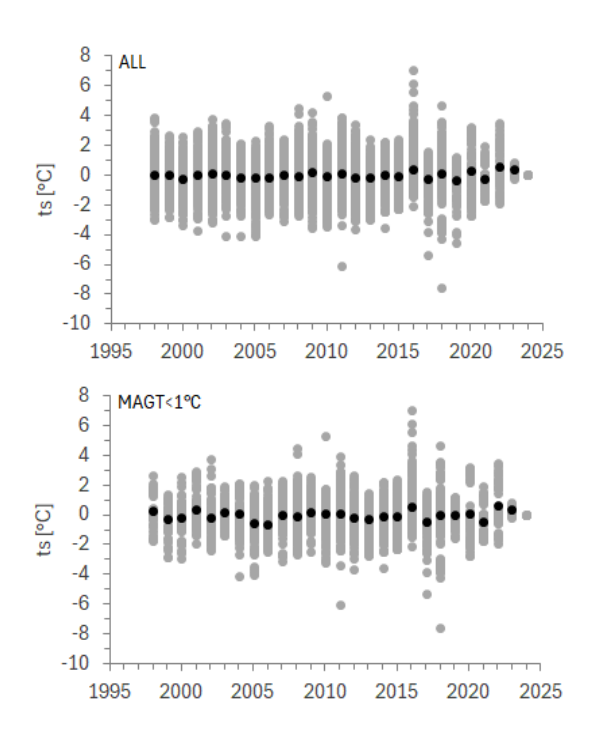


Figure 3.6. Temporal stability (ts, year-to-year change in magnitude of the bias) for the bulk $Permafrost_cci\ GTD\ dataset$ (upper panel) and for the temperature subgroup of the cold sites defined by in situ MAGT < 1 °C (lower panel). Black dots represent the mean values.

The Gleichläufigkeit and the temporal bias stability analyses, see also Tables 3.2, 3.3 and Figure 3.6 show a match in the trend across years with a mean of around 70 % for the Gleichläufigkeit and low bias variations across the years for the bulk data collection and the temperature subgroups, respectively.

Comparison of GTD bias PVIRv4 vs PVIRv5

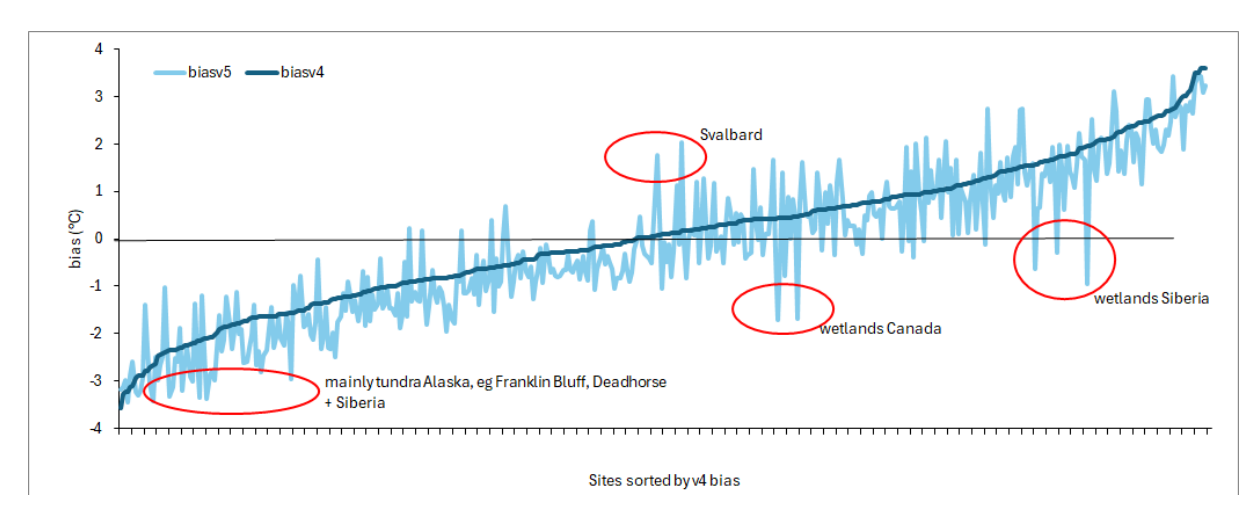


Figure 3.7 Comparison of GTD bias in situ vs Permafrost_cci of PVIRv4 (dark blue) vs PVIRv5 (light blue) per match-up site. Sites are sorted by size of v4 bias from negative to positive. Some wet regions are especially colder in Permafrost_cci than during the last validation, but with a better fit for Siberian wetlands.

D.4.1 Product Validation and Inter-	CCI+ PHASE II – NEW ECVS	Issue 5.1
Comparison Report (PVIR)	Permafrost	30 October 2025

The comparison of the GTD bias in PVIRv4 versus this validation data collection in PVIRv5, Permafrost_cci-Val MAGT, was carried out using only the same sites, i.e. no additional new sites and years, and in addition with the newly removed sites in PVIRv5 also removed in Permafrost_cci GTDv3 (Figure 3.7). This comparison shows that Permafrost_cci GTDv3 performs slightly better at cold tundra and some warmer wetland sites in Canada (i.e. smaller cold bias) than Permafrost_cci GTDv4 (2025). In contrast, Permafrost_cci GTDv4 performs better at several Siberian wetland sites with a smaller warm bias and the warm bias is in generally reduced and smaller. Still, interestingly, at some Svalbard sites Permafrost_cci GTDv4 shows a warm bias.

Regional Assessments

We characterise the Permafrost_cci GTD performance related to regions/countries with permafrost in Table 3.4. These are Russia, United States of America, Canada, Greenland, Iceland, and Scandinavia. Accordingly, we are showing regional maps of North-western America (Figure 3.8), North-eastern America and Greenland (Figure 3.9), Northern Europe (Figure 3.10), North-western Siberia (Figure 3.11) and North-eastern Siberia (Figure 3.12).

Table 3.4. GTD match-up and summary (bias and absolute bias) and temporal statistics (glk and ts) for different countries/regions.

Region	#	bias a	bs_bias	glk	ts
Russia	10327	-1.11	1.64	0.70	-0.01
US	1411	-0.85	1.65	0.58	-0.09
Canada	2126	0.46	1.31	0.68	-0.02
Greenland	25	0.45	1.42	0.90	0.42
Iceland	25	1.41	1.41	0.55	0.00
Scandinavia (Norway, Sweden)	631	0.97	1.36	0.67	-0.05
China	10	-0.79	0.79	0.78	0.09
Mongolia	6	-0.70	0.70	0.50	-0.07

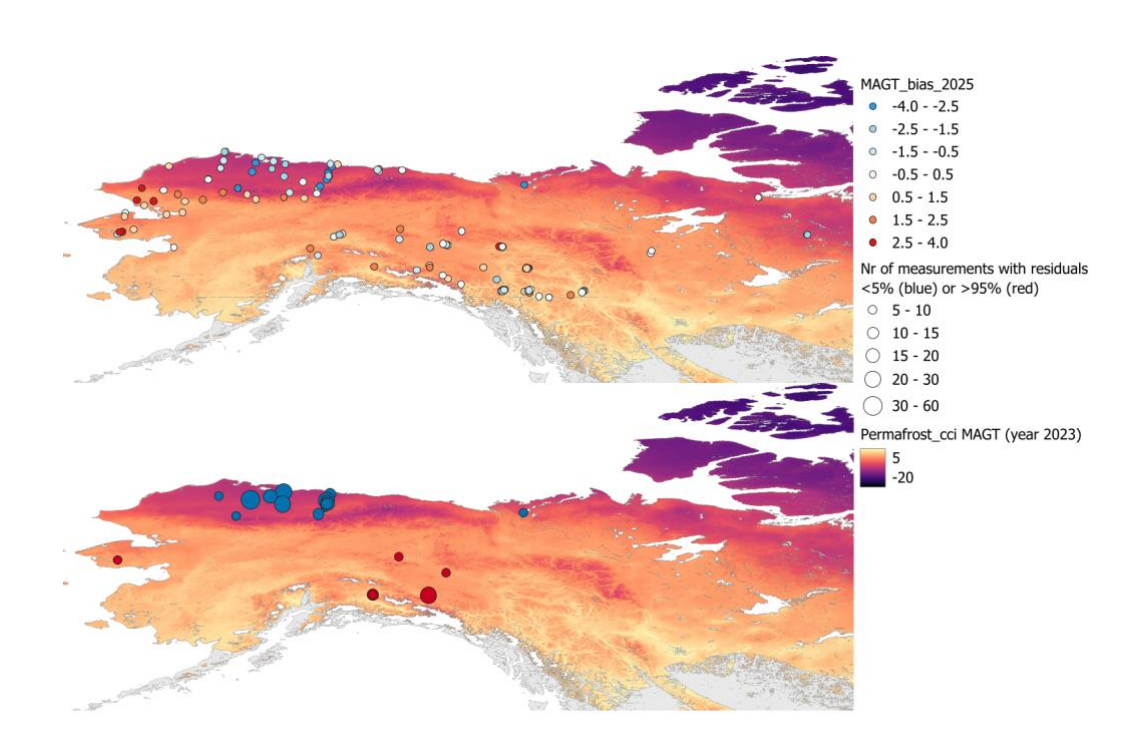


Figure 3.8. (upper panel) GTD bias (color-coded point symbols) and (lower panel) residuals (color-coded point symbols) over mapped Permafrost_cci GTD 2023 (2 m) in north-western America.

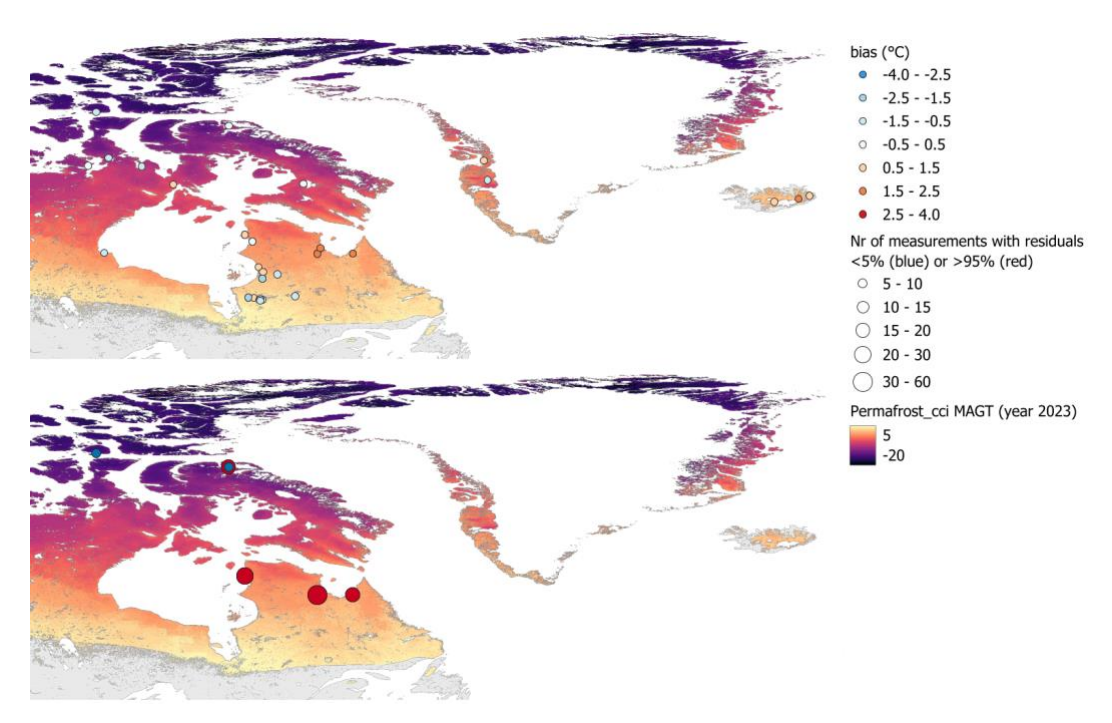


Figure 3.9. (upper panel) GTD bias (color-coded point symbols) and (lower panel) residuals (color-coded point symbols) over mapped Permafrost_cci GTD 2023 (2 m) in north-eastern America and Greenland.

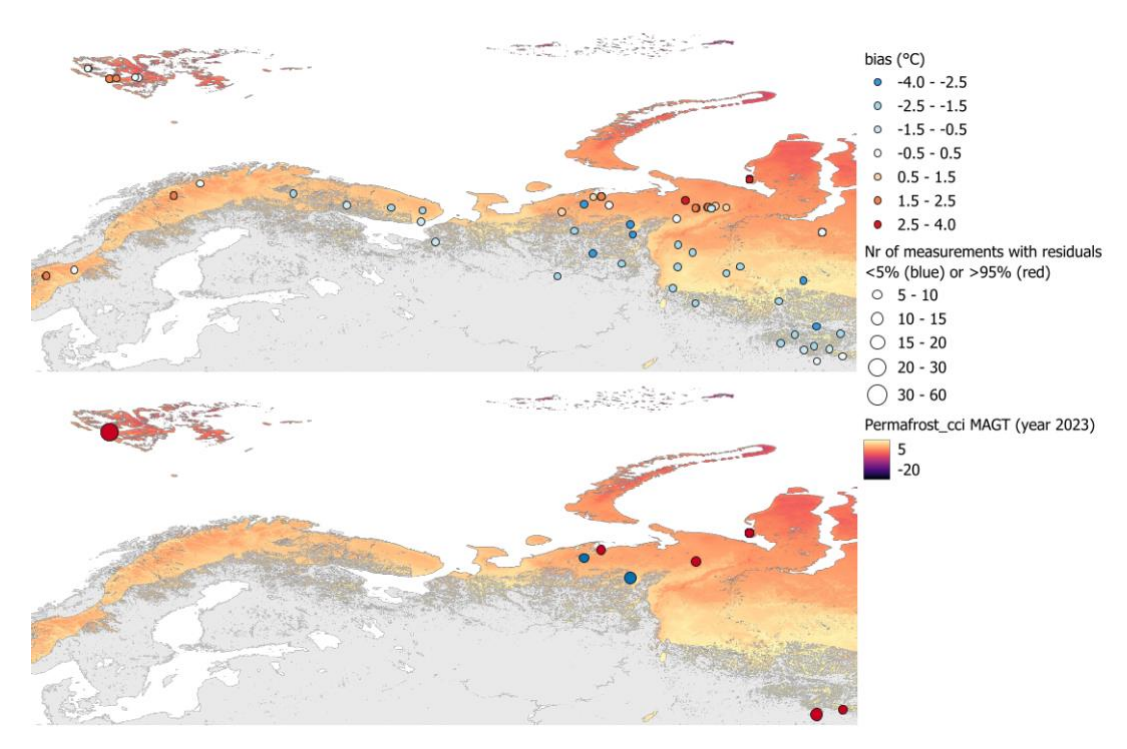


Figure 3.10. (upper panel) GTD bias (color-coded point symbols) and (lower panel) residuals (color-coded point symbols) over mapped Permafrost_cci GTD 2023 (2 m) in northern Europe and western Siberia.

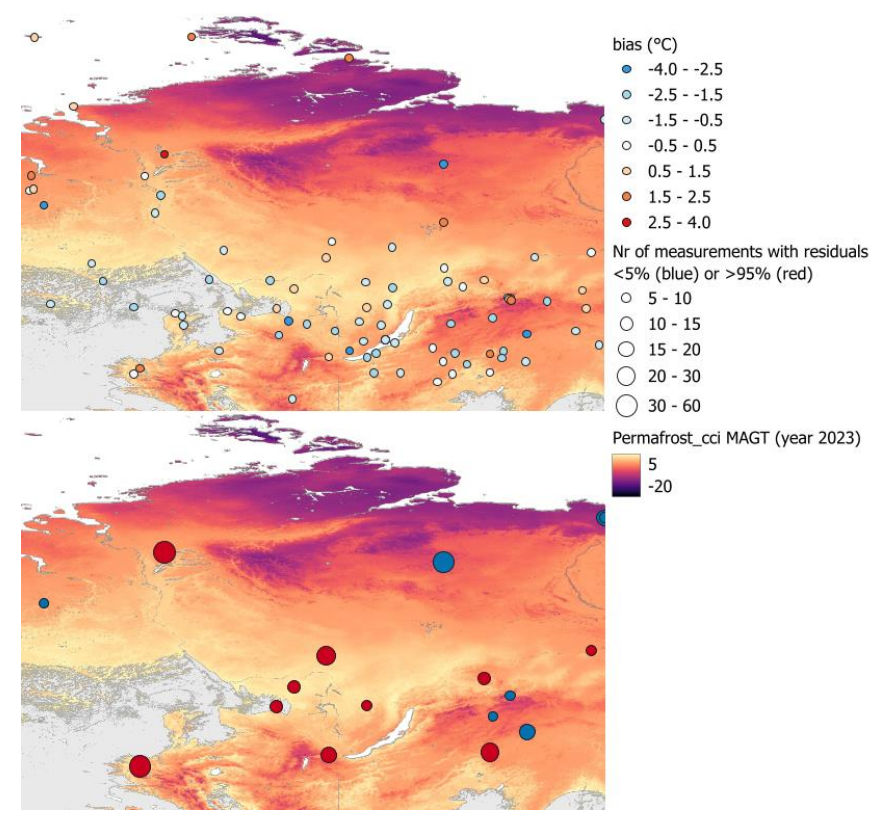


Figure 3.11. (upper panel) GTD bias (color-coded point symbols) and (lower panel) residuals (color-coded point symbols) over mapped Permafrost cci GTD 2023 (2 m) in western to central Siberia.

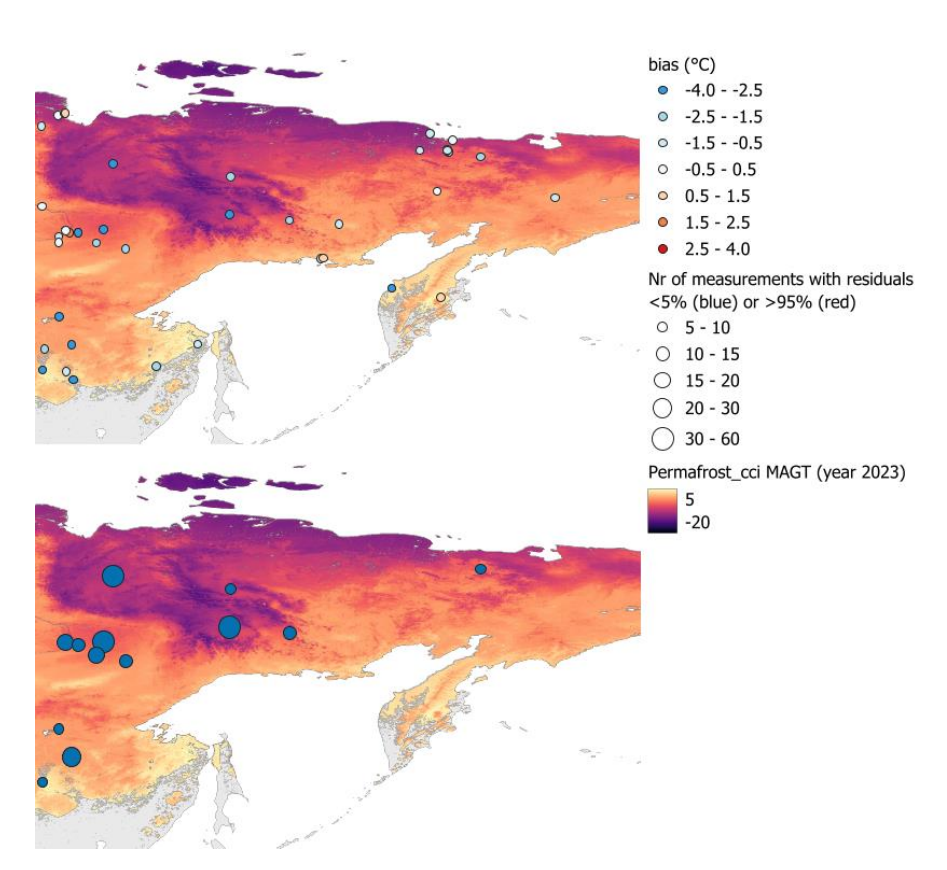


Figure 3.12 (upper panel) GTD bias (color-coded point symbols) and (lower panel) residuals (color-coded point symbols) over mapped Permafrost_cci GTD 2023 (2 m) in central to eastern Siberia.

Regional assessments - GTD bias and temporal trends in Antarctica

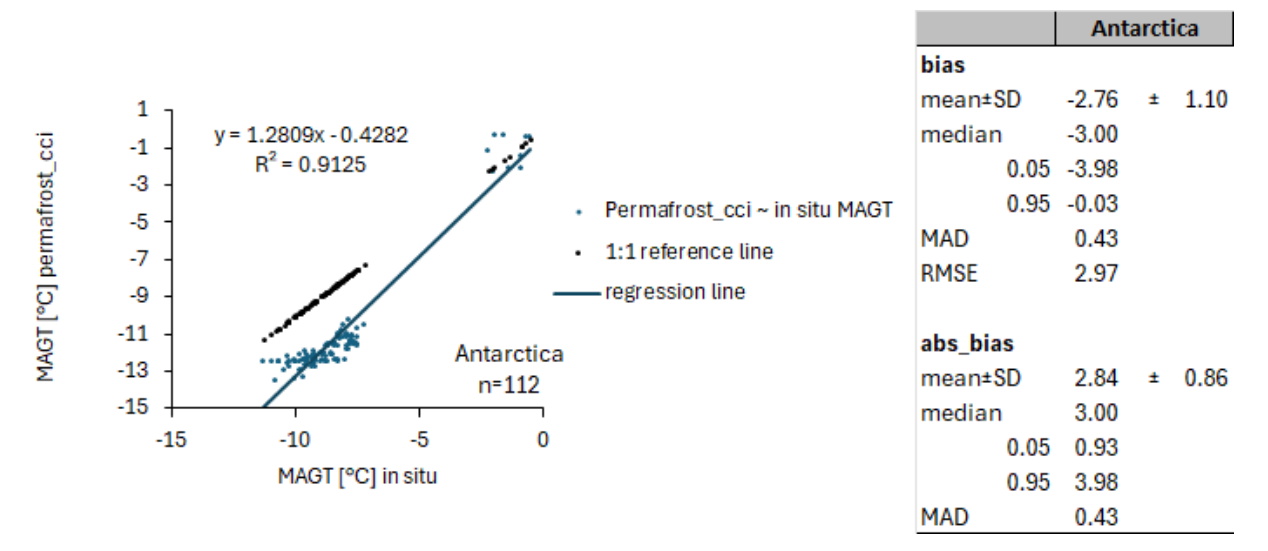


Figure 3.13. Regression of Permafrost_cci GTD versus in situ MAGT in all discrete depths and across all years (1997-2023) for all sites in Antarctica.

D.4.1 Product Validation and Inter-	CCI+ PHASE II – NEW ECVS	Issue 5.1
Comparison Report (PVIR)	Permafrost	30 October 2025

For the inland ice-free permafrost regions in Antarctica data are not sufficient for a thorough statistical analysis. In general, the in-situ data locations represent a wide gradient: cold permafrost between MAGT around MAGT \sim -10 °C and warm permafrost \sim -2 °C. The tendency of Permafrost_cci GTD compared to the available in situ data is negative (Figure 3.13, 3.14), i.e. Permafrost_cci performs with too cold GTD (mean cold bias -2.76 °C \pm 1.10; median cold bias -3 °C).

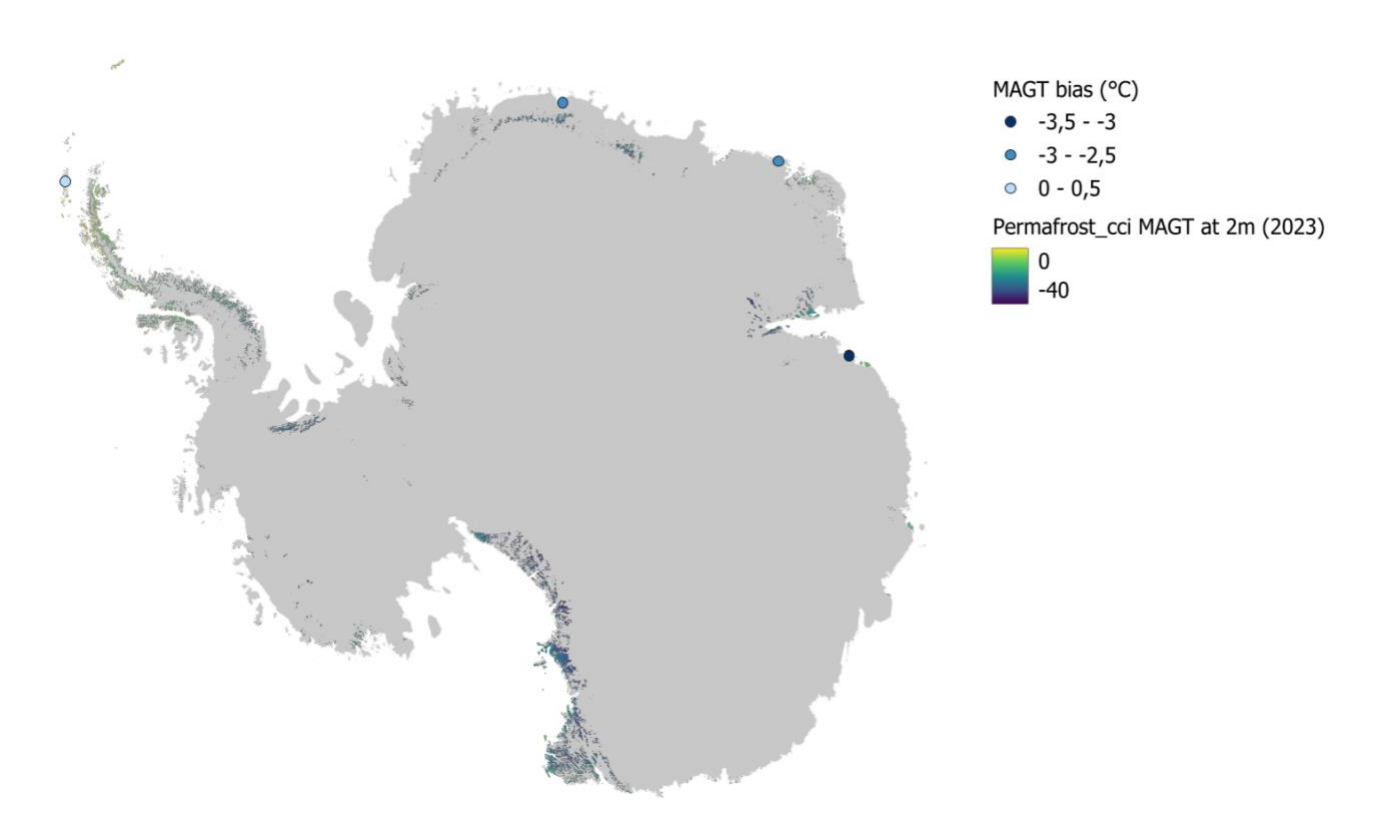


Figure 3.14. GTD bias over mapped Permafrost_cci GTD 2023 (2 m) in Antarctica (source background map: Quantarctica, Matsuoka et al. 2021)

The temporal trend of GTD is well captured by Permafrost_cci at three from five measurement sites (Figure 3.15). One site is warming too fast, while a second one shows no variability in Permafrost_cci GTD.

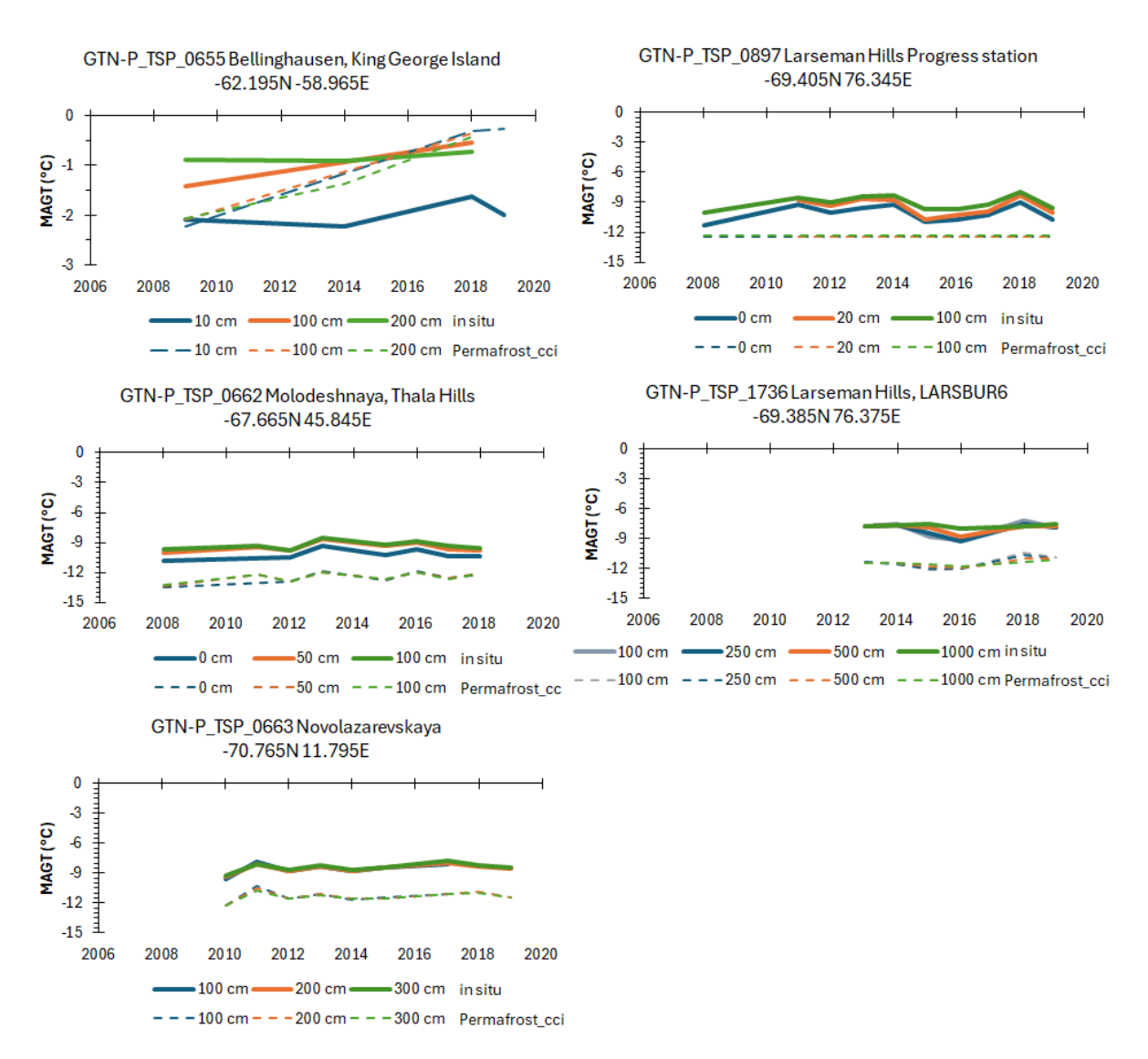


Figure 3.15 Temporal trends of in situ MAGT (solid) and Permafrost_cci GTD (dashed) temperature at different depths for five sites in Antarctica.

D.4.1 Product Validation and Inter-	CCI+ PHASE II – NEW ECVS	Issue 5.1
Comparison Report (PVIR)	Permafrost	30 October 2025

In summary, Permafrost_cci GTD (1997–2023) shows the following performance characteristics:

- Permafrost_cci GTD *CRDPv4* is characterised by a mean bias of -0.76 °C \pm 1.73, and a median bias of -0.95 °C (5 % -3.3 to 95 % 2.3 °C) for the bulk data set, the mean bias is -0.87 °C \pm 1.69, and the median bias is -1.12 °C (5 % -3.3 to 95 % 2.1 °C) for the depth-interpolated bulk dataset.
- Match-up pairs from in situ measurements with MAGT < 1 °C and thus from reliable permafrost sites show an even better performance with a mean bias of 0.03 °C ±1.9, and a median bias of 0.23 °C (5 % -3.3 to 95 % 2.9 °C), compared to the bulk dataset and notably in comparison to MAGT > 1 °C with a median bias of -1.33 °C. For the depth-interpolated dataset, this accounts to a median of 0.26 °C for MAGT < 1 °C and -1.40 °C for MAGT > 1 °C.
- For MAGT < 1 °C without the surface temperature at 0 m the performance is only slightly higher with a mean bias of -0.01 °C, a median bias of 0.18 °C, i.e. the performance of Permafrost_cci surface temperature considerably improved compared to *CRDPv3*. GTD bias across depths is stable with a slightly larger negative mean bias in shallow depths (0 to 1 m), mainly caused by a negative bias in match-up pairs of the warmer sites (MAGT > 1°C).
- Few extreme residuals consistently appear with < 5 % quantile mainly in Northern Alaska and Northern Eastern Siberia in cold permafrost and with > 95 % quantile mainly in Southern Alaska, and Eastern Siberia and in Svalbard in the warm permafrost regions. Permafrost_cci GTD bias is mainly negative (cold bias) at the southern boundary zones in Siberia and Northern America. Regional assessments of GTD bias and temporal trends show a higher absolute bias in Russia, North America and on the Tibetan plateau (China) (> 1 °C) for the bulk dataset.
- the trends over years generally match well between the in situ measurements and Permafrost_cci GTD, with a high Gleichläufigkeit (median glk (1997 to 2023) ~ 70 %) and temporal bias stability (ts ±0.5 °C) in all years for the bulk dataset.
- For the inland ice-free permafrost regions in Antarctica data are not sufficient for a thorough statistical analysis. The tendency of Permafrost_cci GTD compared to the available in situ data is negative, i.e. Permafrost_cci performs with too cold GTD. The temporal trend of GTD is well captured by Permafrost_cci at three from five measurement sites. One site is warming too fast, while a second one shows no variability in Permafrost_cci GTD.

3.3 Permafrost cci GTD Comparison with PERMOS Permafrost Temperature

The comparison of the evolution of the mean in situ measured MAGST and Permafrost_cci GTD at 0 m over the Swiss Alps within the PERMOS domain from 1997 to 2023 shows that Permafrost_cci GTD at 0 m has a slight cold bias of -0.078 °C compared to the in situ measurements (the RMSE is +0.317 °C). The warming tendency observed in the in situ measurements is well reproduced by the Permafrost_cci GTD product (Figure 3.16a) as well as the inter-annual variations (e.g., the warm year 2003 and the cold year 2021). The standard deviation of the in situ measurements, although limited to 23 sites, is larger than the standard deviation of the Permafrost_cci GTD product at 0 m over the entire Swiss Alps between 2500 m a.s.l. and 3000 m a.s.l. This is emphasised in Figure 3.16b which shows the measured MAGST for each single logger in the PERMOS network compared to the minimum and maximum Permafrost_cci GTD at 0 m depth in-between 2500 m and 3000 m a.s.l. in the Swiss Alps. The measured in situ MAGST data ranges from around -4.1 °C to +8 °C, whereas Permafrost_cci GTD ranges from around -0.5 °C to +2.4 °C.

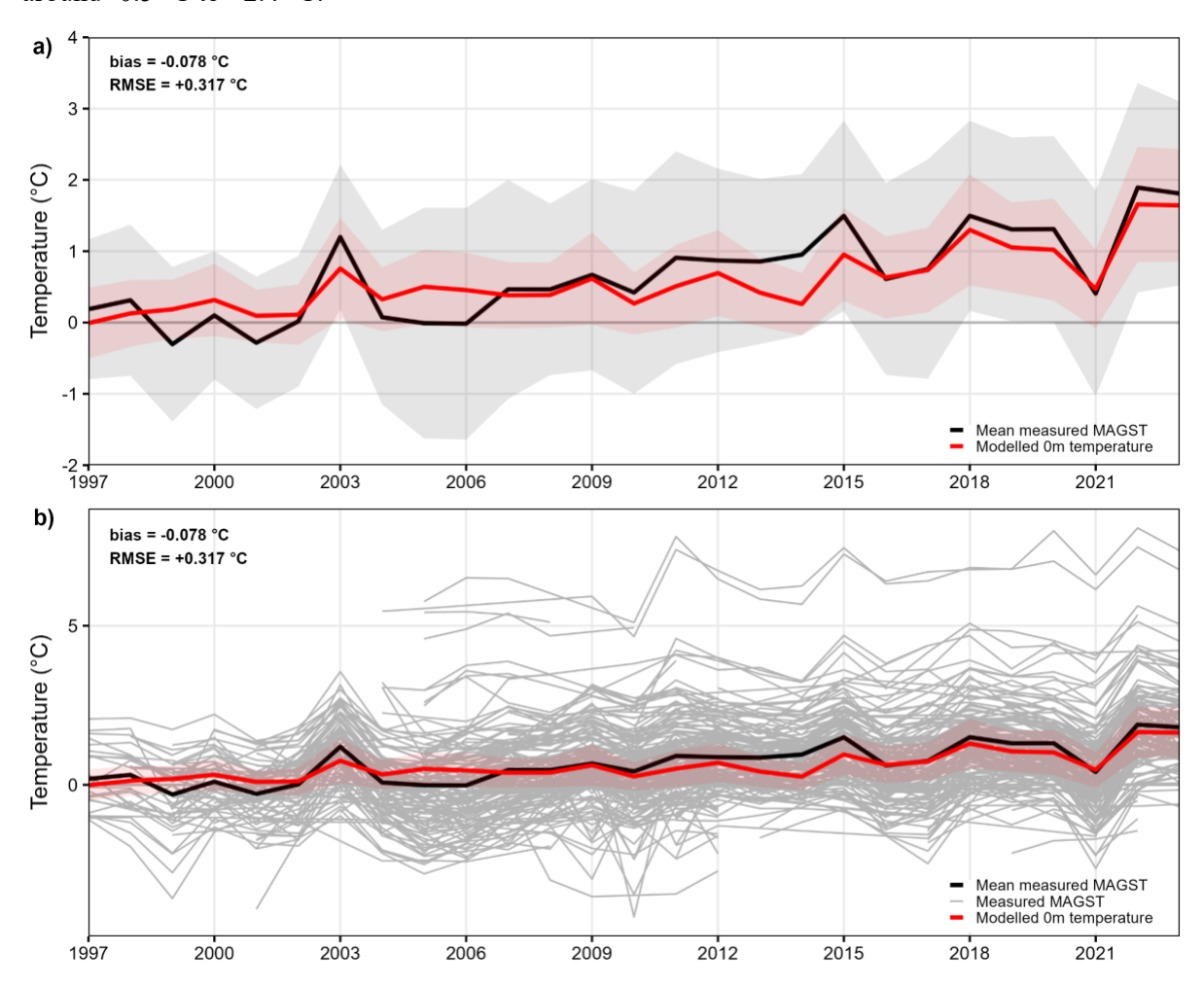


Figure 3.16. Temporal evolution of the in situ measured mean MAGST (black) in Switzerland (a) and measured MAGST at each logger (b) compared to the mean Permafrost_cci GTD at 0 m depth (red) over the entire Swiss Alps between 2500 m a.s.l. and 3000 m a.s.l. The shaded area represents \pm one standard deviation.

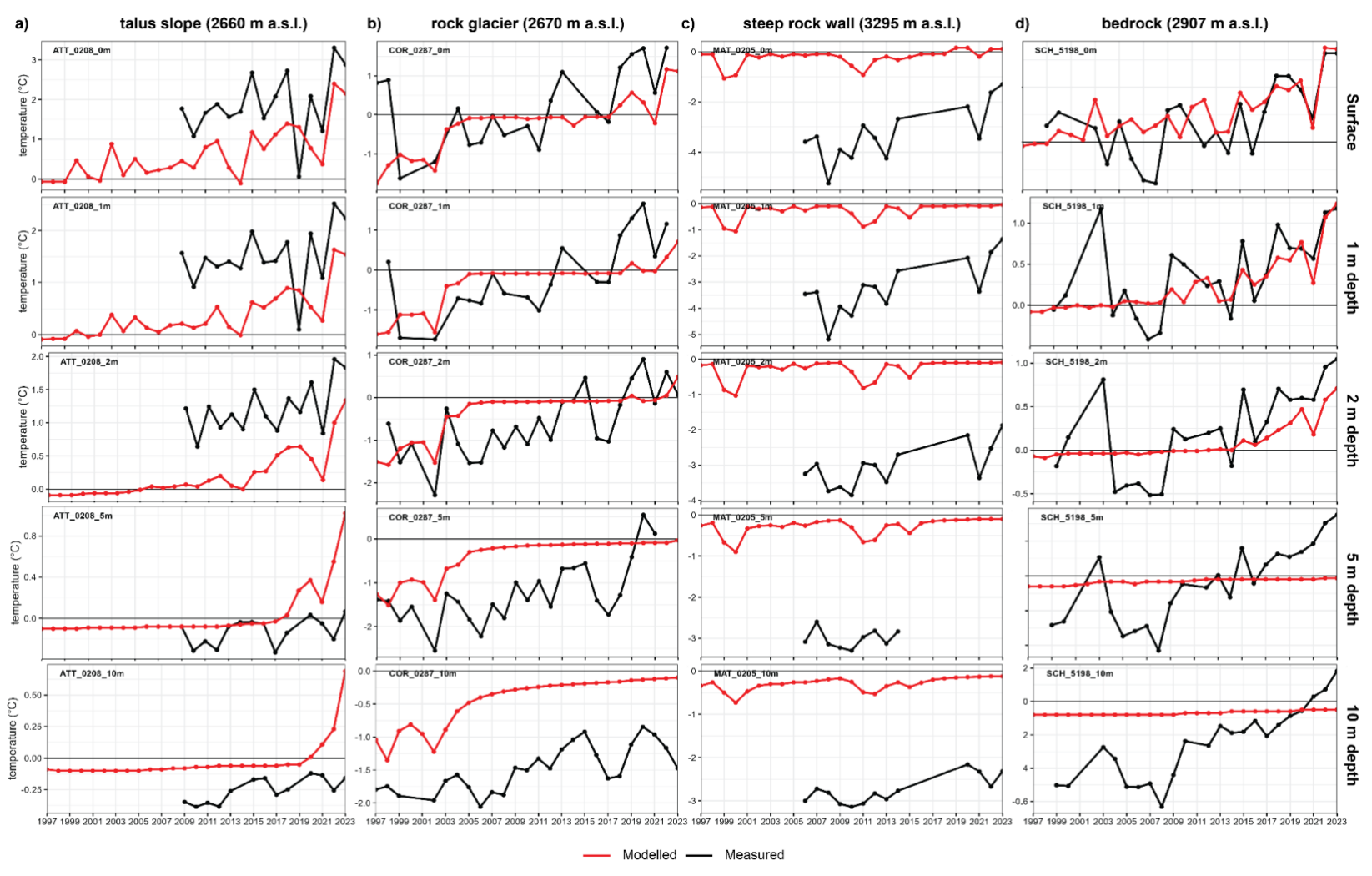


Figure 3.17. Comparison of mean Permafrost_cci GTD (red) and in situ measured MAGT (black) at 0, 1, 2, 5 and 10 m depth at 4 sites in the Swiss Alps.

Comparing Permafrost_cci GTD at 0, 1, 2, 5 and 10 m depth to the in situ measured MAGT in boreholes (see Figure 3.17), there is no systematic bias of the Permafrost_cci GTD product. The best model fit is found at Murtèl and Schilthorn (Figure 3.17b,d), whereas a cold bias is found at Attelas (Figure 3.17a) and a warm bias exists at the Matterhorn (Figure 3.17c). Based on the data from the 13 PERMOS sites (not shown) Permafrost_cci GTD fit is independent from the landform type, elevation or regional site location. The simulated Permafrost_cci GTD values fit better the in situ observations near the surface (bias is +0.153°C at 0 m and +0.106°C at 1m) than at depth (bias is +0.275°C at 10 m), Figure 3.18a-e.

Although the absolute values are different, both, the measured and the simulated MAGT, show a warming trend over the period 1997-2021. However, Permafrost_cci GTD fails to reproduce the interannual variability. At depth, all in situ measured MAGT in 2017 exhibit a more or less marked cooling effect. This is due to the extremely snow-poor winter 2016/17 in the Swiss Alps, which enabled the cold winter air temperature to cool more efficiently the ground (PERMOS, 2019). This effect is not reproduced in Permafrost_cci GTD, illustrating the difficulty to include snow effects characteristic for high mountain regions with steep topography in global models.

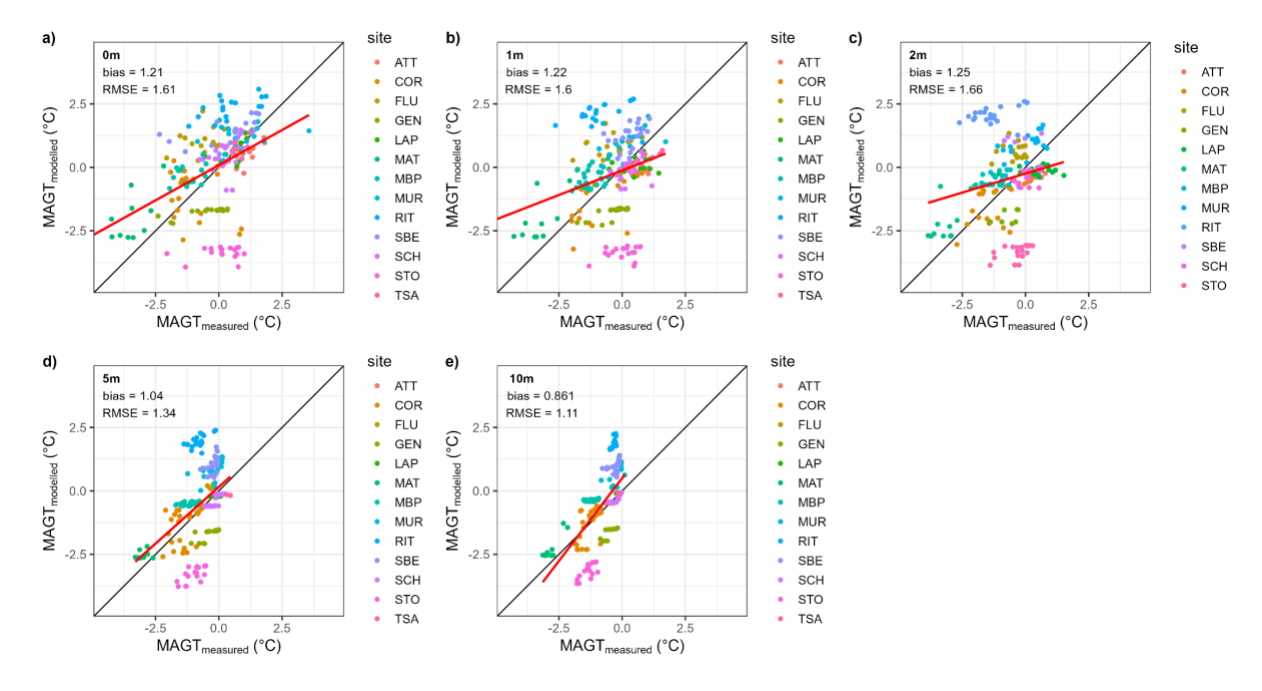


Figure 3.18. Comparison of simulated mean $Permafrost_cci$ (y-axis) and in situ measured MAGT (x-axis) at the surface (a), 1 m (b), 2 m (c), 5 m (d) and 10 m depth (e). The black line represents the one-to-one relationship and the red one the best linear fit. Statistics are displayed for each depth.

D.4.1 Product Validation and Inter-	CCI+ PHASE II – NEW ECVS	Issue 5.1
Comparison Report (PVIR)	Permafrost	30 October 2025

In summary, Permafrost_cci GTD (1997–2023) shows the following performance characteristics in the Swiss high Alps:

- The fit of Permafrost_cci GTD to in situ measured ground surface temperature in the Swiss high Alps improved with a small mean bias of -0.08 °C for *CRDPv4 GTD* compared to a cold mean bias of -0.2 °C for *CRDPv3 GTD*.
- *CRDPv4 GTD* across the ground depth profile shows a good fit with a warm bias around +1 °C with in situ measured ground temperature in the specific Permafrost_cci product depths. However, due to the warm bias *CRDPv4 GTD* fails to represent all permafrost boreholes as cold sites. This explains the better fit since most of the PERMOS permafrost monitoring sites are rather warm with ~-1°C MAGT for the in situ measurements.
- Inter-annual variation of *CRDPv4 GTD* across the ground depth profile does not match the temporal dynamics of the in situ measurements, since there are only small interannual variations in *CRDPv4 GTD* (except for > 0 °C temperature and around -0.5 °C) compared to the large variations in the in situ ground temperature measurements.

3.4 Permafrost cci GTD Comparison with FT2T GT

Regional comparisons of FT2T retrievals for 1 m depth have been made for *CRDPv4 GTD*. FT2T records have been corrected for water fraction as detailed in Bergstedt et al. (2020b).

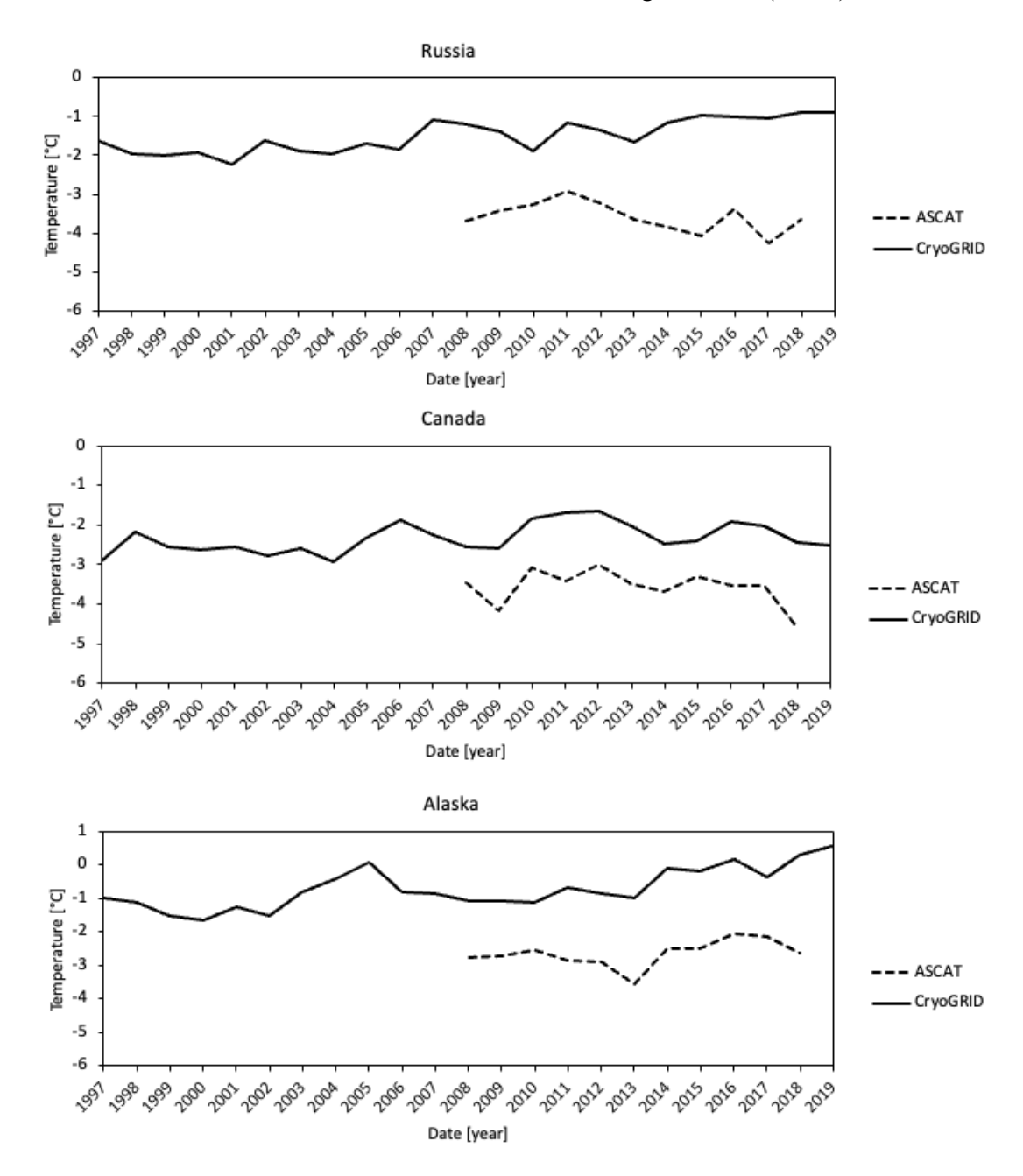


Figure 3.19. Regional ground temperature change (1 m depth) in permafrost regions of selected countries: comparison between surface status derived temperature (C-band scatterometer, Metop ASCAT; FT2T; Kroisleitner et al. (2018), corrected for water fraction according to Bergstedt et al. 2020b)) and transient modelling using land surface temperature (near infrared, MODIS, 1 km²; CryoGRID; Permafrost cci file version CRDPv4, (updated version of Figure 1 in Bartsch et al. 2023).

D.4.1 Product Validation and Inter-	CCI+ PHASE II – NEW ECVS	Issue 5.1
Comparison Report (PVIR)	Permafrost	30 October 2025

The water class of Landcover_cci has been used to assign a water fraction for each original ASCAT footprint (hexagonal approximation as in Högström et al. 2018) overlapping with permafrost according to Permafrost_cci *CRDPv4*. The calibration of FT2T has been revised and extended to include 1 m depth borehole data (North America) and 0.8 m depth data (Russian Arctic) in order to avoid a regional (and temperature range) bias. Regional aggregation of results was applied to countries and administrative districts. Temperature averages partially correlate with R² = 0.34 in Alaska and in Canada. No correlation can be observed for Russia and Greenland. An offset can be observed in case of all selected regions. This bias ranges from 1.42 °C (Canada) to 2.1 °C (Alaska). Similar temporal patterns can be however partially observed (Figure 3.19; as was also observed for *CRDPv2* in Bartsch et al. (2023)).

4 ASSESSMENT RESULTS: ACTIVE LAYER THICKNESS

4.1 Active Layer Thickness User Requirements

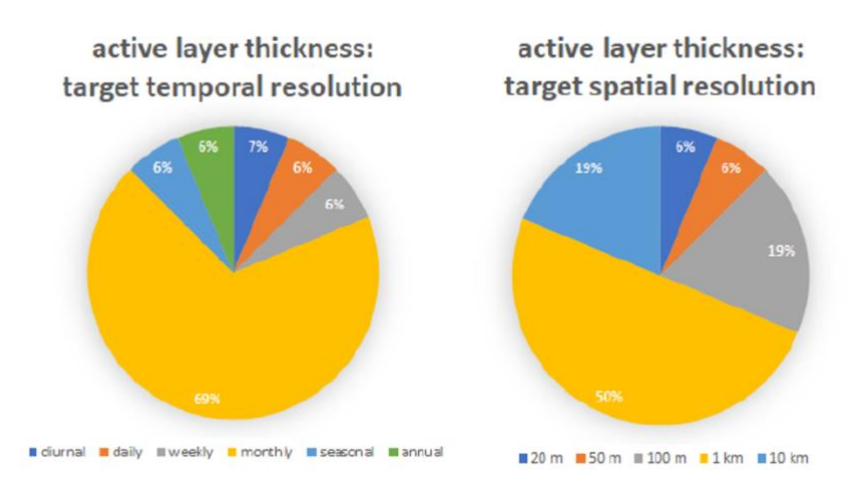


Figure 4.1. User Survey results. ESA CCI Permafrost User Survey results, Figure 4 [RD-12].

Users of potential products of active layer thickness are interested in high temporal resolution: monthly or higher in [RD-12]. Less than 10 % of users rated annual resolution as adequate as target temporal resolution in [RD-12] despite the definition of the true ECV ALT as the maximum thaw depth in summer with a maximum temporal resolution of one year. We assume that user interests in higher temporal resolution are linked to the more frequent active layer depth (ALD) data during summer, however ALD measurements revealing needed data on the progression of the thaw throughout the summer are not the target of our ECV-focused annual temporal resolution approach as seasonal thaw depth evolution is not considered an ECV (see also glossary in section 1.7). Half of the user group are satisfied with a target spatial resolution of 1 km². The first release of the Permafrost_cci *CRDPv0 ALT* provided annual resolution with 1 km² spatial resolution from 2003 to 2017, Permafrost_cci *CRDPv1* to *v4 ALT* provide an annual resolution with 1 km² spatial resolution and in addition covering longer time spans from 1997 to 2018, 1997 to 2019, 1997 to 2021, and 1997 to 2023, respectively.

4.2 Permafrost cci ALT Match-up Analyses with In Situ Data

For each in situ measurement location, the grid cell in Permafrost_cci ALT products closest to the in situ measurement was extracted to produce the match-up dataset and derive comparisons and summary statistics. Note that we assess the fitness of Permafrost_cci ALT with focus on the Northern hemisphere high-latitude continuous permafrost region. The midlatitude discontinuous permafrost regions on high plateaus in Mongolia, Central Asia and the Tibetan Plateau (China) are characterised by very different snow regimes and subground properties requiring further model parameterisation. We therefore excluded all sites in Mongolia, Central Asia, and on the Tibetan Plateau (China) to allow an adequate assessment of mid-latitude to high-latitude permafrost regions.

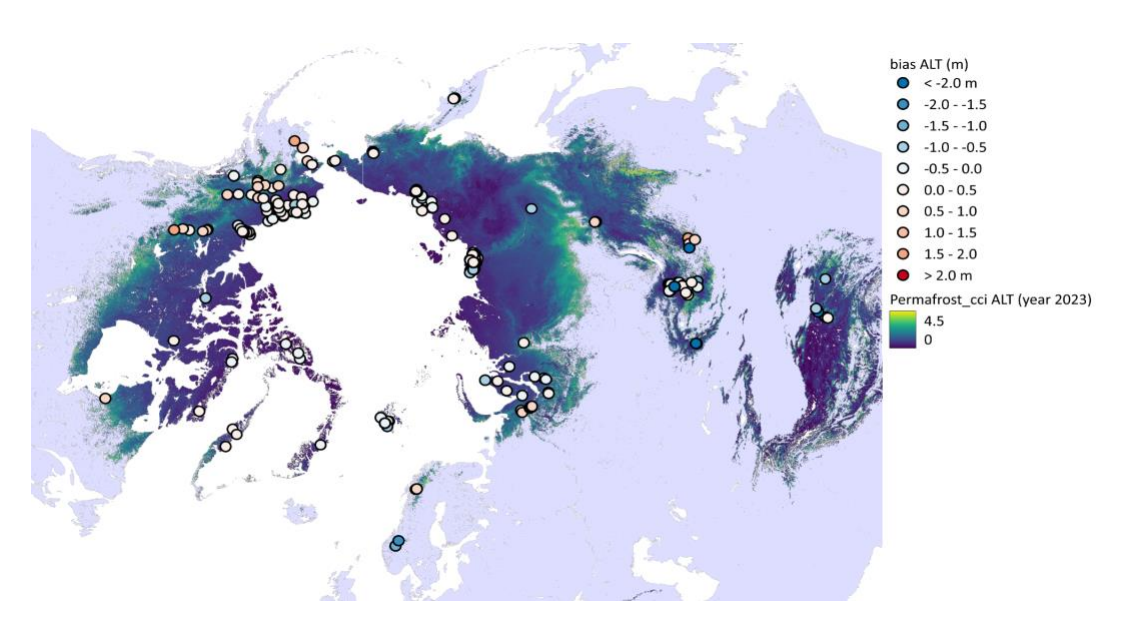


Figure 4.2. ALT bias (color-coded point symbols) over mapped Permafrost_cci ALT 2023 in the Northern hemisphere.

The majority of sites (Figure 4.2) and match-up pairs (Figure 4.3) in the Northern hemisphere range within a bias between -0.5 m to 0.5 m. The majority of these in situ ALT sites are located in the most Northern regions with a shallow ALT below 1 m. The value range of positive bias > 1 m (deep Permafrost_cci ALT versus shallow in situ ALT) occurs in few match-up pairs in Alaska, Canada and Russia at the southern boundary of permafrost in regions with deeper ALT. Large negative bias values > -1 m (shallow Permafrost_cci ALT versus deep in situ ALT) occurs in rocky, dry terrain with a deep in situ active layer, in Svalbard, mountain regions in Scandinavia, the Central Asian mountain plateaus, and on the Tibetan plateau (Figure 4.2, 4.4, 4.5).

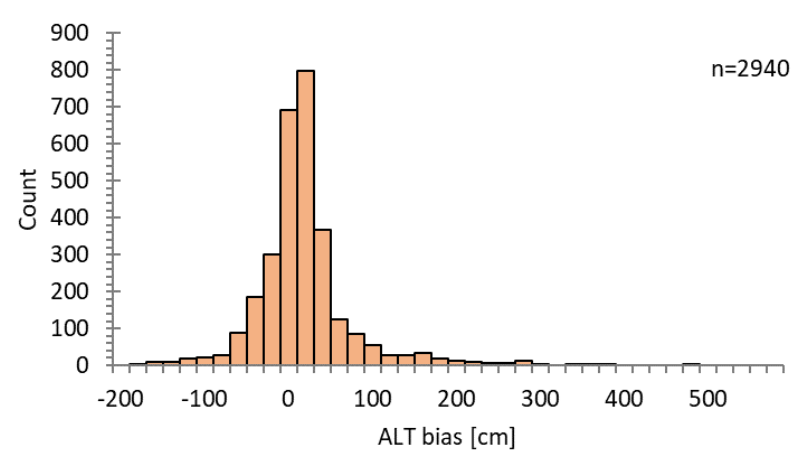


Figure 4.3. Frequency distribution of Permafrost_cci ALT minus in situ ALT. Summary statistics including all ALT match-up data pairs and with locations from Swiss Mountains, Mongolia, and Tibetan plateau (China) excluded (n = 497). Positive bias values are due to deeper Permafrost_cci ALT than the in situ value and negative bias values due to lower Permafrost_cci ALT.

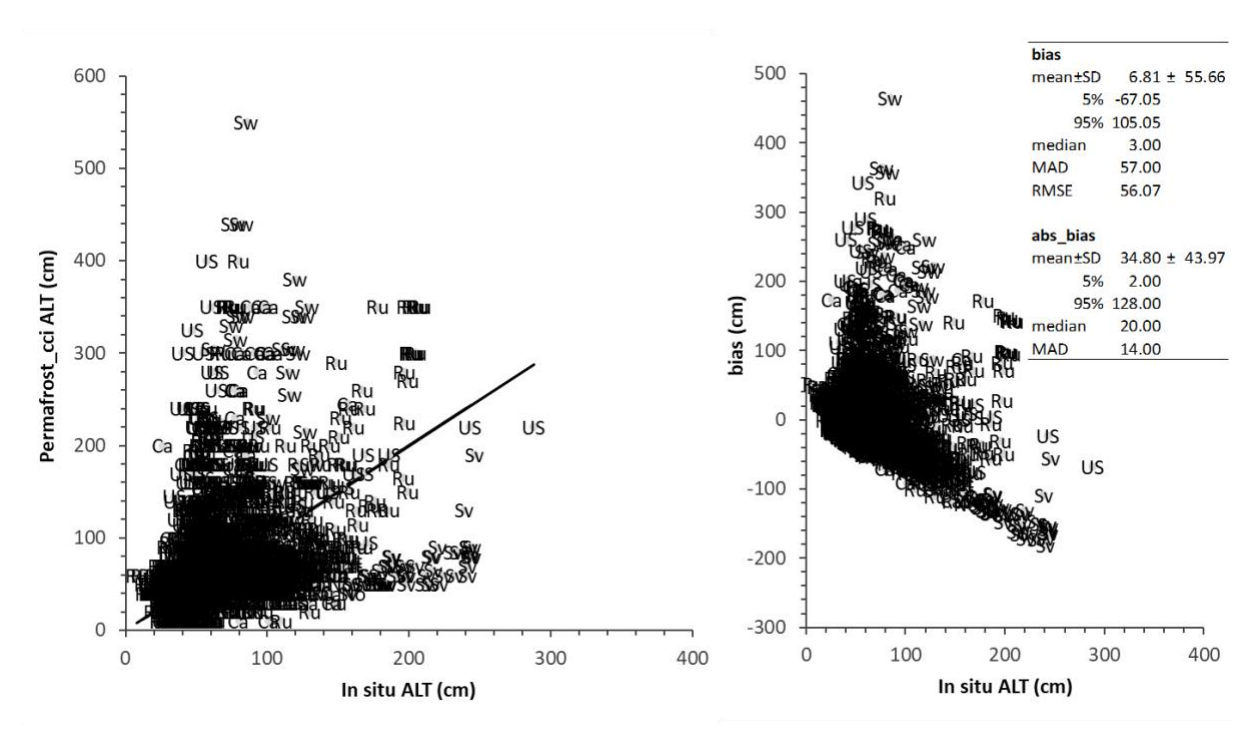


Figure 4.4. Left Panel: x=in situ ALT vs y=Permafrost_cci ALT with a black solid 1:1 reference line. Right Panel: x=in situ ALT, y=corresponding bias (Permafrost_cci ALT minus in situ ALT. Labels = Country. The table-insert includes summary statistics on the bias and absolute bias (SD=standard deviation, MAD=median absolute deviation, RMSE=root mean square error).

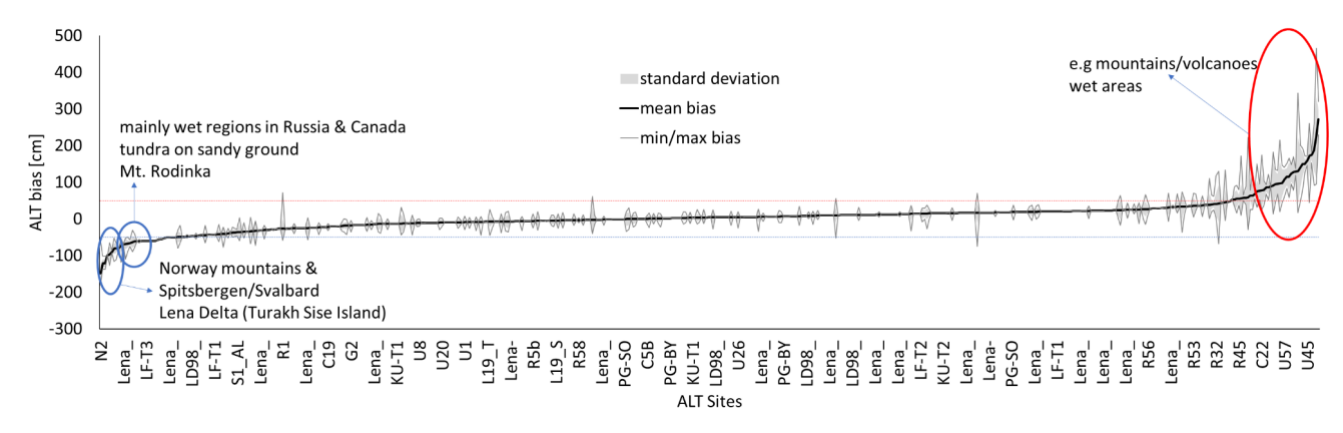


Figure 4.5. Mean bias of ALT (Mongolia, China and Swiss Mountains excluded), including SD and min/max bias. x-Axis shows the single sites, sorted by mean bias. Blue line = bias -50 cm (Permafrost_cci ALT too shallow), red line = bias +50 cm (Permafrost_cci ALT too deep).

Permafrost_cci ALT and in situ ALT consensus in temporal trends

Table 4.1. Gleichläufigkeit (glk) and temporal stability (ts) per year of Permafrost cci ALT time series.

Year	glk	ts	#
1998	0.96	1.39	148
1999	0.83	-2.36	93
2000	0.72	-0.18	92
2001	0.59	1.31	85
2002	0.82	-0.62	92
2003	0.63	-2.97	80
2004	0.67	9.62	88
2005	0.87	1.17	112
2006	0.83	-4.70	93
2007	0.60	4.37	99
2008	0.83	-8.58	115
2009	0.53	6.83	112
2010	0.79	-7.96	120
2011	0.62	6.51	116
2012	0.64	-1.38	114
2013	0.85	-1.55	173
2014	0.78	1.47	143
2015	0.61	1.22	114
2016	0.75	4.32	130
2017	0.70	-2.98	102
2018	0.64	4.09	101
2019	0.89	-5.77	136
2020	0.68	10.37	76
2021	0.82	1.74	107
2022	0.70	0.86	95
2023	0.52	0.87	78
MEAN	0.75	0.54	108.23

Table 4.2. Summary statistics per site for Gleichläufigkeit (glk), temporal stability (ts) and absolute temporal stability (abs_ts) of Permafrost_cci ALT time series.

	glk		ts		abs_ts	
mean±SD	0.73 ±	0.16	0.58 ±	7.84	16.13 ±	13.50
5%	0.00		-15.00		6.21	
95%	1.00		13.88		40.35	
median	0.72		0.29		12.08	

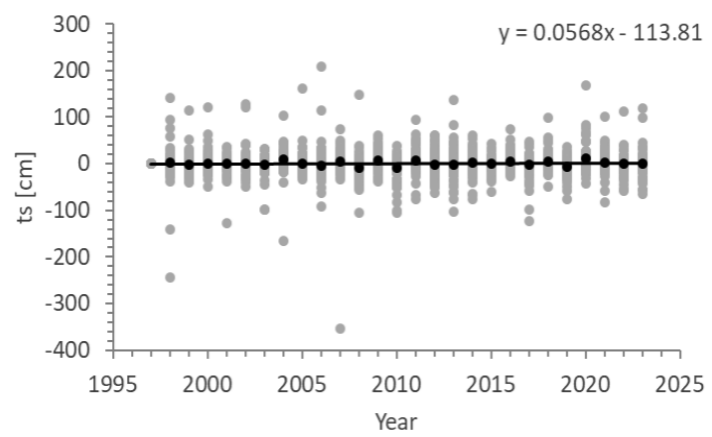


Figure 4.6: Temporal stability (ts, year-to-year change in magnitude of the bias [cm]) for the bulk ALT dataset including updated GTN-P/CALM data (Mongolia, China and Swiss Mountains excluded) and new data sources (ALLENA, MyThaw). Black dots are the mean values, the thin black line is the linear regression through all points.

The Gleichläufigkeit and the temporal bias stability analyses, see also Tables 4.1, 4.2 and Figure 4.6 show a match in the trend across years with a mean of around 73 % for the Gleichläufigkeit and low bias variations across the years for the ALT bulk data collection.

Comparison of ALT bias PVIRv4 vs PVIRv5

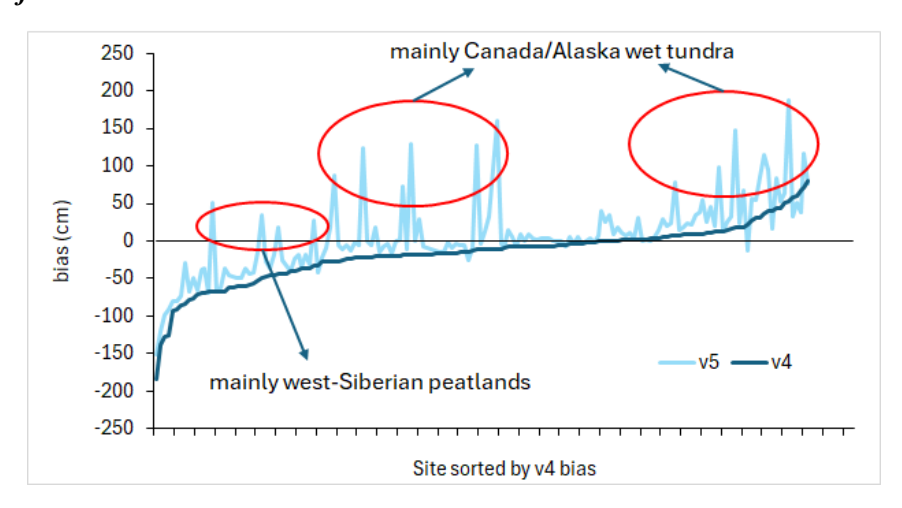


Figure 4.7 Comparison of ALT bias in situ vs Permafrost_cci of PVIRv4 (dark blue) vs PVIRv5 (light blue) per match up site. Sites are sorted by size of v4 bias from negative to positive.

The comparison of the ALT bias in PVIRv4 versus this validation data collection in PVIRv5 was carried out using only the same sites, i.e. no additional new sites or years, and in addition with the newly removed sites in PVIRv5 also removed in Permafrost_cci ALTv3 (Figure 3.7). Permafrost_cci ALTv4 (2025) shows a much better performance with a smaller ALT underestimation for Western Siberian peatlands, i.e. resulting in a much smaller negative bias value range. In general, ALTv4 performs with a lower negative bias, i.e. ALT is less too shallow. However, ALTv4 performs slightly less as ALTv3 at several wet tundra sites in the Canadian and Alaskan tundra region, ALTv4 does show more overestimated ALT compared to in situ shallow ALT, i.e., resulting in a higher positive bias value range than Permafrost_cci ALTv3 (2023).

D.4.1 Product Validation and Inter-	CCI+ PHASE II – NEW ECVS	Issue 5.1
Comparison Report (PVIR)	Permafrost	30 October 2025

Regional Assessments

Table 4.3 Bias, absolute bias, Gleichläufigkeit (glk) and temporal stability (ts) of Permafrost_cci ALT time series per region. Note the high performance for the North American domain (Alaska (US) and Canada).

	bias	abs_bias	glk	ts
Region	(cm)	(cm)		(cm)
Canada	6.03	51.35	0.73	2.35
Greenland	-14.16	18.40	0.65	-0.38
Russia	6.21	31.97	0.81	0.40
Sweden	134.21	136.02	0.80	7.12
Svalbard	-67.13	73.04	0.72	1.06
US	14.78	24.88	0.69	-0.04
China	-101.50	108.61	0.60	0.48
Mongolia	-114.73	159.57	0.56	0.27

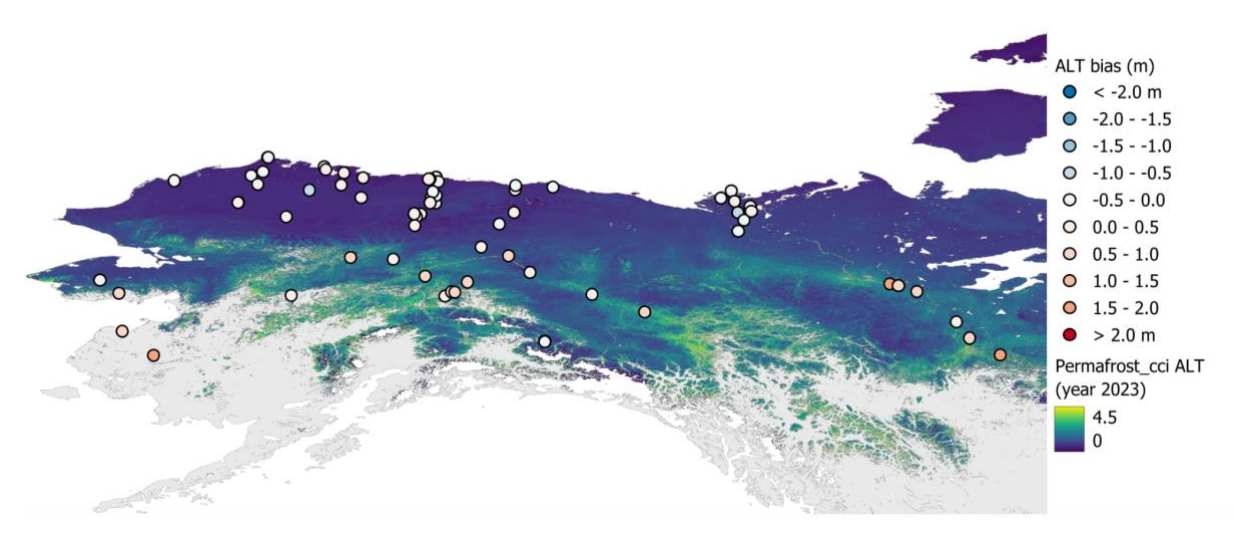


Figure 4.8 ALT bias (color-coded point symbols) over mapped Permafrost_cci ALT 2023 in north-western America.

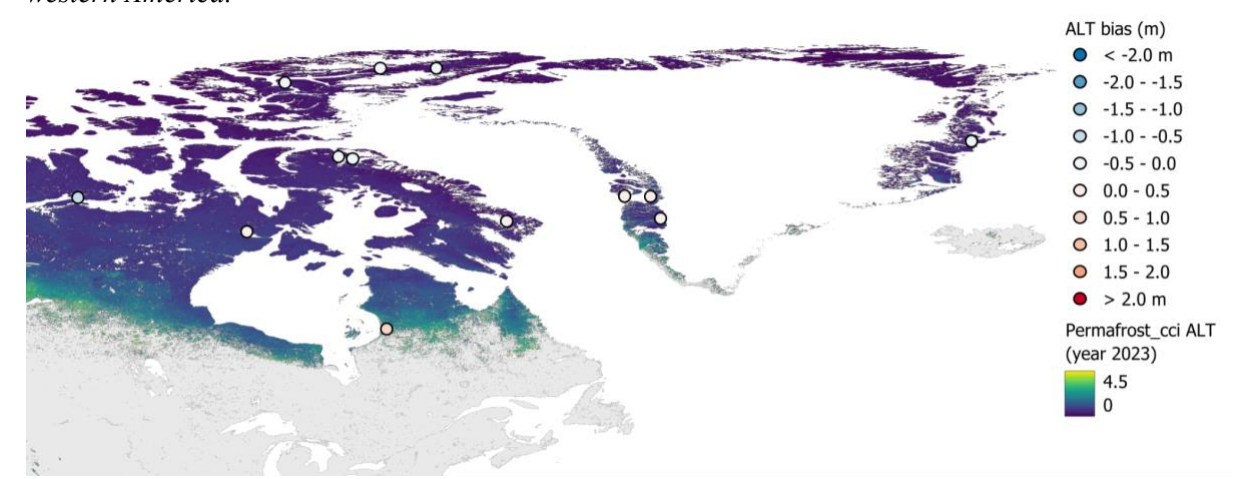


Figure 4.9. ALT bias (color-coded point symbols) over mapped Permafrost_cci ALT 2023 in north-eastern America and Greenland.

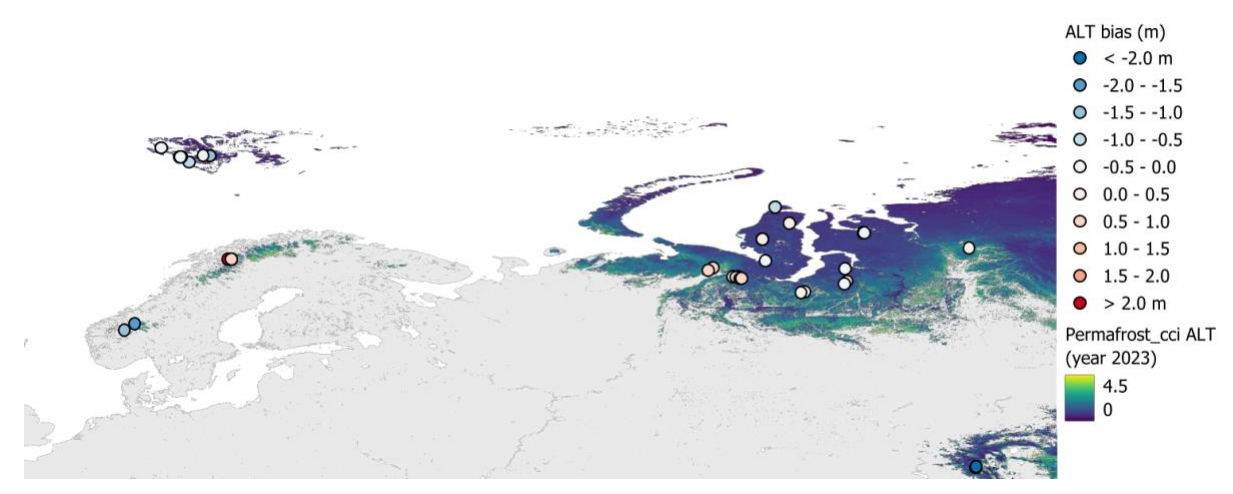


Figure 4.10 ALT bias (color-coded point symbols) over mapped Permafrost_cci ALT 2023 in northern Europe and western Siberia.

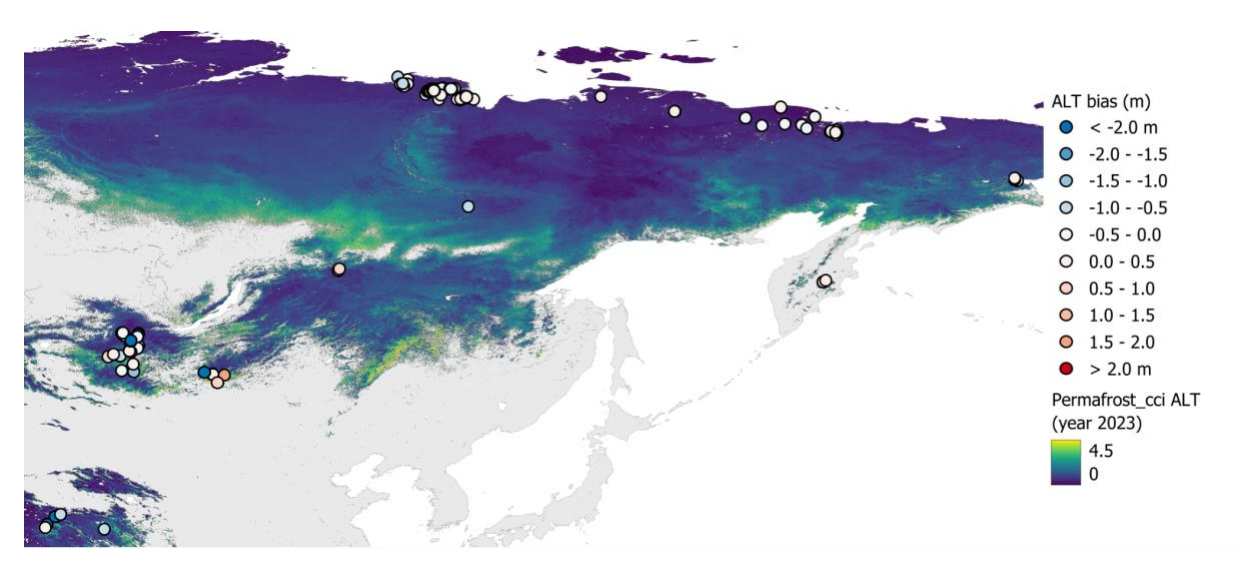


Figure 4.11 ALT bias (color-coded point symbols) over mapped Permafrost_cci ALT 2023 in central to eastern Siberia, Mongolia and Tibetan Plateau (China).

Regional Assessment – Antarctica

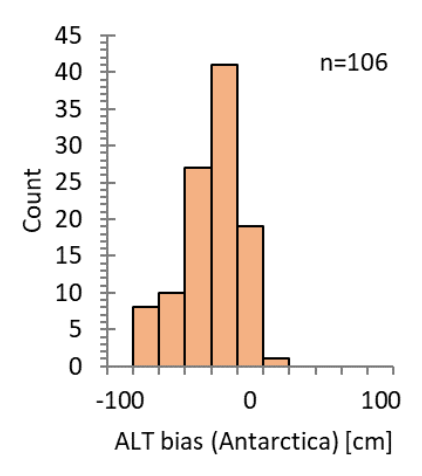


Figure 4.12. Frequency distribution of Permafrost_cci ALT minus in situ ALT in Antarctica. Summary statistics including all ALT match-up data pairs. Positive bias values are due to deeper Permafrost_cci ALT than the in situ value and vice versa.

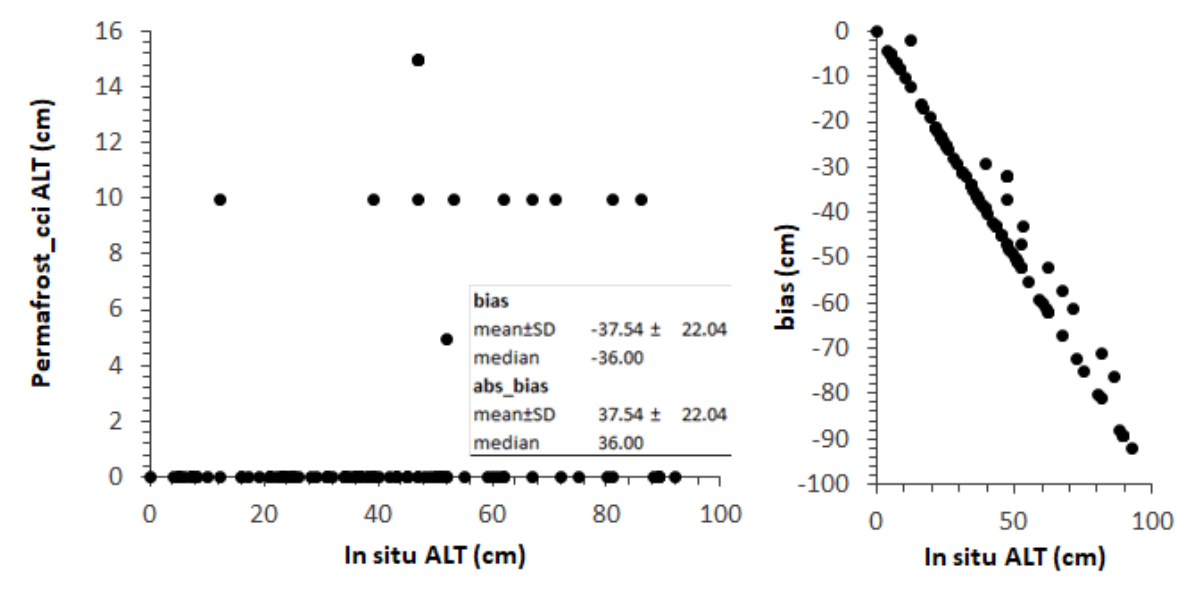


Figure 4.13. Left Panel: x=in situ ALT in Antarctica vs $y=Permafrost_cci$ ALT. Right Panel: x=in situ ALT, y=corresponding bias ($Permafrost_cci$ ALT minus in situ ALT).

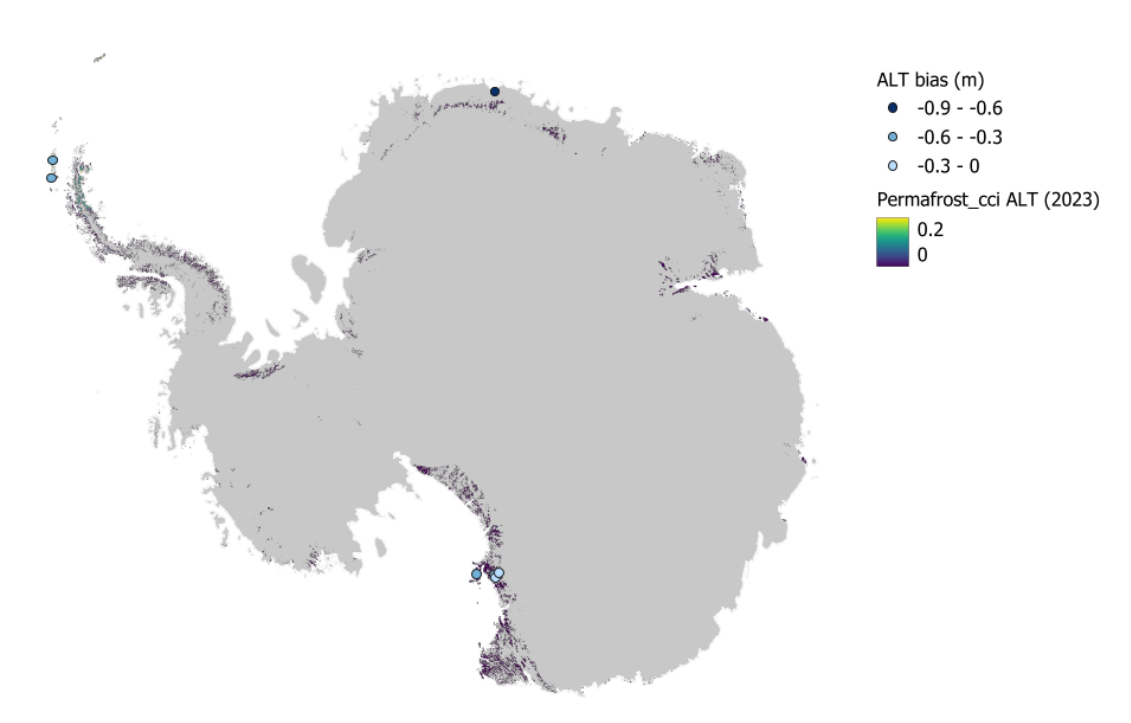


Figure 4.14. ALT bias (color-coded point symbols) over mapped Permafrost_cci ALT 2023 in Antarctica (source background map: Quantarctica, Matsuoka et al. 2021).

For the inland ice-free permafrost regions in Antarctica data are not sufficient for a thorough statistical analysis. In general, the in-situ measurements represent a wide measurement range down to depths of 1 m, in contrast to Permafrost_cci with ALT with a very low value range only < 0.2 m ALT (Figure 4.12).

The tendency of Permafrost_cci ALT compared to the available in situ data for inland ice-free permafrost regions in Antarctica is negative, i.e. Permafrost_cci performs with too shallow ALT depths, despite characteristic for dry, rocky terrain are deep in situ ALT data (Figure 4.13, 4.14).

D.4.1 Product Validation and Inter-	CCI+ PHASE II – NEW ECVS	Issue 5.1
Comparison Report (PVIR)	Permafrost	30 October 2025

In summary, Permafrost_cci ALT (1997–2023) shows the following performance characteristics:

- a mean bias of 0.07 m, however with a large standard deviation of ± 0.56 m and a median bias of 0.03 m, MAD of 0.57 m, RMSE of 0.56 m.
- the high magnitude positive bias occurrence > 1 m (deep Permafrost_cci ALT versus shallow in situ ALT) occurs only in a few match-up pairs in Alaska, Canada and Russia in the southern boundary zones of Permafrost. A high magnitude negative bias occurrence > -1.5 m mainly occurs in Svalbard, and in Northern Scandia in rocky and pebble terrain (shallow Permafrost cci ALT versus deep in situ ALT).
- the mean temporal stability (ts, year-to-year change in magnitude of the bias) ranges around 0.01 m, with variation mainly in the range of ±0.08 m and high gleichläufigkeit (glk, fraction of same-directional year-to-year changes) shows a robust temporal stability around 73 %.
- for the inland ice-free permafrost regions in Antarctica data are not sufficient for a thorough statistical and time series analysis. The tendency of Permafrost_cci ALT compared to the available in situ data for inland ice-free permafrost regions in Antarctica is negative, i.e., Permafrost cci performs with too shallow ALT depths.

5 ASSESSMENT RESULTS: PERMAFROST EXTENT

5.1 Permafrost_cci PFR Match-up Analyses with In Situ Data

The match-up dataset contains in situ binary information on permafrost existence (FALSE/TRUE) and Permafrost_cci PFR across different percentage groups (0,14,29,43,57,71,86,100 %). Using both, ALT and MAGT in situ measurements across the first 300 cm (Figure 5.2) as proxies for permafrost abundance, the match-up dataset contains 7,032 match-up pairs at 1,045 sites (Figure 5.1).

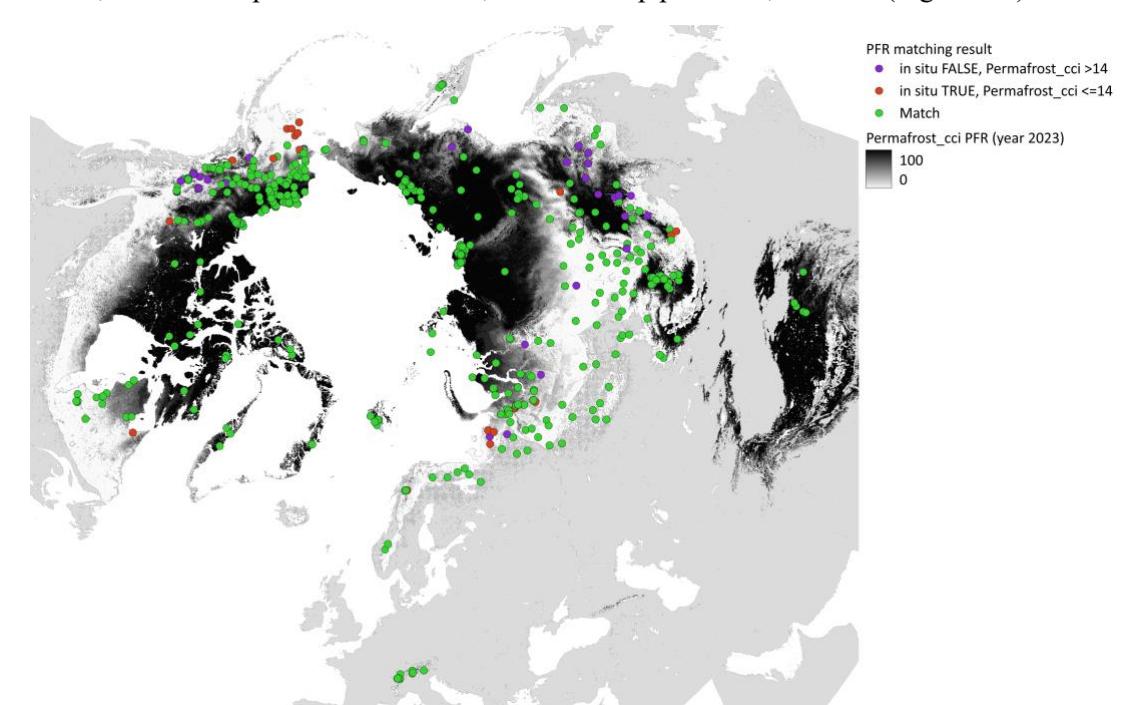


Figure 5.1. PFR match-up sites (color-coded point symbols grouped by matching characteristics with color-coded green points representing 'Match') over mapped Permafrost_cci PFR 2023 in the Northern hemisphere.

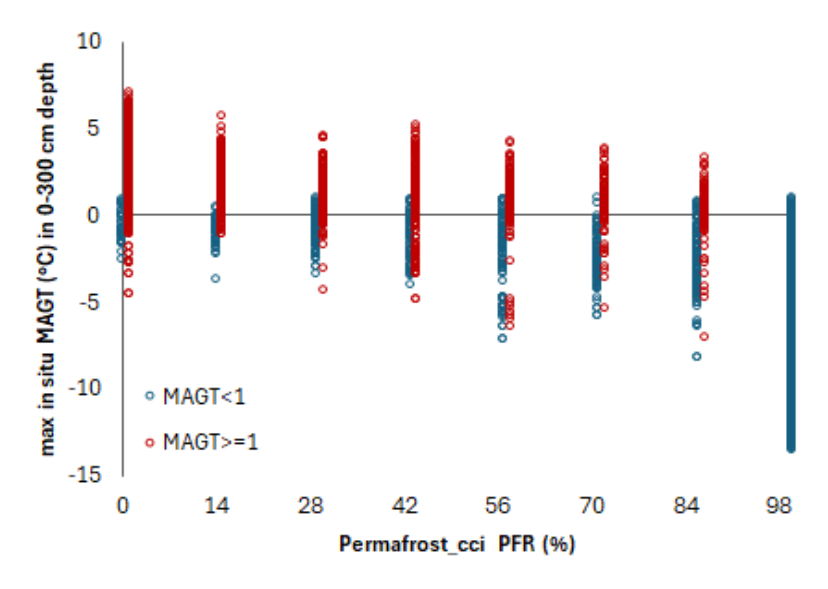


Figure 5.2. Maximum in situ MAGT in 0-300 cm depth per Permafrost cci PFR percentage (%).

As a consequence of the cold bias in the warm temperature range, the binary match-up of 'permafrost' versus 'no permafrost' shows that Permafrost_cci PFR in the grid cell is overestimated compared to in situ-derived 'no permafrost'. Overall, the majority of match-up pairs (88.64 % for case PFR \leq 14 % and 86.66 % for case PFR \leq 29 %) are in agreement between the in situ proxy and Permafrost_cci PFR (Figure 5.3a,b). Notably, Permafrost_cci PFR = 100 % and PFR = 0 % have a high percentage of agreement, with 98.93 % and 90.09 % match, respectively.

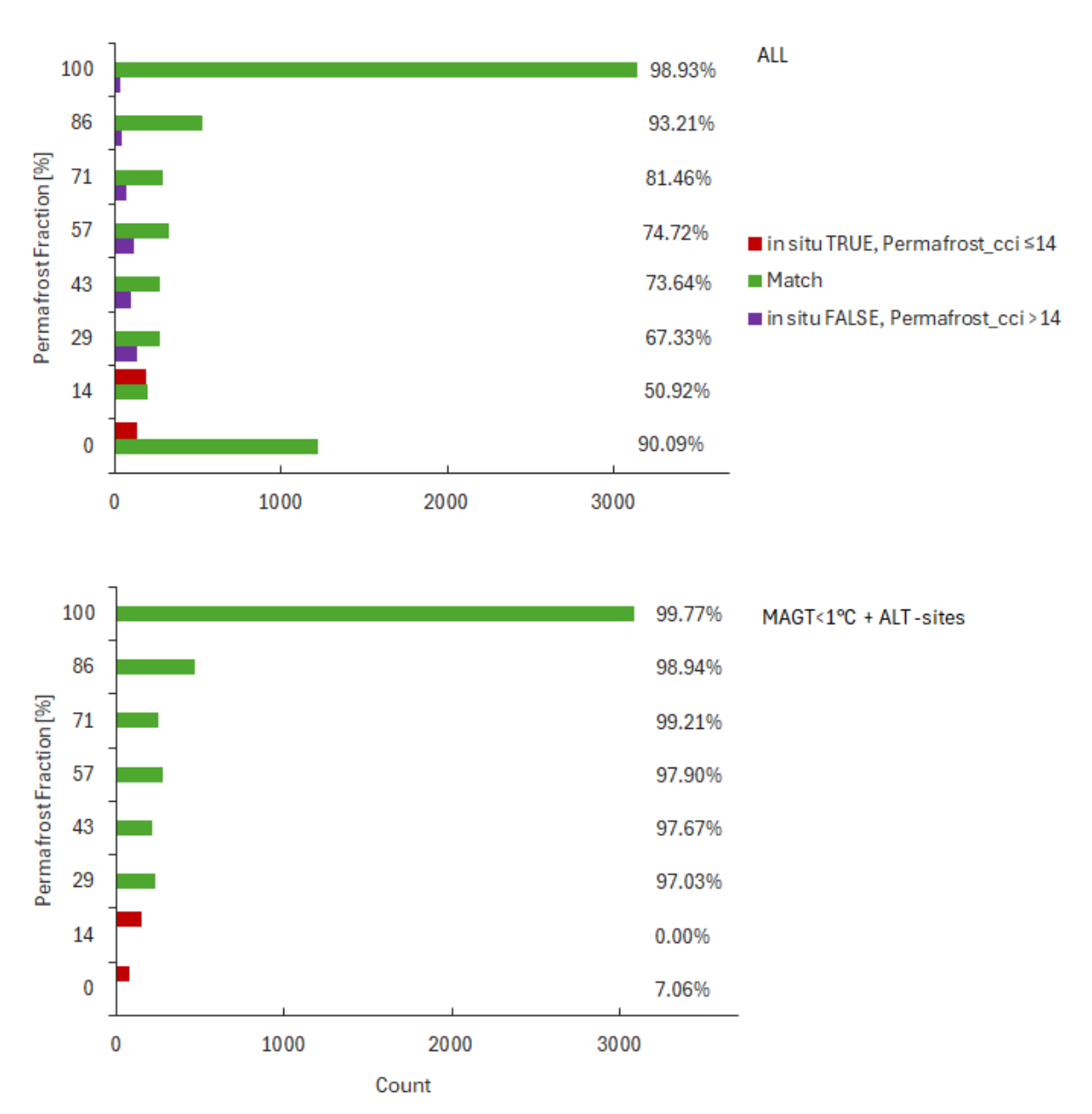


Figure 5.3a. Match-up summary of Permafrost_cci PFR vs. in situ MAGT and ALT datasets. The percentage values depict the amount of matches compared to all match-up pairs. The upper panel consists of all match-up pairs, the lower panel only cold sites with MAGT < 1 °C (all ALT sites are classified as "cold" sites). Permafrost cci PFR \leq 14 % is classified as "no permafrost".

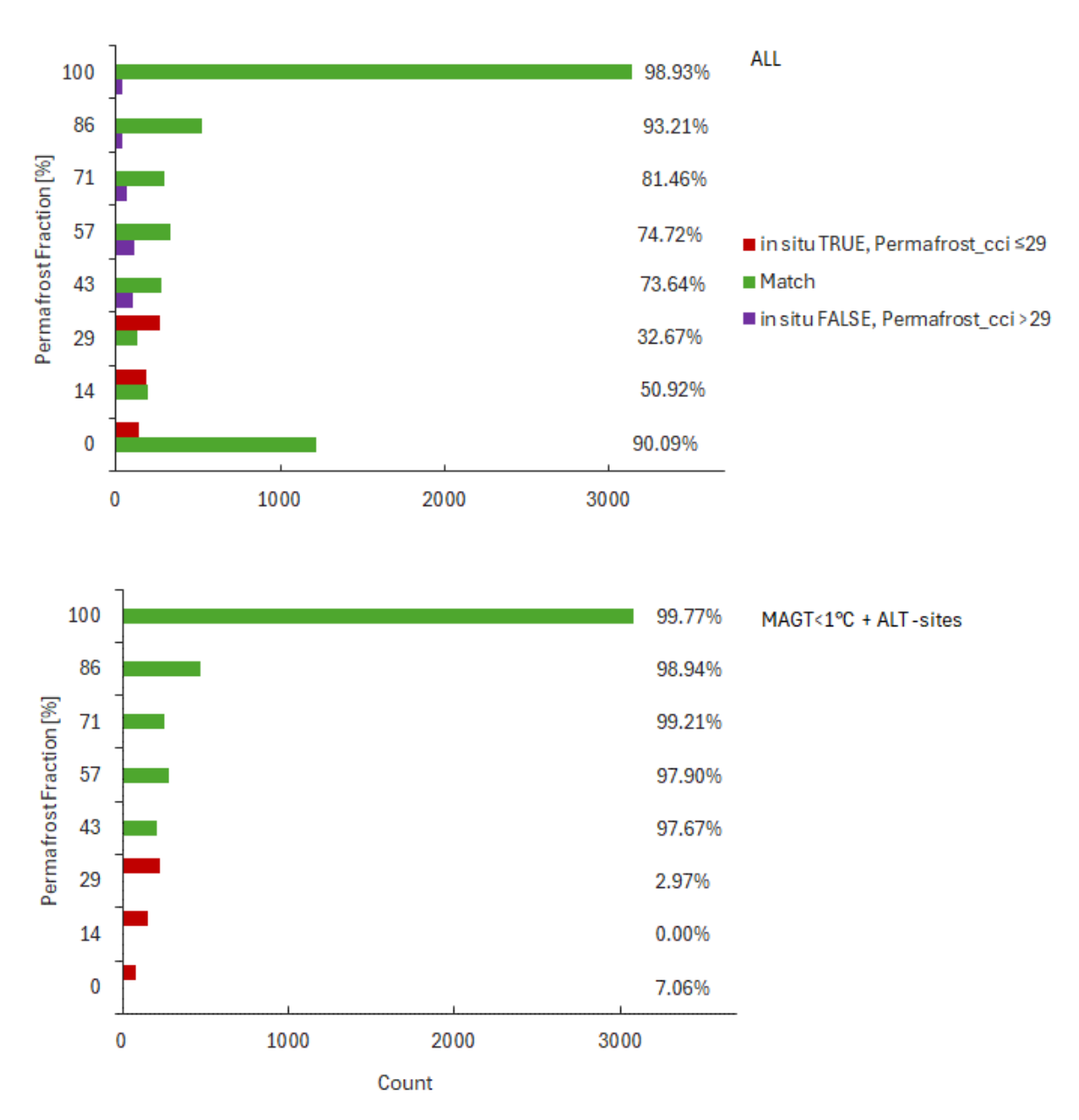


Figure 5.3b. Match-up summary of Permafrost_cci PFR vs. in situ MAGT and ALT datasets. The percentage values depict the amount of matches compared to all match-up pairs. The upper panel consists of all match-up pairs, the lower panel only cold sites with MAGT < 1 °C (all ALT sites are classified as "cold" sites). Permafrost_cci PFR \leq 29 % is classified as "no permafrost".

Permafrost cci PFR and in situ permafrost abundance consensus in temporal trends

We checked for Gleichläufigkeit (glk), by checking the amount of match-up pairs showing changes in the same direction (e.g. from 'permafrost' to 'no permafrost') or no changes. The glk gives the fraction of same-directional changes. The temporal stability was assessed differently to that of MAGT and ALT, as we have only a binary yes/no assessment. We thus checked, in how many cases we get the same result for matches in Permafrost abundance. For ts_all, all matchup-pairs having the same matching result (either a match or no match) from one year to the next get an "1". Different matching results get a "0", ts_all is thus the fraction of no-changes in matching.

For ts_pos, only match-up pairs having a true match get an "1" if this matching is stable from one year to the next. Changing matching results as well as pairs with a no-match get a "0" with ts_pos representing the fraction of no-changes in true matching compared to all match-up pairs. The Gleichläufigkeit shows a high temporal stability across the years across all Permafrost_cci PFR fractions, specifically for the permafrost endmembers 0 % and 100 %. Also, for ts_all, representing no-changes in matching the stability across the years is high for 0 % and 100 %. In contrast, ts_pos shows a high stability for the matching of permafrost abundance for the highest fraction (100 %) across years and a data artefact for not matching anymore in the most recent years, as we do not have updated data anymore from RHM since 2015, the majority of our sites in non-permafrost areas. The result is thus based on very few sites classified as non-permafrost in Permafrost_cci, without a corresponding match in the in situ data.

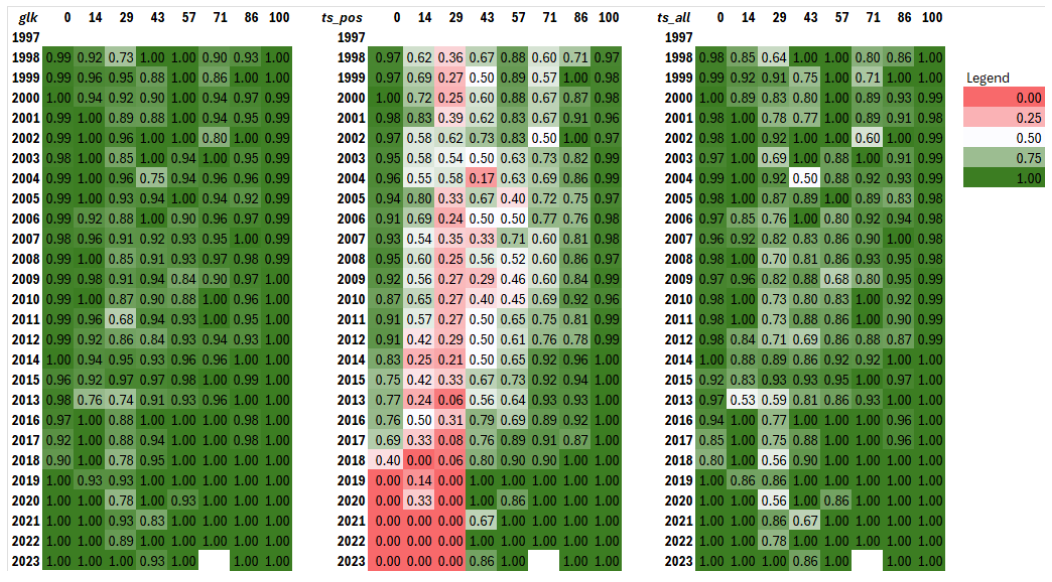


Figure 5.4: Match-up summary of Permafrost_cci PFR in % (0,14,29,43,57,71,86,100 %) with in situ MAGT and ALT dataset over years, with Gleichläufikeit (glk) shown in the left panel, temporal stability of positive matches (ts_pos) in the middle panel (i.e. for how many of all sites the matchup is constantly TRUE in two consecutive years) and temporal stability of all matches (ts_all) in the right panel (i.e. for how many of all sites the matchup is constantly TRUE OR FALSE in two consecutive years). Permafrost_cci PFR \leq 29 % is classified as 'no permafrost'.

Table 5.1 Permafrost abundance matching statistics, Gleichläufigkeit (glk) and temporal stability (ts) of Permafrost cci PFR time series per region.

	in situ FALSE, Permafrost _cci >14	Match	in situ TRUE, Permafrost _cci ≤14	glk	ts pos	ts all
		Count			Fraction	
US	3	119	17	0.99	0.87	0.98
Canada	25	132	17	0.93	0.71	0.87
Greenland	0	8	0	1.00	1.00	1.00
Svalbard	0	16	0	1.00	1.00	1.00
Scandinavia	0	10	7	0.98	0.88	0.97
Europe	0	9	1	1.00	0.96	0.99
Russia	13	581	35	0.97	0.84	0.95
China	0	5	0	1.00	1.00	1.00
Mongolia	0	39	6	0.99	0.88	0.97

D.4.1 Product Validation and Inter-	CCI+ PHASE II – NEW ECVS	Issue 5.1
Comparison Report (PVIR)	Permafrost	30 October 2025

Regional Assessment

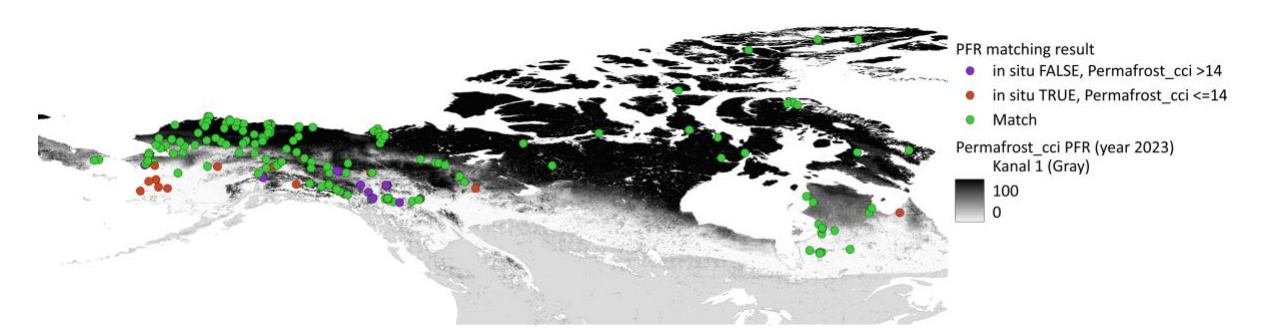


Figure 5.5 PFR match-up sites (color-coded point symbols grouped by matching characteristics with color-coded green points representing 'Match') over mapped Permafrost_cci PFR 2023 in northern America.



Figure 5.6 PFR match-up sites (color-coded point symbols grouped by matching characteristics with color-coded green points representing 'Match') over mapped Permafrost_cci PFR 2023 in Greenland and northern Europe.

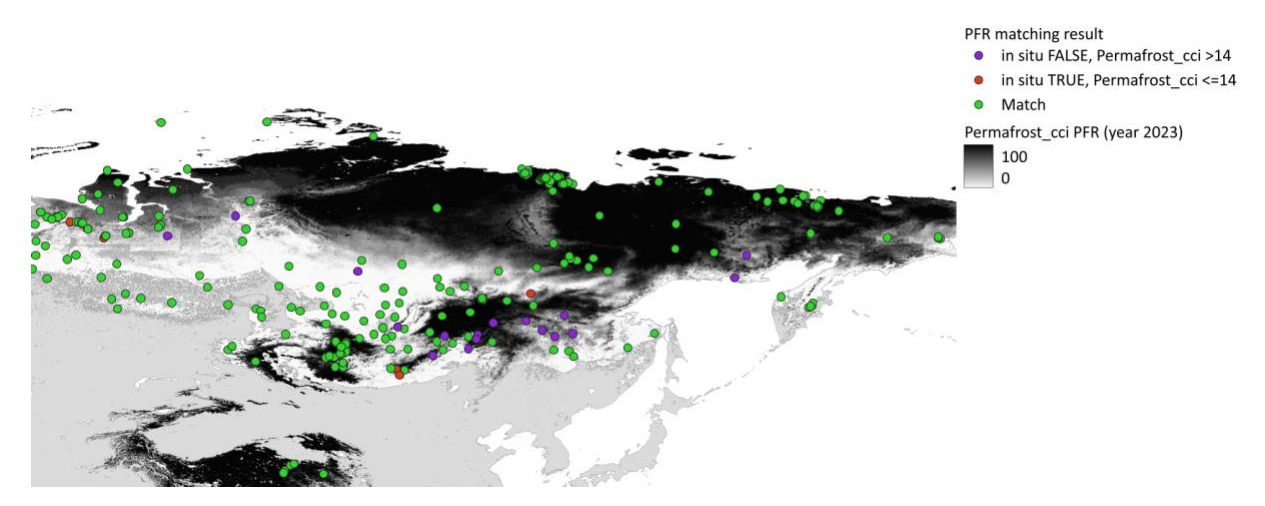


Figure 5.7 PFR match-up sites (color-coded point symbols grouped by matching characteristics with color-coded green points representing 'Match') over mapped Permafrost_cci PFR 2023 in Siberia and Mongolia.

D.4.1 Product Validation and Inter-	CCI+ PHASE II – NEW ECVS	Issue 5.1
Comparison Report (PVIR)	Permafrost	30 October 2025

In summary, Permafrost_cci PFR (1997–2023) shows the following performance characteristics:

- overall, the majority of match-up pairs (88 % for case Permafrost_cci PFR ≤ 14 % and 84 % for case PFR ≤ 29 %) are in agreement between the in situ proxy for permafrost abundance yes / no and Permafrost cci PFR abundance yes / no.
- notably, Permafrost_cci PFR = 100 % and PFR = 0 % show high percentage of agreement, with 99 % and 90 % match, respectively.
- geographically, most mismatches in permafrost abundance are located in the southern boundary of sporadic permafrost for Western Siberia and Alaska.
- the high agreement in the Permafrost_cci PFR = 100 % and PFR = 0 % groups is stable across years with the exception of the most recent years for the warm temperature subgroup as we lose a considerable number of non-permafrost sites from the Roshydromet source (Russia) covering Eurasia that is not provided anymore as open dataset.

5.2 PERMOS Permafrost Extent Comparisons

There is a considerable enhancement of the Permafrost_cci PFR product performance in high mountain landscapes. Figure 5.8 compares Permafrost_cci PFR in 2023 in the Bas-Valais region, Alps, with the locations of the PERMOS boreholes (yellow points) and the ESA GlobPermafrost slope movement inventory for the same region (green polygons).

Similar to the assessment of Permafrost cci CRDP PFR v3, in Permafrost cci CRDP PFR v4, the majority of PERMOS boreholes (n = 12) except two boreholes (n = 2) are located within Permafrost cci PFR ranging from PFR = 14 % to 100 %. Within the ESA GlobPermafrost RGIK inventory (2023), we selected only the landforms classified as active rock glaciers, push moraines or a complex combination of the two, since they are the ones representative of permafrost occurrence. The blue colored grid cells in Fig. 5.8 represent Permafrost cci PFR > 0 % in 2023. In this assessment of Permafrost cci CRDP PFR v4, similarly to the previous assessment of Permafrost cci CRDP PFR v3, the permafrost extent in the Permafrost cci PFR product (i.e. PFR > 0 %) seems too restricted compared to the ESA GlobPermafrost RGIK inventory. The lowermost extremities of the majority of the inventoried permafrost-related RGIK landforms are located outside of Permafrost cci PFR > 0 % indicating that the Permafrost cci PFR lower elevation limit of permafrost is still too high. This is consistent with the Permafrost cci GTD bias reported in 3.3 for the same

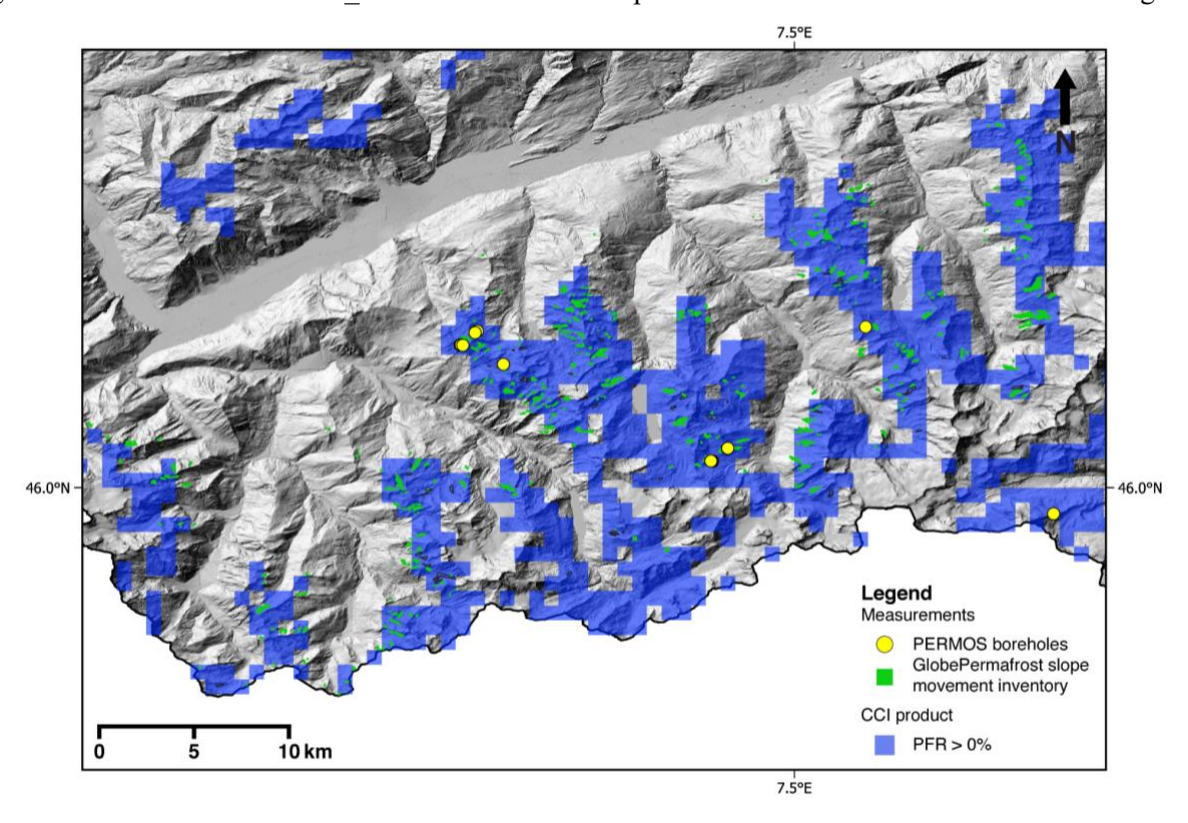
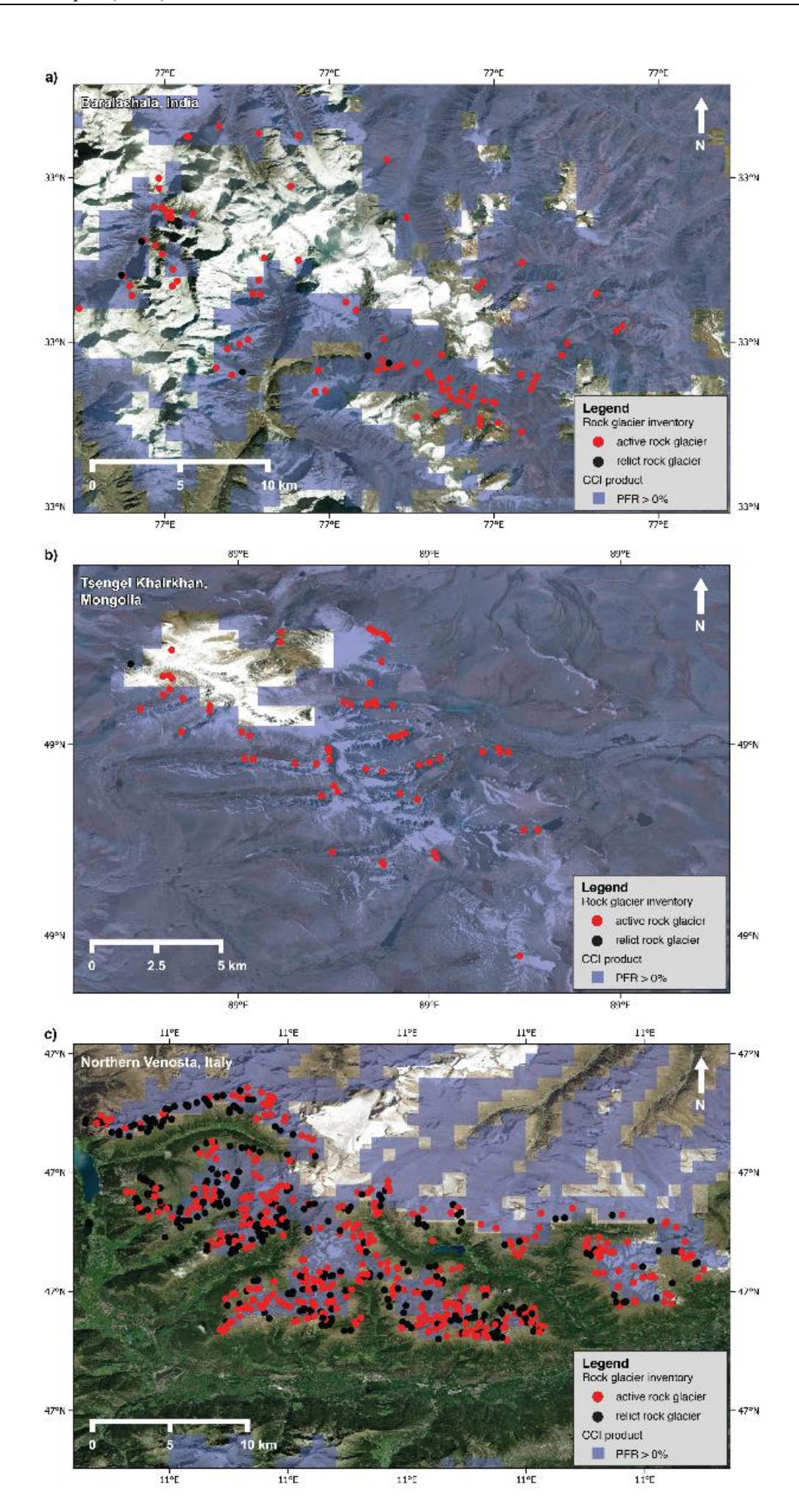


Figure 5.8. Overview of Permafrost_cci PFR in 2023 in Bas-Valais (CH) compared to the ESA GlobPermafrost slope movement inventory and PERMOS permafrost monitoring borehole locations.



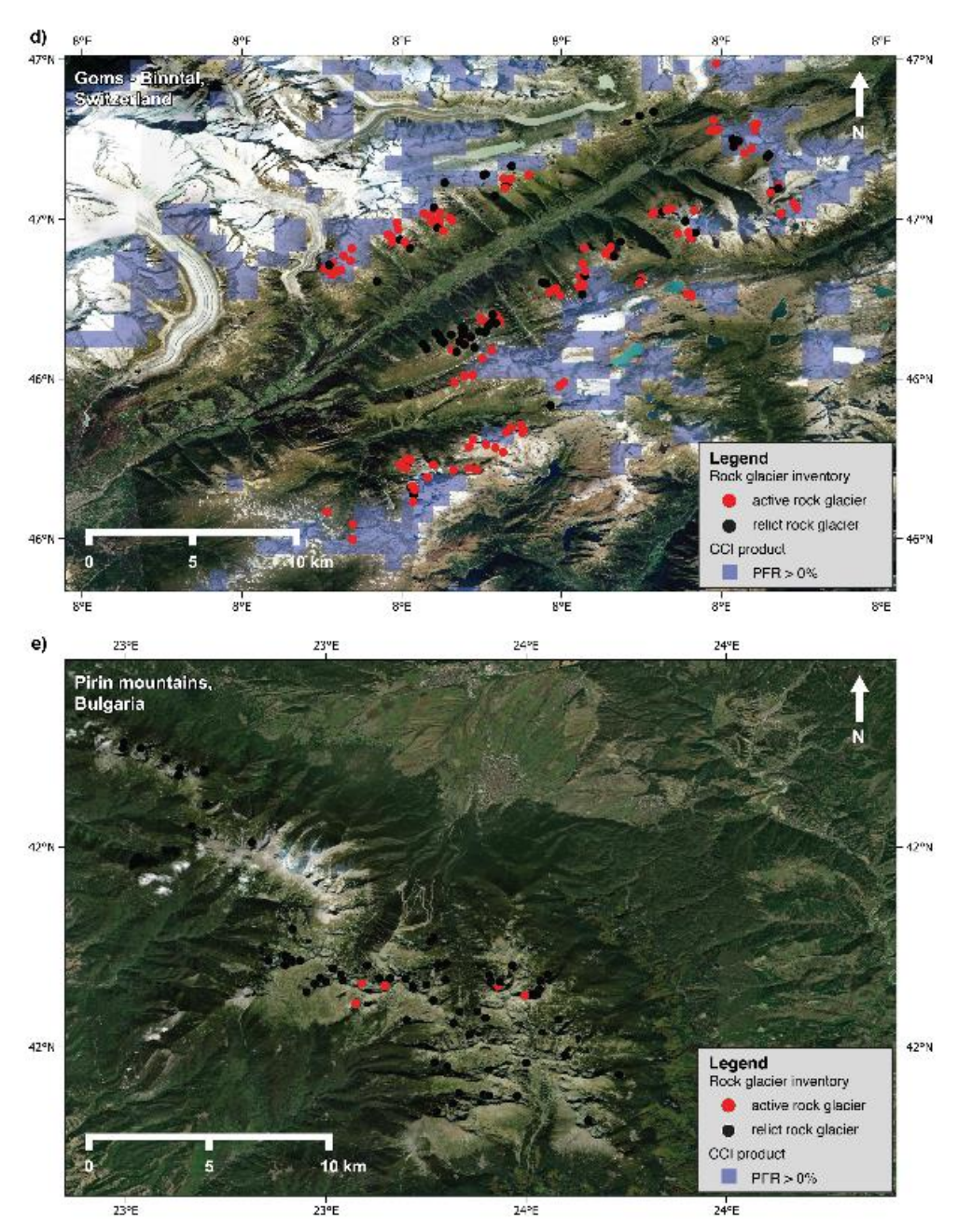


Figure 5.9. Overview of Permafrost_cci PFR permafrost extent in 2023 compared to the Permafrost_cci phase II rock glacier inventories in Baralachala region (India) (a), Tsengel Khairkhan (Mongolia) (b), Northern Venosta (Italy) (c), Goms and Binntal (Switzerland) (d) and Pirin mountains (Bulgaria) (e). The active and transitional rock glaciers are indicated in red circles, the relict rock glaciers are indicated in black circles.

D.4.1 Product Validation and Inter-	CCI+ PHASE II – NEW ECVS	Issue 5.1
Comparison Report (PVIR)	Permafrost	30 October 2025

Looking at additional regions worldwide (Figure 5.9), one can see that the Permafrost_cci PFR permafrost extent fits well with the Permafrost_cci phase II rock glacier inventory products in general. Active rock glaciers can be used as indicators of the occurrence of permafrost whereas relict landforms indicate its absence. In most areas, the 1 km² grid cell resolution Permafrost_cci PFR fails to reproduce the small scale topographical variations and the Permafrost_cci PFR permafrost extent is slightly overestimated in the zones of continuous permafrost. This is true for Disko Island (Western Greenland) and Brooks range (North Alaska). In the discontinuous European permafrost zone of the Troms area (North Norway), at mid-latitudes in Central Asia in the Tien Shan area (Khazastan) and in the Himalayas (India, Nepal and Bhutan) the Permafrost_cci PFR permafrost extent fits well with the inventoried rock glacier and no systematic bias is detected. In the Alps (Goms-Binntal, Southern and Northern Venosta and Vanoise regions), Permafrost_cci PFR shows slightly underestimated permafrost extent, although the majority of the inventoried landforms indicative for permafrost are well represented. In the mountain area of the Carpathians and Pirin mountains, no permafrost is present in the Permafrost_cci PFR product which is consistent with the inventory, where only relict and transitional landforms have been identified.

In summary, Permafrost_cci PFR (1997 to 2023) shows the following performance characteristics in high mountain areas:

- There is a considerable enhancement of the Permafrost_cci PFR product performance across high mountain landscapes worldwide.
- In the Swiss high Alps in general Permafrost_cci PFR is underestimated. Permafrost extent (i.e. PFR > 0%) is too restricted. i.e., most lower extents of inventoried EO-derived rock glacier landforms are located outside of Permafrost_cci PFR > 0 %.
- In the other investigated regions with rock glaciers, Permafrost_cci PFR fits very well. The Permafrost_cci PFR product fits best with the inventoried rock glaciers in the central Asian region (Khazastan), northern Scandinavian region (Troms, Norway) and the Himalayan regions (Nepal, India and Bhutan). In the continuous permafrost area of Brooks mountain range (Alaska), Disko Island (Greenland) and Tsengel region (Mongolia), Permafrost_cci PFR is slightly overestimated (the latter could be due to the conservative criteria for permafrost extent that we defined in this case study as Permafrost_cci PFR > 0%), while in the European Alps (France, Switzerland and Italy) Permafrost_cci PFR is slightly underestimated.

D.4.1 Product Validation and Inter-	CCI+ PHASE II – NEW ECVS	Issue 5.1
Comparison Report (PVIR)	Permafrost	30 October 2025

6 SUMMARY

Permafrost_cci CRDPv4 provides 1 km² pixel resolution ECV products on mean annual ground temperature (MAGT) at discrete depths (product name Ground Temperature per Depth, GTD), Active Layer Thickness (product name ALT) and Permafrost Fraction (product name PFR). All Permafrost_cci CRDPv4 products cover the Northern hemisphere north of 30 °N and new the inland-ice free permafrost regions in Antarctica. Permafrost_cci GTD, ALT and PFR time series from 1997 to 2023 come with an annual resolution. The growing demand for mapped permafrost products needs to accommodate user requirements that span permafrost regions from Scandinavia, Mongolia, Tibetan plateau (China) to higher latitude permafrost in North America, Greenland, Siberia and all altitude ranges from lowland to mountain permafrost. This results in high difficulties of assessing how the Permafrost_cci products perform across a wide range of latitudes, altitudes, climate zones, land cover, and lithologies. The Permafrost_cci product groups (GTD, ALT, PFR) are evaluated using standard match-up statistical approaches, supported by expert knowledge. The match-ups are executed using a pixel-based approach with the in situ data linked to the Permafrost_cci 1 km² product after removing smaller-scale anomalies from the in situ data collection, such as islands, coastal sites, swampy sites and pingos (ice hills).

For in depth Permafrost_cci GTD assessments, the Permafrost_cci product team produced additional GTD at the borehole locations together with Permafrost_cci GTD in 0,1,2,5,10 m depth. The match-up data collection is characterised by a large variability in time, region, and measurement reference depths. Permafrost_cci GTD evaluation shows a mean cold bias of -0.76 °C (std ± 1.73 °C), a median cold bias of -0.95 °C (5 % -3.32 to 95 % 2.26 °C) for the bulk data set and a mean cold bias of -0.87 °C (std ± 1.69 °C), and median cold bias of -1.12 °C (5 % -3.27 to 95 % 2.14 °C) for the depth-interpolated bulk data set. Match-up pairs from the cold temperature subgroup (MAGT < 1 °C) show an even better performance with a small mean bias of 0.03 °C (std ± 1.94 °C) and a median warm bias of 0.23 °C (5 % -3.25 to 95 % 2.89 °C). This cold temperature subgroup shows for the depth-interpolated dataset a small mean bias of 0.06 °C (std ± 1.967 °C) and a median warm bias of 0.26 °C (5 % -3.25 to 95 % 2.93 °C). The trends over years generally match well between the in situ measurements and Permafrost_cci GTD, with a high Gleichläufigkeit (median glk~ 70%) and temporal bias stability (ts ± 0.5 °C) in all years.

In case of the Permafrost_cci PFR assessments, the majority of match-up pairs (88.64 % for case PFR \leq 14 %) is in agreement between the in situ proxies for permafrost abundance and Permafrost_cci abundance yes / no. Notably, Permafrost_cci PFR = 100 % and PFR = 0 % show high percentage of agreement, with 98.93 % and 90.09 % match, respectively. Geographically, most mismatches are located in the Eurasian and Alaskan and Canadian southern boundary of the permafrost extent. The high agreement in the 100 % and 0 % Permafrost cci PFR groups is stable across years.

For the Permafrost_cci ALT assessments, we excluded all sites in Central Asia, Mongolia, on the Tibetan Plateau and in high mountain regions, such as the Alps, due to their different not parameterised lithologies and very high ALT depths. Permafrost_cci ALT performance in high latitude permafrost regions is characterised by a mean bias of 0.07 m, however with a large standard deviation of ±0.56 m and a median bias of 0.03 m, MAD of 0.57 m, and RMSE of 0.56 m. High magnitude positive bias > 1 m (deep Permafrost_cci ALT versus shallow in situ ALT) occurs only in a few match-up pairs in Alaska, Canada and Russia in the southern boundaries of the permafrost zone and high magnitude negative bias > -1.5 m mainly in Svalbard and northern Scandes in rocky and pebble terrain (shallow Permafrost cci ALT versus deep in situ ALT).

D.4.1 Product Validation and Inter-	CCI+ PHASE II – NEW ECVS	Issue 5.1
Comparison Report (PVIR)	Permafrost	30 October 2025

The mean temporal stability shows stable ranges around 0.01 m, with variation mainly in the range of ± 0.56 m and gleichläufigkeit (glk, fraction of same-directional year-to-year changes) shows a robust temporal stability around 73 %.

The mountain permafrost monitoring program PERMOS in Switzerland is specifically assessing the Permafrost cci products for high-mountain permafrost regions, using in situ observations of surface temperature and borehole temperature time series and the ESA GlobPermafrost slope movement inventory. PERMOS investigations in the Swiss Alps show that the performance of Permafrost cci GTD and Permafrost cci PFR improved for mountain regions worldwide. Permafrost cci GTD in the Swiss Alps shows a slight cold bias of -0.08 °C only, RMSE is +0.32 °C). At larger depth, Permafrost cci GTD shows a warm bias of 1.06 °C at 10 m depth. Permafrost cci GTD fits best with the in situ observations near the surface with the bias increasing with depth at all sites. Although the absolute values are different, both PERMOS in situ measurements and Permafrost cci GTD show the consistent warming trend over the period 1997 to 2023. Permafrost cci GTD matches well the inter-annual variability at the surface (i.e. warmer GTD due to the extreme warm years in 2003 and colder GTD due to snow poor winters in 2017 and 2021). At depth, Permafrost cci GTD product fails to reproduce the measured inter-annual variability. When Permafrost cci GTD values are below about -0.5 °C, interannual temperature variations are small and when Permafrost cci GTD values are within about -0.5 and 0 °C there are no variations. Permafrost cci PFR permafrost extent fits well with the distribution of the majority of inventoried ESA GlobPermafrost slope movement products as well as the active rock glaciers inventoried in CCI phase I and II. The Permafrost cci PFR product best fits with the inventoried rock glaciers in central Asian region (Khazastan), northern Scandinavian region (Troms, Norway) and the Himalayan regions (Nepal, India and Bhutan). In the continuous permafrost area of Brooks mountain range (Alaska), Disko Island (Greenland) and Tsengel region (Mongolia) the Permafrost cci PFR is slightly overestimated, while in the European Alps (France, Switzerland and Italy) Permafrost cci PFR is slightly underestimated.

In addition, we innovatively apply the Freeze-Thaw to Temperature (FT2T) product, an EO microwave-derived ground temperature, for comparison with Permafrost_cci GTD. Ground temperature averages partially correlate with $R^2 = 0.34$ in Alaska and in Canada. No correlation can be observed for Russia and Greenland. An offset can be observed in case of all selected regions. This bias ranges from 1.42 °C (Canada) to 2.1 °C (Alaska). Similar temporal patterns can be however partially observed.

For the inland ice-free permafrost regions in Antarctica, data are not sufficient for a thorough statistical analysis. The tendency of the Permafrost_cci dataset compared to the available in situ data is negative, i.e. Permafrost_cci performs with too cold GTD and too shallow ALT depths. The temporal trend of GTD is well captured by Permafrost_cci at three from five measurement sites.

In summary, Permafrost_cci GTD < 1°C shows good performance with a cold median bias of -0.23 °C (mean bias of 0.03 °C \pm 1.94) across all depths and high temporal stability resulting in a well usable CCI ECV product for the climate research communities. Users of Permafrost_cci GTD products should consider that Permafrost_cci GTD > 1 °C outside of the permafrost zones is characterised by a cold median bias of -1.33 °C (mean bias -1.16 °C \pm 1.48). This leads in turn to an overestimation of the areal extent of permafrost at the southern boundaries of Permafrost in discontinuous, and sporadic permafrost regions. We consider Permafrost_cci GTD and PFR products for the Northern hemisphere to be most reliable in the permafrost temperature range with GTD < 1 °C.

7 REFERENCES

7.1 Bibliography

Allard, M., Sarrazin, D. and L'Hérault, E., 2024, Borehole and near-surface ground temperatures in northeastern Canada, v.1.6.0 (1988-2023). Nordicana D8, https://doi.org/10.5885/45291SL-34F28A9491014AFD

Allard, M., Sarrazin, D. and L'Hérault, E., 2020, Borehole and near-surface ground temperatures in northeastern Canada, v.1.5 (1988-2019). Nordicana D8, https://doi.org/10.5885/45291SL-34F28A9491014AFD

Bergstedt, H. and Bartsch, A., 2020a, Near surface ground temperature, soil moisture and snow depth measurements in the Kaldoaivi Wilderness Area, for 2016-2018. PANGAEA, https://doi.org/10.1594/PANGAEA.912482

Bergstedt, H., Bartsch, A., Duguay, C and Jones, B., 2020b, Influence of surface water on coarse resolution C-band backscatter: Implications for freeze/thaw retrieval from scatterometer data. Remote Sensing of Environment, 247, https://doi.org/10.1016/j.rse.2020.111911

Biskaborn, B.K., Smith, S.L.; Noetzli, J., Matthes, H., Vieira, G., Streletskiy, D.A., Schoeneich, P., Romanovsky, V.E., Lewkowicz, A.G., Abramov, A., Allard, M., Boike, J., Cable, W.L., Christiansen, H.H., Delaloye, R., Diekmann, B., Drozdov, D., Etzelmüller, B., Grosse, G., Guglielmin, M., Ingeman-Nielsen, T., Isaksen, K., Ishikawa, M., Johansson, M., Johansson, H., Joo, A., Kaverin, D., Kholodov, A., Konstantinov, P., Kröger, T., Lambiel, C., Lanckman, J.-P., Luo, D., Malkova, G., Meiklejohn, I., Moskalenko, N., Oliva, M., Phillips, M., Ramos, M., Sannel, A.B.K., Sergeev, D., Seybold, C., Skryabin, P., Vasiliev, A., Wu, Q., Yoshikawa, K., Zheleznyak, M. and Lantuit, H., 2019, Permafrost is warming at a global scale. Nature Communications, 10, 264, https://doi.org/10.1038/s41467-018-08240-4

Biskaborn, B.K., Lanckman, J.-P., Lantuit, H., Elger, K., Streletskiy, D.A., Cable, W.L. and Romanovsky, V.E., 2015, The new database of the Global Terrestrial Network for Permafrost (GTN-P). Earth System Science Data, 7, 245-259, https://doi.org/10.5194/essd-7-245-2015

Boike, J., Hammar, J., Goldau, M., Miesner, F. and Anselm, N., 2024a, Circumarctic seasonal measurements of permafrost parameters (thaw depth, snow depth, vegetation and tree height, water level, and soil properties). PANGAEA, https://doi.org/10.1594/PANGAEA.971787

Boike, J., Hammar, J., Goldau, M., Anselm, N., Chadburn, S., Zwieback, S., Martin, J., Abramova, E. N., Coulombe, S., Giamberini, M., Rader, F., Herment, G., Suominen, O., Rudd, D. A., Mastepanov, M., Meléndez González, M., Hille, E., Elias, G., Sjöberg, Y., Greschkowiak, A., Lee, H., Stuenzi, S. M. and Marsh, P., 2024b, T-MOSAiC 2022 myThaw data set. PANGAEA, https://doi.org/10.1594/PANGAEA.971586

Boike, J., Miesner, F., Bornemann, N., Cable, W.L. and Grünberg, I., 2023, Trail Valley Creek, NWT, Canada Soil Moisture and Temperature 2016 et seq. PANGAEA, https://doi.org/10.1594/PANGAEA.962726

Boike, J., Cable, W.L., Bolshiyanov, D.Y., Bornemann, N., Grigoriev, M.N., Grünberg, I. and Miesner, F., 2022, Continuous measurements in soil and air at the permafrost long-term observatory at Samoylov Station (2002 et seq). PANGAEA, https://doi.org/10.1594/PANGAEA.947032

Boike, J., Chadburn, S., Martin, J., Zwieback, S., Althuizen, I. H. J., Anselm, N., Cai, L., Coulombe, S., Lee, H., Liljedahl, A. K., Schneebeli, M., Sjöberg, Y., Smith, N., Smith, S. L., Streletskiy, D. A., Stuenzi, S. M., Westermann, S. and Wilcox, E. J., 2021, Standardized monitoring of permafrost thaw: A user-friendly, multiparameter protocol. Arctic Science, 8(1), 153–182, https://doi.org/10.1139/as-2021-0007

Boike, J., Juszak, I., Lange, S., Chadburn, S., Burke, E., Overduin, P.P., Roth, K., Ippisch, O., Bornemann, N., Stern, L., Gouttevin, I., Hauber, E. and Westermann, S., 2018, A 20-year record (1998-2017) of permafrost, active layer and meteorological conditions at a high Arctic permafrost research site (Bayelva, Spitsbergen). Earth System Science Data, 10, 355-390, https://doi.org/10.5194/essd-10-355-2018

Boike, J., Nitzbon, J., Anders, K., Grigoriev, M.N, Bolshiyanov, D.Y., Langer, M., Lange, S., Bornemann, N., Morgenstern, A., Schreiber, P., Wille, C., Chadburn, S., Gouttevin, I. and Kutzbach, L., 2019, Soil data at station Samoylov (2002-2018, level 1, version 201908). PANGAEA, https://doi.org/10.1594/PANGAEA.905233

Boike, J., Nitzbon, J., Anders, K., Grigoriev, M.N., Bolshiyanov, D.Y., Langer, M., Lange, S., Bornemann, N., Morgenstern, A., Schreiber, P., Wille, C., Chadburn, S., Gouttevin, I. and Kutzbach, L., 2018, Soil data at station Samoylov (2002-2018, level 1, version 1), link to archive. PANGAEA, https://doi.org/10.1594/PANGAEA.891140

Brown, J., Hinkel, K.M. and Nelson, F.E., 2000, The Circumpolar Active Layer Monitoring (Calm) Program: Research Designs and Initial Results. Polar Geography 24, 166-258, https://doi.org/10.1080/10889370009377698

Brown, J., Ferrians, O.J., Heginbottom, J.A. and Melnikov, E.S., 1997, Circum-arctic map of permafrost and ground ice conditions. International Permafrost Association, US Geological Survey.

Brown J., 1970, Permafrost in Canada: Its influence on northern development. University of Toronto Press, Toronto, 234p.

Bryant, R.N., Robinson, J.E., Taylor, M.D., Harper, W., DeMasi, A., Kyker-Snowman, E., Veremeeva, A., Schirrmeister, L., Harden, J. and Grosse, G., 2017, Digital Database and Maps of Quaternary Deposits in East and Central Siberia: U.S. Geological Survey data release. https://doi.org/10.5066/F7VT1Q89

CEN 2020a, Climate station data from Nikku Island in Nunavut, Canada, v. 1.0 (2010-2016). Nordicana D64, https://doi.org/10.5885/45505SL-528A7C505494428A

CEN 2020b, Climate station data from the Biscarat river region in Nunavik, Quebec, Canada, v. 1.0 (2005-2019). Nordicana D62, https://doi.org/10.5885/45495SL-78FA5A95C5FB4D21

CEN 2020c, Climate station data from the Clearwater lake region in Nunavik, Quebec, Canada, v. 1.1 (1986-2019). Nordicana D57, https://doi.org/10.5885/45475SL-5A33FE09B0494D92

CEN 2020d, Climate station data from the Laforge Reservoir region, Quebec, Canada, v. 1.0 (1995-2013). Nordicana D66, https://doi.org/10.5885/45515SL-CFC7E8137E8B4323

D.4.1 Produc	ct Validation and Inter-	CCI+ PHASE II – NEW ECV	S Issue 5.1
Comparison	Report (PVIR)	Permafrost	30 October 2025

CEN 2020e, Climate station data from the Little Whale River region in Nunavik, Quebec, Canada, v. 1.1 (1993-2019). Nordicana D58, https://doi.org/10.5885/45485SL-78F4F9C368364100

CEN 2020f, Climate station data from the Robert-Bourassa Reservoir region, Quebec, Canada, v. 1.1 (1996-2019). Nordicana D60, https://doi.org/10.5885/45470SL-7BD92481E2CF4DC0

CEN 2020g, Climate station data from the Sheldrake river region in Nunavik, Quebec, Canada, v. 1.1 (1986-2019). Nordicana D61, https://doi.org/10.5885/45480SL-C89DEB92A4FE4536

Clow, G.D., 2014, Temperature data acquired from the GTN-P Deep Borehole Array on the Arctic Slope of Alaska, 1973–2013. Earth System Science Data, 6, 201-218, https://doi.org/10.5194/essd-6-201-2014

Fortier, D., Sliger, M., Gagnon, S. and Rioux, K., 2021, Ground temperature in natural conditions along the Alaska Highway at the Beaver Creek Road Experimental Site, Yukon, Canada, v.1.0 (2008-2020). Nordicana D94, https://doi.org/10.5885/45738CE-D75F3C9342D34C83

Grünberg, I., Miesner, F., Bornemann, N., Cable, W.L. and Boike, J., 2025, Meteorological and soil data from Bayelva, Svalbard, homogenised data product (version 2: 1998-09-13 to 2024-12-31, design 2: one row per time-step) [dataset]. PANGAEA, https://doi.org/10.1594/PANGAEA.982254, In: Grünberg, I et al. (2024): Meteorological and soil data from Bayelva, Svalbard, homogenised data product (1998 et seq.). PANGAEA, https://doi.org/10.1594/PANGAEA.969343

GTN-P, 2021, Long-term mean annual ground temperature data for permafrost. PANGAEA, https://doi.org/10.1594/PANGAEA.930669

GTN-P, 2018, GTN-P global mean annual ground temperature data for permafrost near the depth of zero annual amplitude (2007-2016). PANGAEA, https://doi.org/10.1594/PANGAEA.884711

Hammar, J., Goldau, M., Boike, J., Rath, M., Anselm, N., Martin, J., Chadburn, S., Zwieback, S., Carbonnel, M., Herment, G., Coulombe, S., Giamberini, M., Stuenzi, S. M., Suominen, O., Hille, E., Elias, G., Meléndez González, M., Rudd, D. A., Mastepanov, M. and Marsh, P., 2025, 2023 myThaw data set. PANGAEA, https://doi.org/10.1594/PANGAEA.974461

Heginbottom, J.A., 1984, The mapping of permafrost. Canadian Geographer, 28, 1, 78-83.

Heginbottom, J.A. and Radburn, L.K., 1992, Permafrost and Ground Ice Conditions of Northwestern Canada (Mackenzie Region). National Snow and Ice Data Center, Boulder, CO, USA.

Högström, E., Heim, B., Bartsch, A., Bergstedt, H. and Pointner, G., 2018, Evaluation of a MetOp ASCAT-Derived surface soil moisture product in tundra environments. Journal of Geophysical Research: Earth Surface, 123(12), 3190-3205, https://doi.org/10.1029/2018JF004658

Matsuoka, K., Skoglund, A., Roth, G., de Pomereu, J., Griffiths, H., Headland, R., Herried, B., Katsumata, K., Le Brocq, A., Licht, K., Morgan, F., Neff, P.D., Ritz, C., Scheinert, M., Tamura, T., Van de Putte, A., van den Broeke, M., von Deschwanden, A., Deschamps-Berger, C., Van Liefferinge, B., Stein Tronstad and Melvær, Y., 2021, Quantarctica, an integrated mapping environment for Antarctica, the Southern Ocean, and sub-Antarctic islands, Environmental Modelling & Software, Volume 140, 105015, https://doi.org/10.1016/j.envsoft.2021.105015

Kholodov, A.L, Wieczorek, M., Heim, B. and Romanovsky, V.E, 2025, Eleven years of Mean Annual Ground Temperatures across depths from eastern and central Siberia (2008-2018). PANGAEA, https://doi.org/10.1594/PANGAEA.972733

D.4.1 Product Validation and Inter-	CCI+ PHASE II – NEW ECVS	Issue 5.1
Comparison Report (PVIR)	Permafrost	30 October 2025

Kroisleitner, C., Bartsch, A. and Bergstedt, H., 2018, Circumpolar patterns of potential mean annual ground temperature based on surface state obtained from microwave satellite data. The Cryosphere, 12, 2349-2370, https://doi.org/10.5194/tc-12-2349-2018

Kudryavtsev, V.A., 1978, Naeimi, V., Bartalis, Z., Hasenauer, S., and Wagner, W., 2009, An improved soil moisture retrieval algorithm for ERS and METOP scatterometer observations. IEEE Transactions on Geoscience and Remote Sensing, 47(7), https://doi.org/10.1109/TGRS.2008.2011617

Lewkowicz, A.G, Wieczorek, M., Bartsch, A. and Heim, B., 2025, Twenty years of Mean Annual Ground Temperature (MAGT) across latitudinal and elevational gradients in the Yukon Territory (NW Canada). PANGAEA, https://doi.org/10.1594/PANGAEA.971276

Martin, J., Boike, J., Chadburn, S., Zwieback, S., Anselm, N., Goldau, M., Hammar, J., Abramova, E. N., Lisovski, S., Coulombe, S., Dakin, B., Wilcox, E. J., Giamberini, M., Rader, F., Suominen, O., Rudd, D. A., Mastepanov, M. and Young, A., 2023, T-MOSAiC 2021 myThaw data set [Dataset]. PANGAEA, https://doi.org/10.1594/PANGAEA.956039

Miesner, F., Bolshiyanov, D.Y., Bornemann, N., Cable, W.L, Grigoriev, M.N., Grünberg, I. and Boike, J., 2023, Calm data at station Samoylov (2021). PANGAEA, https://doi.org/10.1594/PANGAEA.961867

Muller, S.W, 1943, Permafrost or permanently frozen ground and related engineering problems. U.S. Engineers Office, Strategic Engineering Study, Special Report No. 62, 136p. (Reprinted in 1947, J. W. Edwards, Ann Arbor, Michigan, 231p).

Naeimi, V., Paulik, C., Bartsch, A., Wagner, W., Kidd, R., Park, S.-E., Elger, K., and Boik, J., 2012, ASCAT Surface State Flag (SSF): Extracting Information on Surface Freeze/Thaw Conditions From Backscatter Data Using an Empirical Threshold-Analysis Algorithm. IEEE Transactions on Geoscience and Remote Sensing, 50(7), 2566-2582, https://doi.org/10.1109/TGRS.2011.2177667

Paulik, C., Melzer, T., Hahn, S., Bartsch, A., Heim, B., Elger, K. and Wagner, W., 2014, Circumpolar surface soil moisture and freeze/thaw surface status remote sensing products (version 4) with links to geotiff images and NetCDF files (2007-01 to 2013-12). PANGAEA, https://doi.org/10.1594/PANGAEA.832153

RGIK, 2023, Guidelines for inventorying rock glaciers: baseline and practical concepts (version 1.0). IPA Action Group Rock glacier inventories and kinematics, 25 pp, https://doi.org/10.51363/unifr.srr.2023.002

Rouyet, L., Bolch, T., Brardinoni, F., Caduff, R., Cusicanqui, D., Darrow, M., Delaloye, R., Echelard, T., Lambiel, C., Pellet, C., Ruiz, L., Schmid, L., Sirbu, F. and Strozzi, T., 2025, Rock Glacier Inventories (RoGIs) in 12 areas worldwide using a multi-operator consensus-based procedure. Earth System Science Data, 17(8), 4125–4157, https://doi.org/10.5194/essd-17-4125-2025

Staub, B., Hasler, A., Noetzli, J. and Delaloye, R., 2017, Gap-filling algorithm for ground surface temperature data measured in permafrost and periglacial environments. Permafrost and Periglacial Processes, 28(1), 275-285, https://doi.org/10.1002/ppp.1913

Streletskiy, D.A., Wieczorek, M., Heim, B. and Bartsch, A., 2025, GTN-P CALM: 35 years of Active Layer Thickness (ALT) across latitudinal and elevational gradients in the Northern Hemisphere. PANGAEA, https://doi.org/10.1594/PANGAEA.972777

D.4.1 Product Validation and Inter-	CCI+ PHASE II – NEW ECVS	Issue 5.1
Comparison Report (PVIR)	Permafrost	30 October 2025

van Everdingen R.O., 1985, Unfrozen permafrost and other taliks. Workshop on Permafrost Geophysics, Golden, Colorado, 1984 (J. Brown, M.C. Metz, P. Hoekstra, eds). U.S. Army, C.R.R.E.L., Hanover, New Hampshire, Special Report 85-5, 101-105

van Everdingen, R.O., 1976, Geocryological terminology, Canadian Journal of Earth Sciences, 13, 862-867, https://doi.org/10.1139/e76-089

Veremeeva, A., Morgenstern, A., Gottschalk, M., Jünger, J., Laboor, S., Abakumov, E., Adrian, I., Angelopoulos, M., Antonova, S., Boike, J., Bornemann, N., Cherepanova, A., Evgrafova, S., Fedorov-Davydov, D., Fuchs, M., Grigoriev, M.N., Günther, F., Hugelius, G., Kizyakov, A., Kut, A., Lashchinskiy, N., Lupachev, A., Maksimov, G.T., Meyer, H., Miesner, F., Minke, M., Nitzbon, J., Opel, T., Overduin, P.P., Ramage, J.L., Liebner, S., Polyakov, V.I., Rivkina, E., Runge, A., Schirrmeister, L., Schwamborn, G., Siewert, M.B., Tarbeeva, A., Ulrich, M., Wetterich, S., Zubrzycki, S. and Grosse, G., 2025, ALLena: Thaw depth measurements of the active layer in the Lena River Delta region from 1998 to 2022, Northeastern Siberia. PANGAEA. https://doi.org/10.1594/PANGAEA.973813, In: Veremeeva, A et al. (2025): ALLena: Compilation of thaw depth measurements of the active layer in the Lena River Delta region from 1998 to 2022, Northeastern Siberia. PANGAEA, https://doi.org/10.1594/PANGAEA.974408

Wang, K., 2018, A Synthesis Dataset of Near-Surface Permafrost Conditions for Alaska, 1997-2016. https://doi.org/10.18739/a2kg55

Wieczorek, M., Lewkowicz, A.G., Kholodov, A.L., Romanovsky, V.E., Nicolsky, D., Streletskiy, D.A., Boike, J., Heim, B., Bartsch, A., Biskaborn, B.K., Christiansen, H.H., Elger, K. and Irrgang, A.M., 2025, GTN-P: 41 years of Mean Annual Ground Temperature (MAGT) across latitudinal and elevational gradients in the Northern Hemisphere. PANGAEA, https://doi.pangaea.de/10.1594/PANGAEA.972992 (dataset in review)

Williams, J.R., 1965, Ground water in permafrost regions, An annotated bibliography. U.S. Geological Survey, Professional Paper 696, 83p.

D.4.1 Product Validation and Inter-	CCI+ PHASE II – NEW ECVS	Issue 5.1
Comparison Report (PVIR)	Permafrost	30 October 2025

7.2 Acronyms

ALT Active Layer Thickness

AWI Alfred Wegener Institute Helmholtz Centre for Polar and Marine Research

B.GEOS b.geos GmbH

CALM Circumpolar Active Layer Monitoring

CC3 Permafrost_cci CryoGrid 3

CEN Center for Northern Studies in Canada

CCI Climate Change Initiative

CRDP Climate Research Data Package

ECV Essential Climate Variable

EO Earth Observation

ESA European Space Agency

FT2T Freeze-Thaw to Temperature
GAMMA Gamma Remote Sensing AG

GCOS Global Climate Observing System

GCW Global Cryosphere Watch

GT Ground Temperature

GTD Ground Temperature per Depth

GTN-P Global Terrestrial Network for Permafrost

GTOS Global Terrestrial Observing System

GUIO Department of Geosciences University of Oslo

IASC International Arctic Science Committee

IPA International Permafrost Association

IPCC Intergovernmental Panel on Climate Change

MAGT Mean Annual Ground Temperature
NSIDC National Snow and Ice Data Center

PE Permafrost Extent

PERMOS Swiss Permafrost Monitoring Network

PFR Permafrost FRaction
RD Reference Document

TSP Thermal State of Permafrost

UNIFR Department of Geosciences University of Fribourg

URD Users Requirement Document

WMO World Meteorological Organisation